Universidade de Aveiro

2014

Departamento de Eletrónica, Telecomunicações e Informática

Krzysztof Mirosław Bartos

Controladores LED eficientes para aplicações de iluminação geral

Efficient LED Drivers for General Illumination Applications

Universidade de Aveiro

2014

Departamento de Eletrónica, Telecomunicações e Informática

Krzysztof Mirosław Bartos

Controladores LED eficientes para aplicações de iluminação geral

Efficient LED Drivers for General Illumination Applications

Dissertação apresentada à Universidade de Aveiro para cumprimento dos requisitos necessários à obtenção do grau de Mestre em Engenharia Eletrónica e Telecomunicações, realizada sob a orientação científica do Dr. Luis Filipe Mesquita Nero Moreira Alves, Professor Auxiliar do Departamento de Electrónica Telecomunicações e Informática da Universidade de Aveiro

For my family for their love,
support and endless faith

o júri

presidente   Professor Doutor Rui Manuel Escadas Ramos Martins

Professor Auxiliar do Departamento de Electrónica Telecomunicações e Informática da Universidade de Aveiro

Professor Doutor Marcin Janicki

Associate Professor of Department of Microelectronics and Computer Science, of Faculty of Electrical, Electronic, Compute**r** And Control Engineering, Lodz University of Technology, Lodz, Poland

Professor Doutor Luis Filipe Mesquita Nero Moreira Alves

Professor Auxiliar do Departamento de Electrónica Telecomunicações e Informática da Universidade de Aveiro

resumo

As tendências de consumo de energia cada vez maior e seu impacto sobre o meio ambiente tem captado a atenção a nível mundial. Isso tem motivado várias medidas, tais como o Protocolo de Quioto, ou a estratégia Europeia 20 20 20, visando a redução do consumo de energia. Globalmente, estas medidas defendem um uso melhor e eficiente da energia disponível. Este, por sua vez, está fortemente ligado à consciência pública e à introdução de equipamento eletrónico eficiente. A iluminação pública é um bom exemplo dessas tendências, em que ambos os aspetos são de extrema importância. A introdução de LEDs como dispositivos de iluminação tem motivado vários avanços que lidam com essas estratégias. De um lado, os LEDs são capazes de oferecer uma maior eficiência quando comparados com dispositivos de iluminação convencionais. Isso provocou a substituição de luminárias convencionais por luminárias baseadas em LED. No entanto, o custo elevado destes dispositivos tem impedido a adoção plena e na fase atual, está mesmo a atuar como uma força negativa contra esta tendência de substituição. Melhores soluções estão sob investigação no âmbito de vários projetos europeus.

Os LEDs são dispositivos de estado sólido, capazes de suportar a comutação rápida, uma característica que não é totalmente suportada por dispositivos de iluminação convencionais. Combinando esta característica com sensores ambientais e controlo inteligente pode-se ambicionar melhores poupanças energéticas. Uma abordagem simples seria a de considerar o que as exigências de iluminação reais dependem do uso das ruas e os níveis de iluminação circundantes. Para este efeito, a combinação de sensores de crepúsculo, detetores de movimento e regimes de controlo inteligentes podem propiciar uma abordagem adequada. Desta forma, os requisitos reais de iluminação podem ser efetivamente considerados, fornecendo luminárias capazes de consumir apenas a energia necessária. Para que isto se torne uma realidade vários desafios têm de ser vencidos. Um dos desafios mais importantes é o projeto LED driver.

Nos sistemas de iluminação modernos baseados em LEDs, substitui-se os balastros convencionais por LED drivers. Quando a eficiência é importante, como no caso da iluminação pública, O LED driver têm de ser concebido de forma a ser o mais robusto e eficiente possível. Soluções recorrentes usam a fontes de alimentação comutadas, capazes de suportar o escurecimento adaptativo do fluxo luminoso. Um dos problemas principais no projeto destes drivers é o facto de a sua eficiência diminuir para níveis de regulação mais baixos. Isto é de extrema importância para a iluminação pública, pois na maioria dos casos durante a noite, as luminárias estão num nível de iluminação de baixo. Assim, com a finalidade de promover uma melhor economia de energia, a eficiência do driver deve ser elevada para ambas as condições de iluminação. Drivers comercialmente disponíveis, exibem eficácias na gama de 90% com elevado fluxo luminoso, e apenas 40% a 60% na condição de baixo fluxo luminoso. No âmbito desta dissertação de mestrado foi investigado o problema do projeto de driver LED visando a maior uniformidade possível da curva de eficiência, sob diferentes condições de carga e de fluxo luminoso. A abordagem escolhida foi baseada no conversor flyback quasi-ressonante, apoiado por um bloco de correção de fator de potência ativa. O driver projetado suporta configuração e monitorização remota, bem como de integração de sensores. Os resultados alcançados mostram que este driver atinge um pico de eficiência de 93% na condição de carga máxima e máximo fluxo luminoso. A eficiência em condições de baixo fluxo luminoso é superior a 75%.

keywords

LED ,efficency drivers, lighting system, two switch quasi-resonant flyback, active PFC, wireless comunication.

abstract

The ever growing energy consumption trends and its impact on the environment has triggered worldwide attention. This has motivated several measures, such as the Kyoto protocol, or the 20 20 20 European strategy, aiming at the reduction of energy consumption. Globally, these measures defend a better and efficient usage of the available energy. This in turn is strongly linked to public awareness and the introduction of efficient electronic equipment. Public street lighting is a good example of these trends, where both aspects are of the utmost importance. The introduction of power LEDs as future lighting devices has motivated several advances coping with these strategies. On one side, LEDs are able to deliver higher efficiency when compared to conventional lighting devices. This has triggered the replacement of old style luminaires by LED based ones. However, their high cost has prevented full adoption and at the present stage, is acting as a slowing down force against this replacement trend. Better solutions are under research on the framework of several European projects.

Power LEDs are solid-state devices able to support fast switching, a feature which was not fully supported by conventional lighting devices. Combining this feature with environmental sensing and intelligent control may lead to better power savings. A simple approach would be to consider the that the actual lighting demands depend on the street usage and surrounding lighting levels. For this purpose, the combination of twilight sensors, motion detectors and intelligent control schemes may provide a suitable approach. This way, the real lighting demands can be effectively taken into consideration, providing luminaires able to consume the least possible energy. For this to become a reality several challenges have to be addressed. One of the most important challenges is the LED driver design.

Modern lighting systems based on LEDs, replace the traditional ballasts by LED drivers. When efficiency is a major concern, such as in public street lighting, these drivers have to be designed in order to be the most robust and efficient as possible. Recurring solutions resort to switched mode power supplies, able to support light dimming. One of the major problems with these drivers is the fact that their efficiency decreases for lower dimming levels. This is of the utmost importance for public street lighting, as most of the time during night, the luminaires are on a low lighting level (as changes to high lighting conditions depend on street usage). Thus, in order to promote better power savings, the efficiency of the driver should be high for both lighting conditions. Commercially available drivers, exhibit efficiencies on the 90% range for the high lighting conditions, with only 40% to 60% under the low lighting. On the framework of this master dissertation it was investigated the problem of LED driver design aiming at the highest possible uniformity of the efficiency curve, under different loading and dimming conditions. The selected approach was based on quasi-resonant flyback converter, backed up by an active power factor correcting block. The designed driver supports remote configuration and monitoring as well as sensor integration. The archived results show that this driver achieves a peak efficiency of 93% under maximum load and 100% duty-cycle. The efficiency for low dimming conditions (10% duty-cycle) achieves 75%.

Table of contents

List of figures

1.Introduction

Discoveries in the 18th and 19th centuries led to a knowledge of electromagnetic phenomenon. In result, the profession of electrical engineering was born and the massive production of electric energy was started [1]. Electric energy is a very convenient and flexible form of energy. It is easy to transform into other forms of energy like heat, light, mechanical, amongst others. It brought accelerated civilization development. Nowadays it is hard to imagine world without electricity. It is present in offices, factories, homes, entertainment, communications and health care. Production of electric devices is increasing, what entail growing demand for electricity. According to International Energy Agency, the consumption of electricity in years 1973 – 2011 increased from 439 to 1582 Million Tonnes of Oil Equivalent (Mtoe), what is more than three and half times [2].
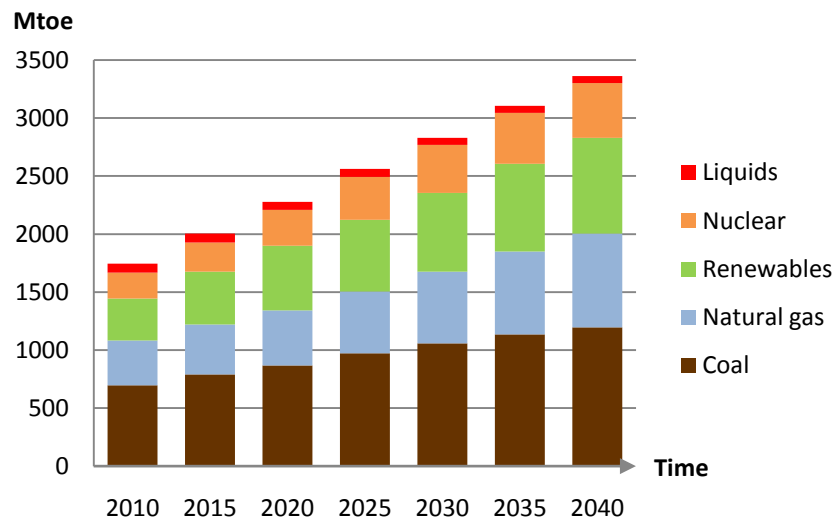
Figure 1.1 Prediction energy sources usage participated in electricity production [3].

Forecasts indicate that growth will remain at the level of 2.2% per annum and by 2040 will exceed the 3353 Mtoe [3]. However, the methods used to produce electricity will not change to a large extent. Figure 1.1 shows a planned participation of energy sources used to produce electricity. The share of fossil fuels in energy production will exceed 60%. This means an increase of CO_2 emissions into the atmosphere, which is the main product of burning fossil fuels. It can be also expected an increase in energy prices due to shrinking fuel resources. The issue of environmental protection and impact on climate change, has become a widely discussed in recent years. High developed countries have taken international cooperation in the United Nations Framework Convention on Climate Change, which resulted in the signing of an agreement in Kyoto in 1997 [4]. One of the main purposes of the agreement was to reduce emissions of greenhouse gases (including carbon dioxide) in the period 2008-2012 by at least 5% compared to 1990. European Union has taken even greater steps contained in the so-called 3 x 20 climate and energy package [5], which intends to:

• cutting greenhouse gases emissions by at least 20% of 1990 levels (30% if other developed countries commit to comparable cuts),

• limiting energy consumption by 20% of projected 2020 levels - by improving energy efficiency,

• increasing use of renewable energy source (wind, solar, biomass, etc) to 20% of total energy production (currently ± 8.5%).

The authorities carry out in the educational aspect to protect the environment. It is organized many campaigns and actions aimed at raising awareness of average citizen about the need to use modern, green and efficient technologies. The unquestionable advantage for the consumer is to reduce electricity costs. This causes that people are willing to use environmentally friendly devices. However, they are expected good performance, ease and convenience of use.

1.1 Problem Statement

Nearly one-fifth of the electricity produced is used for lighting purposes. [6] Lighting market brings tens of billions of Euros of income per year, of which the main part is due to general lighting. To meet the demands of today's lighting systems, lighting manufacturers have to reach for the latest technical achievements. The current trend in lighting is LED-based applications. The development of semiconductor technology and streamlining production processes of high power LED made it a useful and cost-effective type of lighting. It is expected that LED lighting will be the leader in lighting systems in the next two decades [7].

The main advantage is the high efficiency of LEDs compared to other common light sources. The efficiency is defined as the ratio of the light flux per unit of supplied electricity. The efficiency of LEDs is several times higher than traditional incandescent bulbs or halogen, which means a reduction in consumption, resulting in a significant decrease of electricity costs [8]. Today, modern Compact Fluorescent Lamp (CLF) can compete with LED lighting in terms of efficiency. However, a great progress in recent years in the field of LED and new performance records can change it. LED are solid-state devices with fast turn on and turn off times. At the start, it achieves full functionality with no extra time to warm up and stabilization. Light dimming or intensity adaptation is easily obtained employing Pulse Width Modulation (PWM). This brings huge advantages in lighting applications that require continuous changes in light intensity or rapid response. Possible applications may be intelligent lighting management systems that analyze signals and data from the environment and properly control the light intensity to provide the best lighting conditions as well as minimize energy consumption. Another feature of the LED, which is important in lighting systems, is their long life [9]. It is estimated that the average effective operation of the LED, under appropriate conditions, is 100,000 hours. For comparison, the life of incandescent lamp is estimated at 1000 hours, and at about 5000 hours for CLF, but time is strongly dependent on operating conditions, and in particular, the device's temperature. LED lighting has several advantages over other existing light sources. However, for proper operation, it requires suitable control. Due to the nonlinear characteristics of the LED control schemes often require current stabilization. Each LED has an optimum value of the current at which it

delivers highest efficiency and offer longer lifetime. Above this value, the device undergoes rapid degradation. Furthermore, the characterization work is very dependent on temperature, which forces constant monitoring and driving.

The LED driver is responsible for providing adequate working conditions. Primarily, its proper functioning allows to use all the advantages of the LED. In addition to meeting the above requirements, it is expected that it will not introduce additional complexity. Its design should be compact and robust. It cannot occupy a lot of space, so it can be easily built-in into the lamp housing. In addition, high efficiency is expected in order to make use of benefits, which the LED brings. To save energy and to control of luminance intensity according to ambient condition, the dimming is also wide spread in use. We can distinguish two types of LED driver design - Linear and Switched [10]. In the first case, the controller has a simple and compact structure, it is cheap in design and production. However, because the power semiconductor elements operate in the linear range, much heat is dissipated. It results in a relatively low efficiency. This creates the need for large and heavy heat sink, which increases the size and weight of the whole structure. This means that in most cases linear driver are not able meet requirements. The second type of controller is based on a switched converter. Its design and construction has higher complexity and requires the use of expensive high-speed semiconductor devices. However, its efficiency is higher. This causes less problems with heat dissipation and using modern integrated circuits allows for a small and lightweight design. Switched LED drivers are able to meet the imposed requirements and are widely used.

In recent times, the development of communication technology and the miniaturization of electronic devices allowed the installation of communications modules, even in small devices that operate autonomously. The implementation such a module in a LED driver would broaden its capabilities for managing and monitoring. In addition, it would give grounds for the inclusion of the controller to the entire lighting management system in order to increase the effectiveness and efficiency.

1.2 Thesis objective

The main objective of this work is the design and construction of the power supply and controller for LED applications. The most important requirement is to obtain the overall greatest efficiency. In addition it should be incorporated a digital control system based on microcontroller, to monitor and manage the output power, depending on the external environment conditions and enable wireless communication.

To achieve the objectives, it is necessary to investigate existing lighting systems. Then review of power supply techniques for LED purpose and power converters configurations. It should be noted that the device must not affect the operation of the power grid. Power supply and the LED driver should be allowed to cooperate with LED module available in the laboratory. The digital system should collect information of temperature, ambient light level, and the presence of people nearby. Then, analyzing the collected data, it has to control properly the light flux of LED module. In addition, it should estimate the power consumption from the grid for statistical purposes. The user needs to have access to relevant factors in order to fit the system to own needs. To facilitate the management, these data should have wireless access.

1.3 Structure of the dissertation

The whole dissertation is divided into five chapters. This chapter presents an introduction to the project development. It shows the situation on the energy market which indicates that LED technology is a promising future light source, and convenient for modern lighting systems. At the same time the power supply, as an integral part of the illumination system, is also the area on which it is worth to work and to develop it. Chapter 2 presents the theoretical part, which contains a description of present lighting sources and systems available in the field of power supply, taking into account the chosen solution. In Chapter 3 it is described in detail the requirements of the project. It shows the process of calculating and designing particular modules of the device and the selection of appropriate components. Also contains a implementation of the management system and the algorithm of the program. Chapter 4 presents the design of transformers and describes the design of PCB. It includes description of start-up and measurements process. After the devices is tested and analyzed. The obtained waveforms and measurement results are discussed. The last chapter presents obtained results and conclusions about dissertation.

2. State of the art survey

This chapter introduces the lighting systems with particular emphasis on the LED and power systems. At the beginning, popular light sources will be discussed. This will allow the reader to refer to the situation in the lighting market. Next, the LED operation and its characteristics will be described. It is necessary to familiar with the power supply methods and used topologies. The issue of power quality and power factor correction also will be touched.

2.1 Illumination

Lighting or illumination is the use of light to achieve a practical or aesthetic effect. Lighting includes the use of both artificial light sources like lamps, as well as natural illumination by capturing daylight during daytime. Proper lighting can enhance task performance, improve the appearance of an area, or have positive psychological effects on occupants [52].

2.1.1 A brief history of light sources

Primitive man needed to prolong livelihood in the darkness after sunset. Perhaps he learned how to use the fire as a light source about 500 thousand years ago [11]. The first torch was a piece of burning wood. The next notable invention was a burning fiber soaked in molten fat. These were the first candles used by ancient civilizations, and they are dated back to about 3000 BC. As a fuel, numerous kind of animals fat and vegetable oils was used. In the Middle Ages, candles were made of tallow and later beeswax or paraffin. In the 1800s gas lamps became popular as street lights [12]. It had no wick, however the main drawback was an open flame that produced considerable flicker. Electric lights became popular early 1900s after the incandescent lamp was developed independently by Sir Joseph Swan in England (1878) and Thomas Edison in the United States (1879). XX century has seen a huge increase in the number of available light sources in the marketplace. In 1901, Peter Cooper Hewitt, an American electrical engineer and inventor, patented the mercury vapor lamp, generating a bluish-green light. Low-pressure sodium vapor lamp was invented in 1919 by Arthur Holly at Compton of Westinghouse Electric in the United States. Edmund Germer was a German inventor who patented an experimental fluorescent lamp in 1927 together with Friedrich Meyer and Hans Spanner. The fluorescent lamps based on the fluorescence emission from the tube inner walls coated with a phosphor material when subjected to ultraviolet (UV) irradiation from discharge reached in mercury vapor under low-pressure. Later Germer sold his patent to General Electric where it was improved to practical fluorescent lamp. General Electric (GE) first developed the high-pressure sodium lamp in Schenectady (New York) and Nela Park (Ohio). It appeared in the market in 1964. The development of rare-earth phosphors in the late 1970s enabled the production of compact fluorescent lamps (CFL). Evolution of semiconductors technology and development new materials in 50s brings a invention of first practical visible spectrum light emitted diode in 1962. It was done by Nick Holonyak Jr. also called as *the father of the LED*. However first

publications about semiconductors light emission was already appeared in 1927, written by Russian Oleg Vladimirovich Losev.

2.1.2 Nature of light

Light is a form of electromagnetic energy. In vacuum [11], light propagates at a steady speed c = 2.99 × 10^8 m/s, which is taken as a universal constant. In nonvacuum media, this speed changes. Light has dual nature moving through space. It behaves like a wave or discrete particle called photon. A photon is a massless and chargeless particle. Its energy is calculated by the formula 2.1

$$E = h \cdot v = \frac{h \cdot c}{\lambda}$$

(2.1)

where E is the energy in joules, h is Planck's constant $= 6.625 \cdot 10^{-34}$ J/s, v is the frequency of light in Hz, c is the speed of light $= 2.998 \cdot 10^8$ m/s for vacuum, and λ is its wavelength in meters.

As energy carrier, photon can be absorbed or emitted. Light energy is propagated in the form of electromagnetic waves [12]. This wave consists of two transverse electric and magnetic fields, changing in space and time. Both of fields have the same frequency of oscillation. Visible light is contained in the specific frequency range as also wavelength. Visible spectrum is defined from 380nm for violet color to 780nm for dark red color.
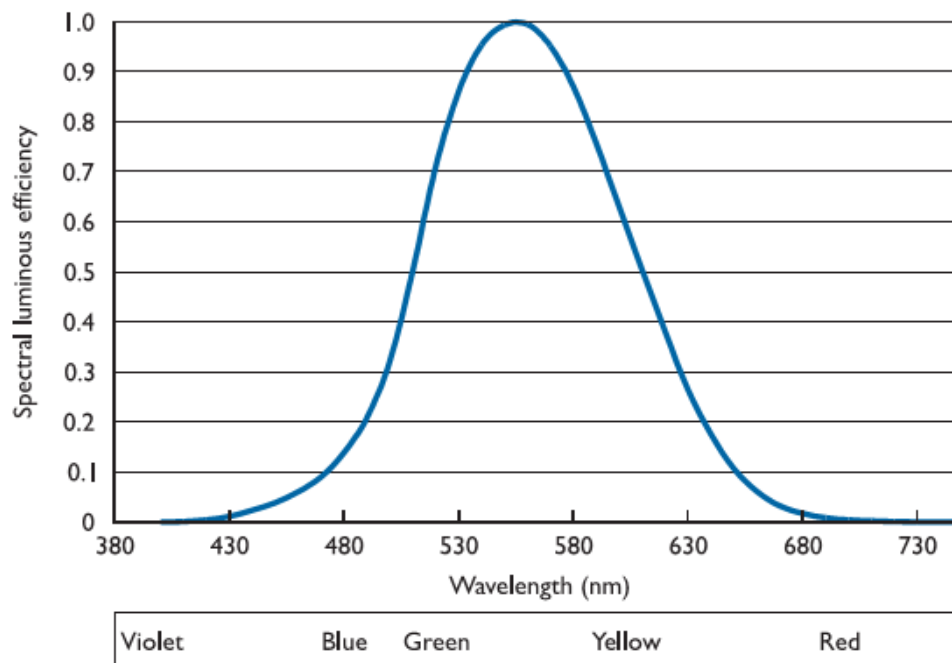
Figure 2.1 The relative spectral sensitivity of the human eye [9].

The human eye receives certain wavelengths of light with different sensitivity. Highest sensitivity is achieved for the green-yellow light which corresponds to waves with a length of 550-570nm. The relation of human visual sensitivity depends on light wavelength and it is described by the luminous efficiency function depicted on Figure 2.1. It is very important for lighting system. The efficiency of the lamp, defined as the total light energy emitted per unit of energy input, does not reflect the quality of light. It can be measure using luminous flux. It is the spectral density of radiant flux, also called spectral power distribution, multiplied by luminous efficiency function and integrated over the full visible spectrum. The unit of luminous flux is the lumen (lm). Accordingly, a lamp's energy performance is defined by the lamp's efficacy, which in broad terms is the ratio of the visually useful light emitted to the energy consumed. Its unit is lumen per watt (lm/W). Illuminance is the total luminous flux incident on a surface, per unit area. The unit of illuminance is lux and it is equal

$$1 lux = \frac{1\ lm}{1\ m^2}$$

(2.2)

Light sources can have different colors. The factor that characterizes the color of the light source is called a Correlated Color Temperature (CCT) given in Kelvin (K). The relationship between color and Kelvin temperature is derived from heating a black body radiator. The blackbody is artificial body, which absorbs all light radiation that falls on it. However, it can also emit energy in light form during heating. When the blackbody is sufficiently heated, it begins to emit dull red light. Continue heating, it becomes yellow, then white, and ultimately blue. A low color temperature is ascribed to warmer or yellow/red light while high color temperature is associated with a colder or blue light. This phenomena is stated by the Stefan–Boltzmann law which says that the total energy radiated per unit surface area of a black body across all wavelengths per unit time is directly proportional to the fourth power of the black body's temperature T. The color of emitted light corresponds to energy and hence to temperature. The color of light emitted by some source is referred to the color of heated black body, and on this base, its state the temperature of color of light source. There is one more factor corresponding with color, which is important to define the quality of light, the color rendering index (CRI). It is a quantitative measure of the ability of a light source to reveal the colors of various objects faithfully in comparison with an ideal or natural light source. It is rated on a scale running from 1 to 100. The smaller the CRI rating, the less truthfully reproduced are the colors. Light sources with high CRI have spectrum responses similar to incandescent lamp. In contrast, a low pressure sodium lamp, which produces monochromatic light, has 0 CRI

2.1.3 Description of light sources

At the present, there are many types of light sources on the lighting market. Each of them has its own characteristics, which define its purpose and area of use. There are main parameters, which describe a light source:

- efficacy [lm/W],
- color temperature [K],
- color rendering index,
- lifetime [hours].

There are other characteristics of light sources that can affect the comfort or usefulness in some area of application. These include

- start up time and light stability,
- dimming capabilities,
- size,
- cost,
- supply voltage range,
- need for ballast and ignition systems.

There are many sources that, although they were invented a long time ago and their development had stopped, still meet the requirements and are in use. New technologies are constantly developing and expand its area of application. However, sometimes due to the financial aspects, they are not able to displace the older solutions. This causes diversity in the lighting market which is constantly evolving. Figure 2.2 shows diagram of light source families.
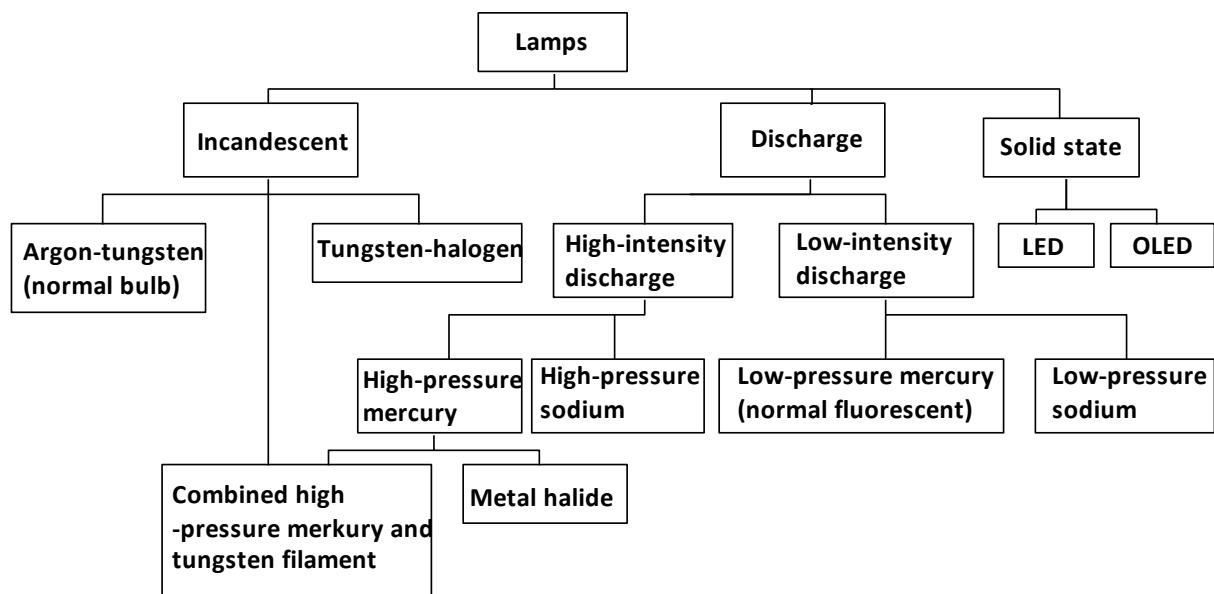
Figure 2.2 Structure of main light sources on market [9].

2.1.4 Incandescent filament bulb

This light source, despite its long history is still used. The construction is very simple (Figure 2.3). The glass bulb filament is made of tungsten. It is connected with cap via two wires. A cap serves as mounting of the light bulb. The tungsten filament is used due to its high melting point and low evaporation pressure. To reduce the evaporation of the tungsten filament, the bulb is filled with inert gas, usually argon. During operation, the filament heats up to high temperatures, which causes glowing and emission of visible light. Nevertheless, most of the emitted energy is in the infrared range.
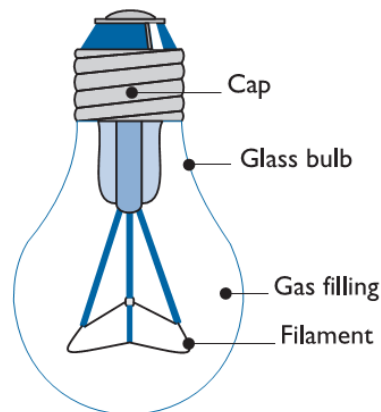
Figure 2.3 Incandescent lamp constructions.

Incandescent lamps have many advantages. Due to the simple construction, the cost of production is very small. The materials used and the method of operation does not cause danger to humans and animals. The lamp can be easily adjust to the desired voltage, and provide dimming. The bulb immediately obtains full light intensity. The light is emitted equally in all directions, but can be used a reflector that focuses the light flux in the desired direction. Because the filament can be treated as a black body, the incandescent bulb gives a comfortable warm shade of light in the range 240-3100K and the color rendering index (CRI) can reach 100. Despite the efforts, the tungsten filament evaporates relatively quickly so that the bulb life is poor and is approximately 1000 hours. The life of a filament decreases after exceeding the permissible operating voltage. Bulbs have a low efficacy - at the level of 10-16 lm/W, and are a source of unwanted heat. Up to 95% of the supplied energy is emitted in the infrared range. Therefore, operating costs are high.

2.1.5 Tungsten halogen lamp

Halogen lamps operate on the same principle as incandescent bulbs with the exception of the halogen regeneration cycle. Halogen gas is placed inside a bulb. During operation the tungsten filament particles vaporizes and deposited on the walls of the bulb. The halogen circulating in the bubble combines with tungsten particles. When it is near the filament, tungsten is released and deposited on the filament. This results in regeneration of the filament and extend the life of the bulb to 2000-6000 hours. To invoke halogen cycle, the temperature of the bulb should be greater than 260 degrees C.

Owing to the halogen cycle, a whiter light with a color up to 3200K and the shift of the emitted light spectrum toward the blue color can be obtained. The efficacy of the lamp is in the range of 18 -33 lm/W while color rendering index can reach 100. Usage of halogen gas and high-temperature glass, halogen lamp costs is higher than incandescent. Dimmed tungsten-halogen lamps should be run periodically at full power to initiate the halogen cycle.

2.1.6 Fluorescent Lamp and Compact Fluorescent Lamp

The fluorescent lamp is a low-pressure discharge lamp in which the phenomenon of fluorescence occurs. It is constructed mostly out of a tube ended on both sides on tungsten electrodes. The tube is filled with mercury and an inert gas (usually argon), and its walls are covered with phosphor. Current flowing between the electrodes creates a glow discharge, that excites the mercury vapor and thereby produces ultraviolet radiation. This in turn excites the phosphor coated glass tube, which emits visible light. Fluorescent lamps need a ballast to regulate the current and input voltage when turning on and assure stability while working. The efficacy of a fluorescent lamp is in the range of 60-104 lm/W, and its lifetime 7500-30000 hours. These values strongly depend on the diameter and length of the tube. A typical value of the CRI is 86%. Depending on the choice of phosphor mixture, lamps can be designed in a wide range of CCT ranging from 2700-7500K. These characteristics combined with reasonable lamp prices have led to fluorescent lamps to a dominant position in the lighting market, especially in offices and public buildings.

As previously mentioned, the development of rare-earth phosphors lead to the introduction of compact fluorescent lamps in the early 80s. Their principle of operation is the same as the linear fluorescent lamp, but the dimensions are considerably smaller. This allows the use of CLFs as direct replacements for traditional incandescent lamps. CFL Power rating ranges from 4 to 120 W and their efficacies from 35 to 80 lm/W. Another important benefit is that, they have relatively longer lifetimes ranging from 5000 to 25000 hours. Typical color rendering index is in range of 82-86%, which is good enough for most applications.

2.1.7 Discharge lamps

There are several types of discharge lamps. They are divided into low and high intensity discharge lamps. Table 2.1 shows the main properties of discharge lamps. Their action is based on the emission of light created by electrical discharges in vapors of various substances. These substances include mainly mercury, sodium, halogen metals and noble gases such as argon or neon. Their structure is similar, it consists of the arc tube filled with the active substance. The internal atmosphere allows the electrical discharge between two electrodes. Often, an auxiliary electrode is used for speed up evaporation of the active substance after start. The arc tube is enclosed in a glass bulb, which is often coated with an anti ultraviolet layer or phosphor to stop UV radiation. Most of the lamps need a ballast to initiate discharge during startup. Warm-up time takes about 10-15 minutes.

Table 2.1 Discharge lamps characteristics [11].

	Efficacy (lm/W)	CCT (K)	CRI	Lifespan(h)
High pressure mercury vapor lamp	25-65	2900-5700	15-62	6000-28000
Low pressure sodium (LPS) vapor lamp	up to 200	1800	0	10000-16000
High pressure sodium (HPS) vapor lamp	70-140	1900-2500	21-83	5000-28000
Metal halide lamp vapor lamp	47-105	3000-6500	65-92	6000-20000

High-pressure mercury lamp is the oldest high-intensity discharge lamp. During the operation, arc discharge occurs between the mercury vapor. The high-pressure mercury emits a bluish-green light. However, a large part of the radiated energy is in the ultraviolet spectrum. Therefore, the bulb surrounding the arc tube is made of UV-absorbing glass and coated with phosphor. The phosphor is excited by UV rays and emits visible light. This increases the efficacy of the lamp and prevents harmful UV rays. Mercury lamps have a low color rendering index and relatively low efficacy compared to other discharge lamps. The mercury lamp has found widespread usage in street lighting due it its low cost and high reliability. It is also used as a source of ultraviolet radiation. There are also mercury incandescent lamps. They do not require ballast, its role serves tungsten filament bulb connected in series with the arc tube. Such lamps have improved color rendering index, but at the expense of efficacy.

In sodium lamps, sodium vapor is the working medium. Low-pressure sodium lamps are the most efficient light sources in use. They emit a yellow light in a very narrow spectrum. This causes its high efficacy, because the light spectrum is very close to the peak light sensitivity of human vision. However, due to the monochromatic light, color rendering index is very low. Therefore, their use is limited only where color rendering is not important, for example, lighting highways and tunnels. Due to the low pressure, the lamp does not need time to cool down for restart.

Raising the pressure of the sodium vapor inside the arc tube, widens the spectrum of high-pressure sodium light compared to low-pressure. This increases the color rendering index, unfortunately at the expense of efficacy. Nevertheless, due to the relatively high efficacy, long life times and improvement visual perception in dust and fog, these lamps are the most popular for lighting roads, factory squares and open spaces. Because the spectrum of the sodium lamps is in the range of photosynthetic active radiation, they are also used in the cultivation of plants.

In the metal halide lamp, the electrical discharge occurs in a mixture of mercury, rare gas argon and a multitude of halide salts. We can distinguish the metal halide lamp with a quartz or ceramic arc tubes, which was recently develop intensively. Metal halide lamps have a very high efficacy, high color rendering index and a wide range of color temperature. The metal halide lamps also have a long life but a disadvantage of this type of lighting is a significant

decrease in light flux with age. Another problem is to maintain stable production parameters and costs. They are widely used for lighting shop windows, billboards, advertisements and architectural objects.

2.2 Light-emitting diode

Light-emitting diode (LED) belong to solid state lighting (SSL) devices category. The LED is a semiconductor electronic component that emits light under current conduction [11].

2.2.1 LED operation

LED consists of two electrodes: anode and cathode. It conducts current in one direction from the anode to the cathode (positive polarity), and blocks the current flow in the second direction (reverse polarization), as a normal diode. Semiconductors are doped by some impurity materials that create free charge. The LED is composed of two types of semiconductors: P-type in which the main charge carriers are holes, and N-type in which the main role is played by electrons. At the junction of these two materials, the free charges combine and this creates a narrow region depleted from free charge. This region creates energy barrier, which opposes any further free charge recombination. In effect, we have a junction diode.
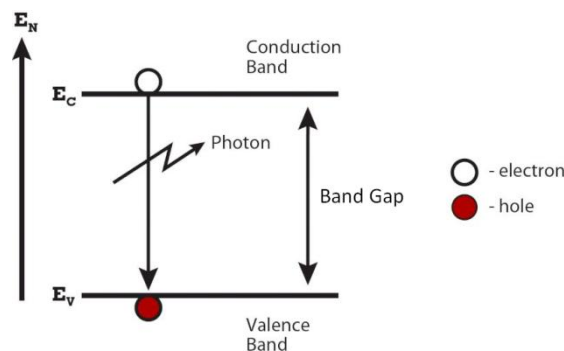
Figure 2.4 Radiative recombination in band model of semiconductor [adopted from 51].

The current that crosses the junction, follows a model based on energy bands. In the model, the energy bands represent energy levels for electrons in the conduction and valence band (Figure 2.4). Electrons have to overcome the band gap to change from valence to conduction [13]. The energy required to overcome the band gap depends on its width and is called the energy band gap (E_G). The energy released in this process can be emitted as a photon. This process is called radiative recombination. The energy of the photon corresponds to the wavelength of light according to the formula 2.1. There is an intimate relationship between the energy band gap and the wavelength of the emitted photon, as depicted in Figure 2.5.
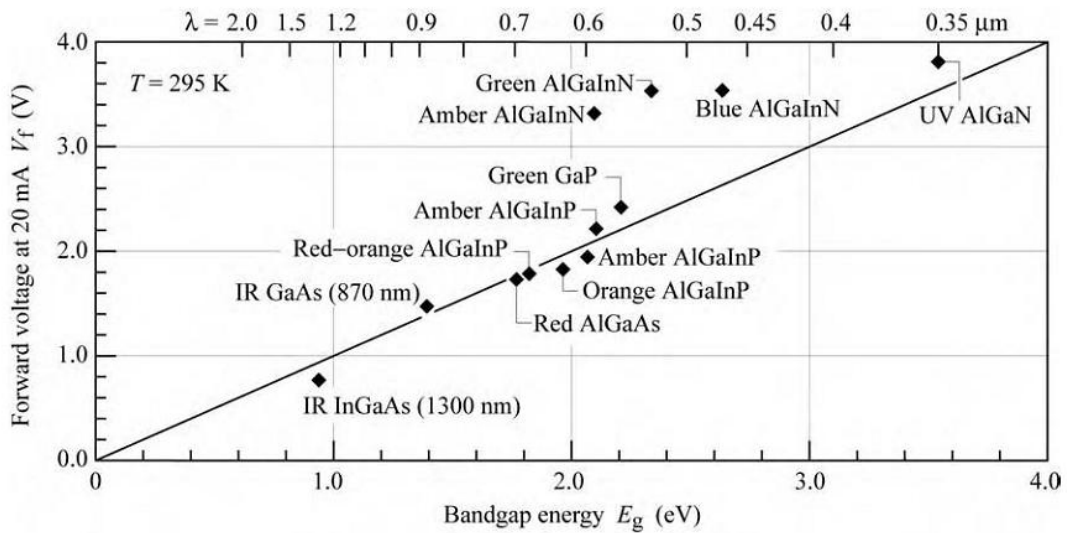
Figure 2.5 Relationship of forward voltage of LED to bandgap energy of semiconductor and wavelength of emitted light with marked materials of semiconductor [13].

The energy's band gap width depends on the material of the semiconductor. To obtain the different light colors, various materials are used for LED production. The diode forward voltage increases with the width of the bandgap. The current-voltage characteristic of the LED is similar to normal diode as depicted on Figure 2.6. After crossing the voltage threshold, which is characteristic for a given material, the diode current increases exponentially with the supplied voltage. The characteristics of the diodes of the same type may vary. This may result in different values of current for the same voltage. Exceeding the permissible current causes damage to the diode. Therefore, current limiting resistors or current sources are used to power the LEDs.
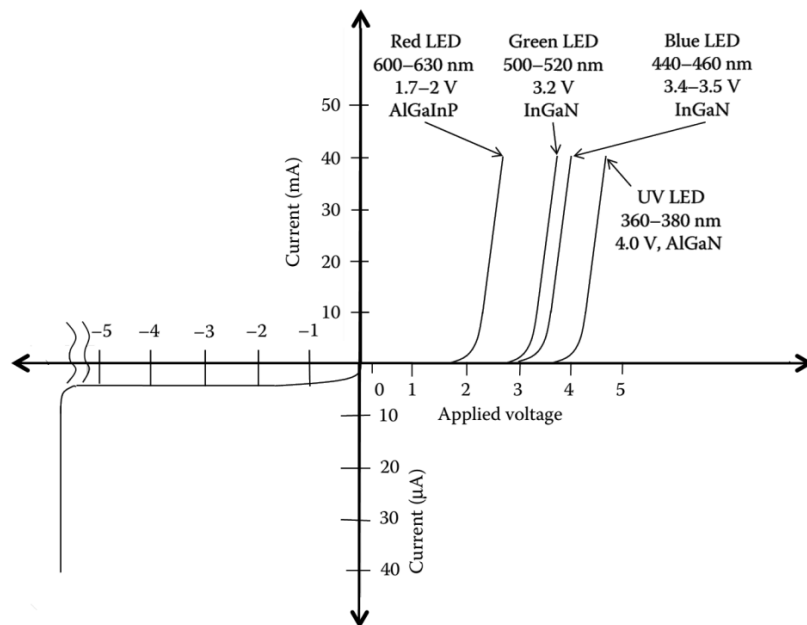
Figure 2.6 Voltage-current characteristic of LED [11].

The breakdown voltage of LEDs is relatively small compared to rectifier diodes. To protect the LEDs against high reverse voltages, an additional rectifier diode it is used, connected in parallel and reverse polarization.

2.2.2 The LED lighting systems

The first LEDs, due to very low efficiency values, have been used only as indicating decives [9]. On the beginning, only red color was available. Orange, yellow, green and infrared LEDs were developed later. The huge challenge was to develop blue and ultraviolet LEDs. The latter appeared in the mid 90s. This allowed the production of white LEDs. They are produced in 3 ways. The first is to put a diode in the red, green and blue in one housing (RGB diode). The combined power of the tree colors is carefully adjusted, in order to produce white light. Another way is to use a blue LED with a yellow phosphor. The last method is similar to fluorescent lamps and consists in the use of ultraviolet light-emitting diodes and a mixture of phosphors that performs wavelength up conversion from blue to visible range.

Thanks to colors mixing, a wide range of color temperature can be obtained in the range from 2700 to 6500K. The color rendering index is in the range of 60-90%. Unfortunately, lamps with high CRI are less efficient [14]. Several research trends on LED technology are currently under investigation. The Haitz's law is an expresion of this research trends, by which the efficiency of LEDs is doubled every two years. Lamps available on market have efficacy about 50-120 lm/W [15]. In the first quarter of 2014 year, the company CREE INC. announced the achievement of LED with efficiency of 303 lm/W [16]. A major challenge for LED manufacturers is to obtain high efficiency in high power LEDs. Therefore, LED modules are often composed of many LEDs to provide sufficient light intensity at high efficiency. Another barrier is the heat dissipation. Despite the fact that LEDs have a high efficiency, heat is generated in the small diode's structure. The diode's parameters are strongly dependent on temperature. The maximum LED junction temperature should not exceed 150 of degrees. Therefore, LEDs require heatsink to ensure adequate operating conditions. LED are point light source. This is a drawback for use as a general lighting source. To solve this inconvenience, various kinds of reflectors are used to ensure even light flux. A major advantage is the ability to match the shape of the lamp to the housing, which broadens the applications. In addition, LEDs are devices with long life times. Commercial LEDs lifespan is from 15,000 to 50,000 hours.

2.3 LED driving

LEDs can be described as a constant voltage source with equivalent series resistance (R_{on}) [10]. The voltage drop depends on the internal energy barrier required for the photons of light to be emitted, as described earlier. Due to changes in production, the voltage drop is not constant and may vary by ± 10% sample to sample. The temperature increase in the junction enables electrons to pass the energy barrier (band gap) easier. This causes the

decrease of voltage drop across the diode, about 2 mV per degree with increasing temperature.

Driving LEDs with a constant voltage source is very difficult, because it is only the difference between the supply voltage and the load voltage, which is dropped across the series resistance R_{on}. The value of R_{on} is usually small. For low-power LEDs, R_{on} value is about 20 ohms. However, high power LED of 350 mA has about 1-2 ohms of R_{on}. This means that the difference of 1V power supply implies an increase in a current of 1 ampere. Therefore, the LED is not controlled by voltage regulators but, use current source instead. In the simplest applications, a resistor is connected in series to limit the current. Such a circuit is sensitive to changes in supply voltage and temperature. Using this method, the LED cannot be operated with maximum possible current. Moreover, the voltage drop across the resistor causes energy losses. This solution is applied when a diode is used as an indicator. Active current control is used for proper LED power supplies. There are two solutions: linear current regulators and switched-mode power supplies (SMPS). The latter will be discussed in detail in the next section, due to the variety of configurations.

2.3.1 Linear drivers

Linear power supplies are preferred for driving LEDs for a number of reasons. Due to the linear operation, they do not emit any electromagnetic interference (EMI), what is a very significant feature in some applications. Another important commercial reason is low cost. In addition, current stabilization is very accurate. Their main disadvantage is low efficiency and hence the introduction of thermal problems. In order to solve them, heavy and bulky heat sinks have to be used. Linear driver usage is limited to applications where the supply voltage is higher than the maximum LED voltage.

Linear drivers are based on linear current sources. The current sensor is connected in series with the LED array to measure the current flow. The sensor signal is compared with a reference signal and the obtained error signal controls the power device. An example of a current source, based on the operational amplifier is shown in Figure 2.7. Diode current I_D can be adjust by changing the reference voltage V_{ref} and the sensor resistance R_S according to the formula

$$I_D = V_{ref} / R_S \tag{2.3}$$

By adjusting the reference voltage, the LED current can change also during operation.
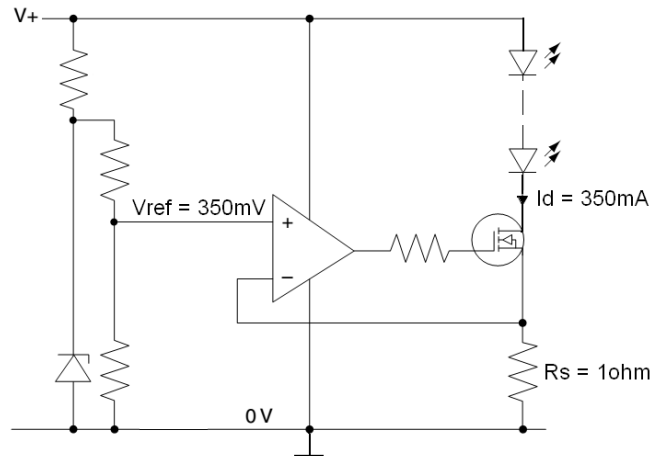
Figure 2.7 Linear LED driver [10].

During operation, there is a transistor voltage drop, which is dependent on the supply voltage and the voltage drop across the LEDs. To ensure proper operation, the minimum supply voltage must always be higher than the voltage drop across the diodes, sense resistor and the saturation voltage of the transistor. However, much higher line voltage than the voltage drop across the diodes increases the voltage across the transistor and leads to temperature problem. LEDs have a relatively long life time. Therefore, the controller should be robust and able to work under critical conditions. The LEDs may be damaged, causing an open circuit or short circuit. The driver should keep stability, detect and indicate failure. In the case of an open circuit fault, the current disappears and the LEDs stop emitting light. If the LEDs are damaged on a short circuit, then the voltage drop on the power transistor increases, which also leads to an increase of heat dissipation. The circuit must be able to dissipate the heat or turn off if the voltage exceeds a safety threshold. Such security can be achieved by using a Zener diode and two resistors. Diode's cathode is connected to the collector of the main transistor, and anode is connected to the ground by resistors. Damage of the LEDs will cause increase of the collector voltage thus leads to diode breakdown and voltage rise across resistors what will trigger protection. The circuit of protection is shown on Figure 2.8.
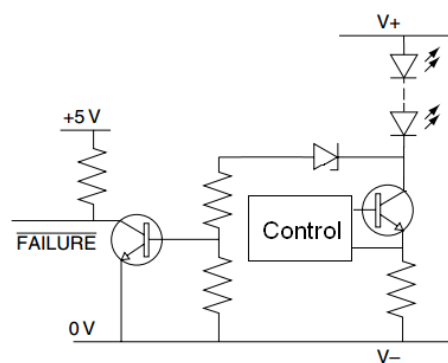
Figure 2.8 Shorted Load Indication (adapted from[10]).

2.4   Switched mode Power supplies for LED Applications

Switching power supplies are widely used to power the LED lamp [18]. Conversion of voltage and current is realized by switching reactive elements such as capacitors and inductors. Elements of the switches are semiconductor devices. For appliances of small and medium-voltage, MOSFET transistors are used most often due to lower losses and higher switching speed than bipolar transistors. Since the ideal coil, capacitor and transistor in turn on/off state does not cause the losses, the theoretical efficiency of the switching power supply is 100%. In practice, there are losses due to device imperfections, but in most cases, power supplies have a much higher efficiency than linear power supplies.

2.4.1   Controlling and topology selection

The most common method for driving the transistor is pulse-width modulation (PWM) [19]. The control signal (depicted on Figure 2.9a) is a square wave with variable pulse width and a certain, usually fixed frequency. The ratio of the pulse width to the signal period is defined as by the duty-cycle

$$D = \frac{t_{ON}}{t_{ON} + t_{OFF}} = \frac{t_{ON}}{T} \tag{2.4}$$

where T is the period of the duty-cycle of the drive signal and the t_{ON} and t_{OFF} means respectively the time when the transistor is turned on and off. By changing the duty-cycle, the operation of the inverter can be controlled. There are two basic modes of control: voltage-mode control and current-mode control. Theirs circuits are depicted in Figure 2.9b,c.

In voltage-mode control, the output of the switching power supply is sampled, compared with a reference voltage and compensated using and error amplifier. Then the error voltage at the output of the error amplifier is compared to a sawtooth signal, generating the driving signal for the switching transistor. The voltage-mode control is a **single loop** control technique.

Current-mode control is consist of **multi-loop** control scheme. The outer loop is a voltage-loop, where output voltage is still sensed and compared to a reference. However, in this case, the error amplifier output provides a reference for the inner current loop. In the inner loop a current in the system is sensed and compared to the reference from the voltage loop. The error signal together with a clock signal goes to a RS flip-flop where the switching signal for the power transistor is generated.

There are several topologies of power supplies, with different features. The selection of a suitable topology depends on the application, the required power and the input and output voltage. Table 2.2 shows the main topologies, their properties and application range.

a)

t_{on} t_{off}

T T time

b)

error amplifier

voltage sense

U_{ref}

reference source

output to switching device

comparator

ramp generator

c)

CLOCK

clock generator

error amplifier

voltage sense

V_{ref}

reference source

output to switching device

S
Q
R
Latch

comparator

current sense
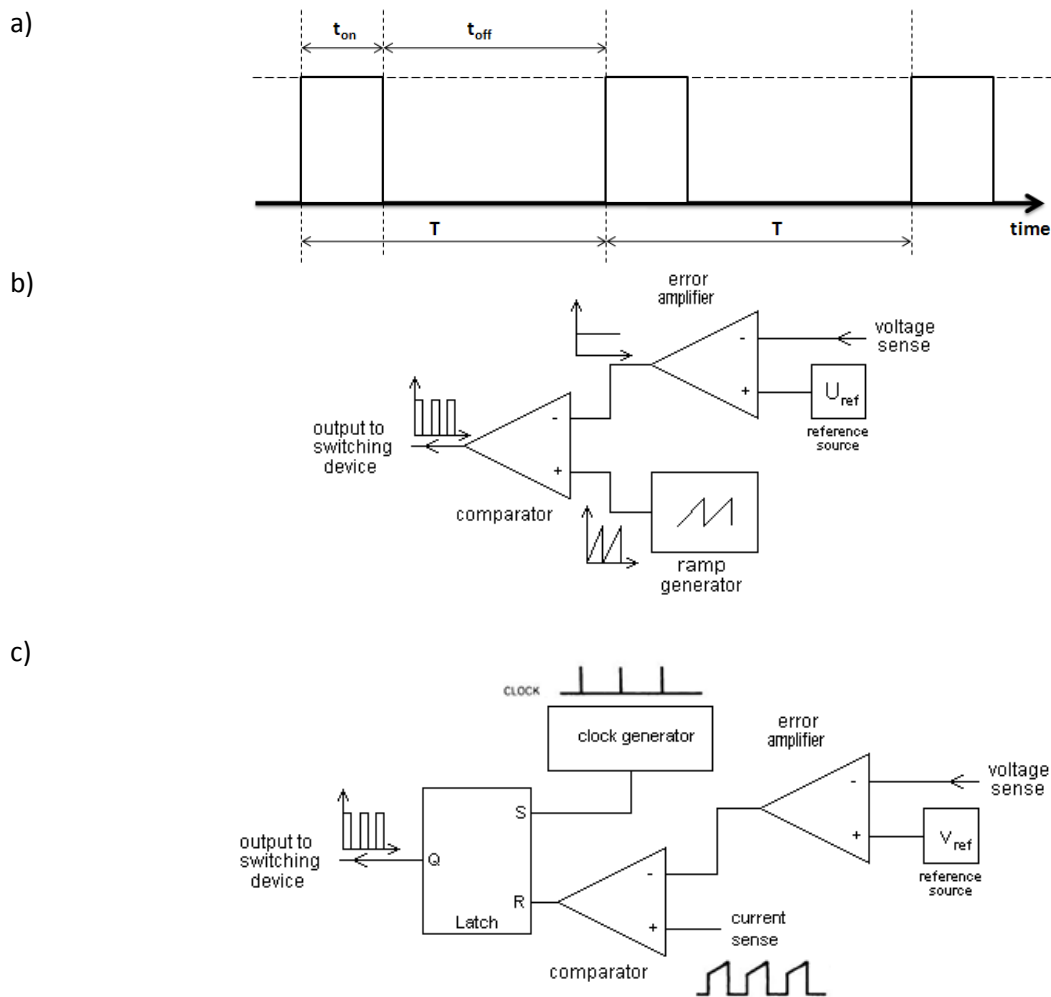
Figure 2.9 PWM signal waveform a); control mode circuits: b) voltage mode control, c) current mode control.

Table 2.2 Characteristic of SMPS topologies [17]

Topology	Power Range (W)	Vin(dc) Range	In/Out Isolation	Typical Efficiency (%)
Buck	0-1000	5-40	No	78
Boost	0-150	5-40	No	80
Buck-boost	0-150	5-40	No	80
1T forward	0-150	5-500	Yes	78
Flyback	0-150	5-500	Yes	80
Push-pull	100-1000	50-1000	Yes	75
Half-bridge	100-500	50-1000	Yes	75
Full-bridge	400-2000+	50-1000	Yes	73

Converters can be divided into two types: with galvanic isolation between input and output or without isolation. Isolation is provided by a transformer. If the converter works with voltage higher than 40VDC, topologies with galvanic isolation should be considered. In high-power converters, the energy density is too large for a single transistor. Therefore,

topologies with more transistors are used to let the transistors operate in a safe operating area (SOA). These topologies are more complicated in the operation and control. Pulsed operation at high frequency requires using fast but expensive and technologically advanced components. In addition, the SMPS is a source of broad spectrum of electromagnetic interference [20]. Electromagnetic interferences are due to the parasitic reactances of the components that cause voltage spikes and current surges. To maintain electromagnetic compatibility, it is possible to use suppression filters, a special design of printed circuit board (PCB) and varying methods of transformers winding.

The most common topologies of switching power supplies that are used for low-voltage power LED applications are circuits without isolation: Buck (step-down), Boost (step-up), Buck-bust (inverter). When the device is powered from the mains, flyback and half-bridge topologies are often employed.

2.4.2 Buck converter

Buck converters are used to reduce the voltage. A simplified schematic is shown in Figure 2.10a. The operation of the converter can be described in two steps.

a)

b)
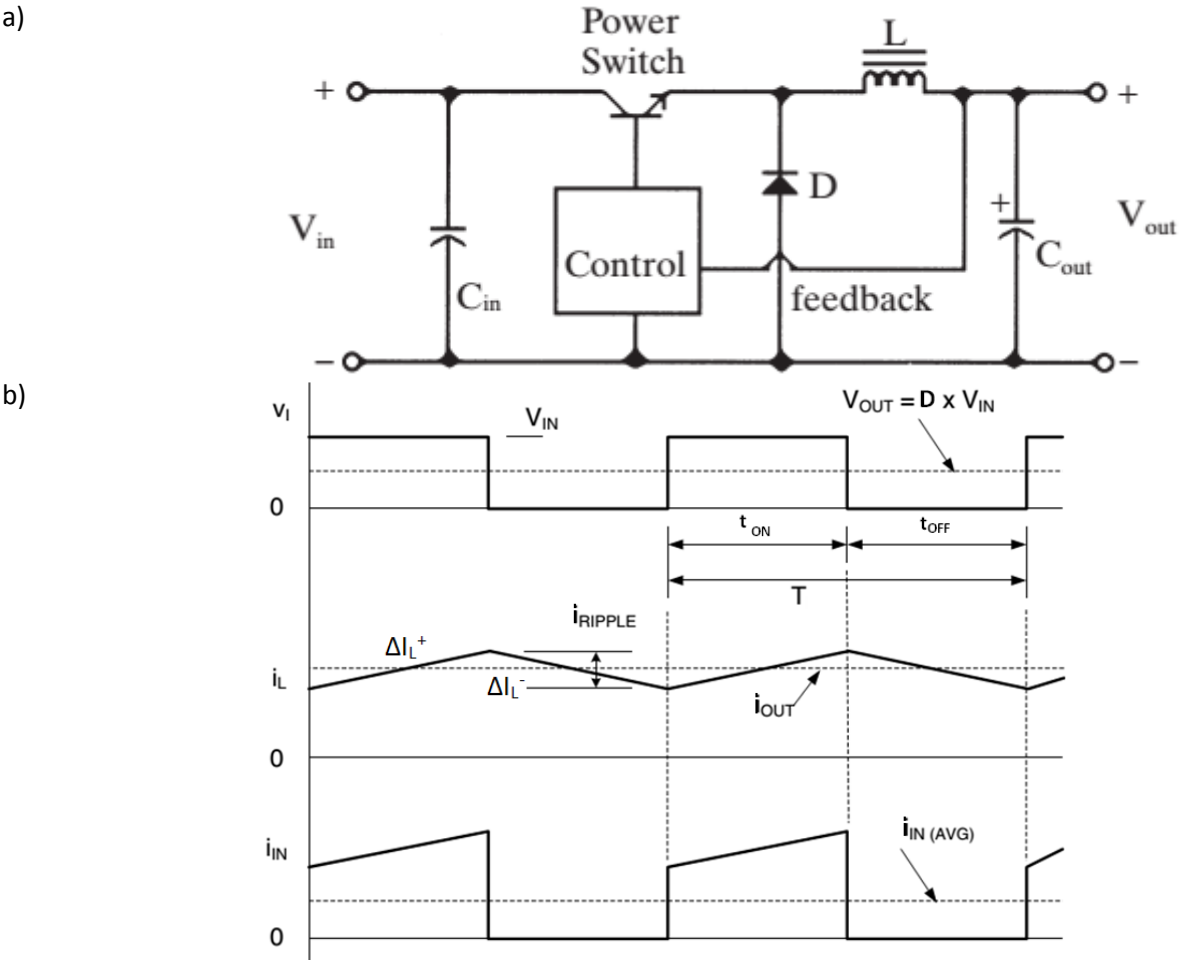
Figure 2.10 Buck converter: a) circuit, b) waveforms[17,19].

In a first step, the power transistor is conducting and the current I_L flows from the input source to the output load capacitor C_{OUT} and through the inductor L. Due to the constant voltage, the coil current increases linearly. At this time, the core of inductor accumulates energy in the magnetic field. In the next step of the power transistor is turned off. Due to the nature of the inductor, to keep the flow of current, the voltage is self-inducted in inductor. At this time, current loop is closed through the diode, and the energy stored in the inductor in the previous cycle is transferred to the output capacitor C_{OUT} and the load. Current and voltage waveforms are shown in Figure 2.10b.

The output voltage depends on the input voltage and transistor turn on time t_{ON} or otherwise duty-cycle D:

$$V_{OUT} = D \cdot V_{IN} \tag{2.6}$$

There can be distinguished two modes of operation depending on the inductor current: continuous conduction mode (CCM) and discontinuous conduction mode (DCM). In the former, the inductor current never falls to zero during the period. This means that there is always a magnetic field in the inductor core and some energy is accumulated. In discontinuous current mode during t_{ON}, the current is increasing from zero and during t_{OFF} drops to zero. This means that during one period all the energy stored in the inductor is transferred to the load.
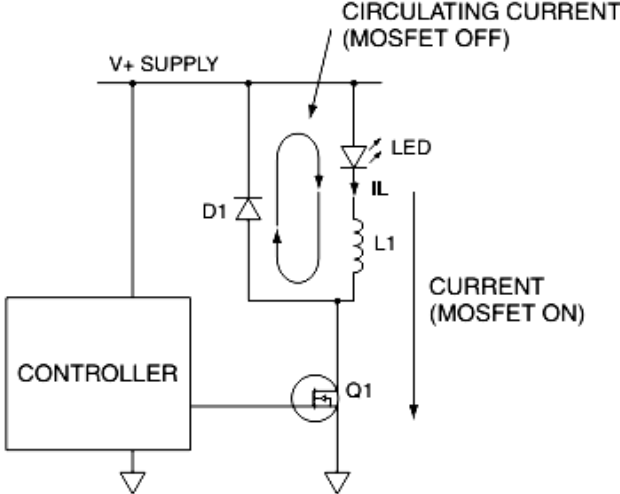
Figure 2.11 Buck converter for LED application [10].

In LED applications, the Buck converter is often used in the configuration shown in Figure 2.11. Because LEDs are current-controlled, the output capacitor can be canceled. At the time when the power transistor is switched off the current circulates in the loop formed by the LED, the inductor and the free wheel diode.

2.4.3 Boost converter

Boost converters are used in applications where the input voltage is lower than the voltage required at the output and the voltage must be increased. This type of converter is often used in battery application because the battery voltage is relatively low and depends on battery's charge level. The Boost converter diagram is shown in Figure 2.12a.

a)

b)
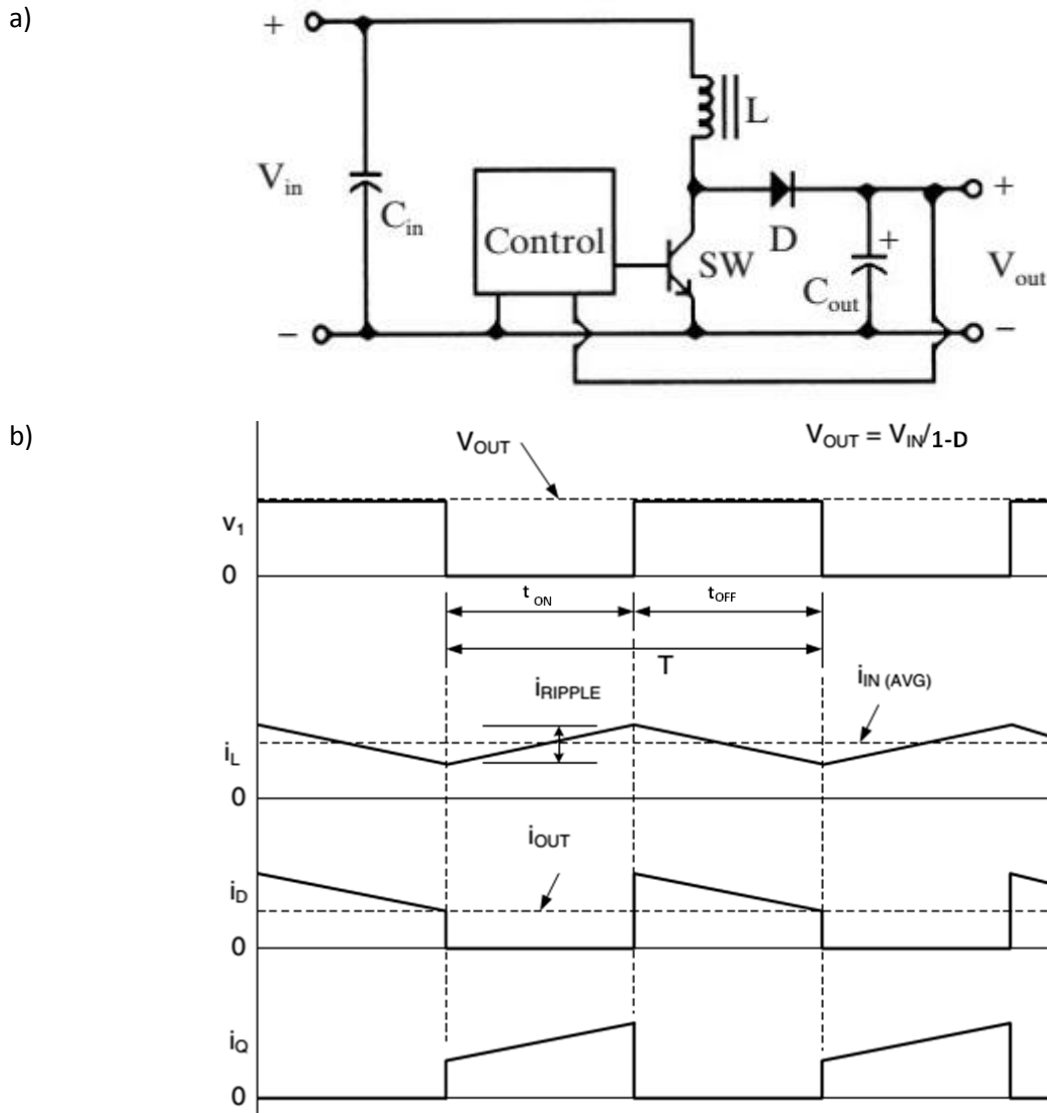
Figure 2.12 Boost converter: a) circuit, b) waveforms[17,19].

The operation can be described in two steps. In the first step, during ton, the inductor is shorted to ground through the switch. At this time, the inductor current I_L is increases linearly. Energy is stored in the inductor core. The load is supplied by the energy stored in the capacitor C_{OUT} from previous period. In an instance of open the switch, current flow path is closed. This leads to the voltage self-induction in inductor to allow continued flow of current. The voltage at the transistor increases to

$$Vsw \ = \ Vout \ + V_f$$

(2.6)

where V_f is the forward voltage diode D. This allows current to flow through C_{OUT} and the load. Equation 2.7 describes transfer function of Boost converter.

$$V_{OUT} = V_{IN} \frac{1}{1 - D}$$ (2.7)

Waveforms of boost converter in CCM are shown in Figure 2.12b. The Boost converter may also be operated in DCM, in the same way as in the buck converter.

2.4.4 Buck-Boost converter

The Buck-Boost converter possesses features of the two previously described converters: the output voltage may be higher and lower than the input voltage. However, it is in opposite polarity with respect to the input voltage. That is why it is also called the inverting converter. Figure 2.13 shows a schematic of a buck-boost converter (a) and waveforms during operation in CCM mode (b). At t_{ON}, the current I_L flows through the switch and the inductor to ground and the energy accumulates in the inductor core. When the switch turns off, a voltage is inducted in inductor. Since one end of the inductor is connected to ground, negative voltage appears at the second end to maintain current flowing. The inductor current decreases linearly and flows through the diode and inductor to the capacitor C_{OUT} and to load. In result the negative voltage appears on output according to formula

$$V_{OUT} = -V_{IN} \frac{D}{1 - D}$$ (2.8)

2.4.5 Flyback converter

This type of converter is widespread in the market due to the simple construction and control, a relatively wide range of power and output voltages and relatively low cost [21].The Flyback is based on Buck-boost topology but it provides galvanic isolation, due to the use of a transformer. The transformer consists of a primary winding with Np turns and secondary winding with Ns turns. The transformer turns ratio is equal to Np / Ns. Contrary to the normal transformer, the flyback transformer is inherently an inductor that provides energy storage, coupling and isolation. In the general transformer, energy is transmitting in one step and the current flows in both the primary and secondary winding at the same time. However, in the flyback transformer, energy transmission proceeds in two steps. In first, the current flows only in the primary winding while the energy is stored in the core. In the second step current flows in the secondary winding while the energy in the core is released [31]. Therefore, the transformer core acts as energy accumulator. Usually air-gap is introduced between the core halves to increase the energy storage capacity. The important thing is that the windings are reversed coupled. Schematic and voltage waveforms are shown in Figure 2.14.

a)
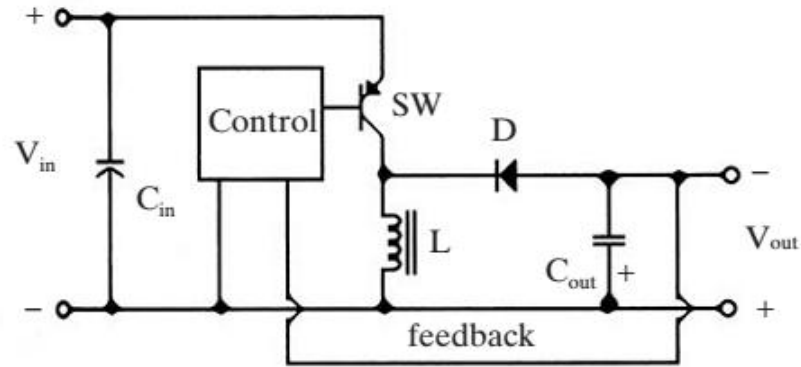
b)
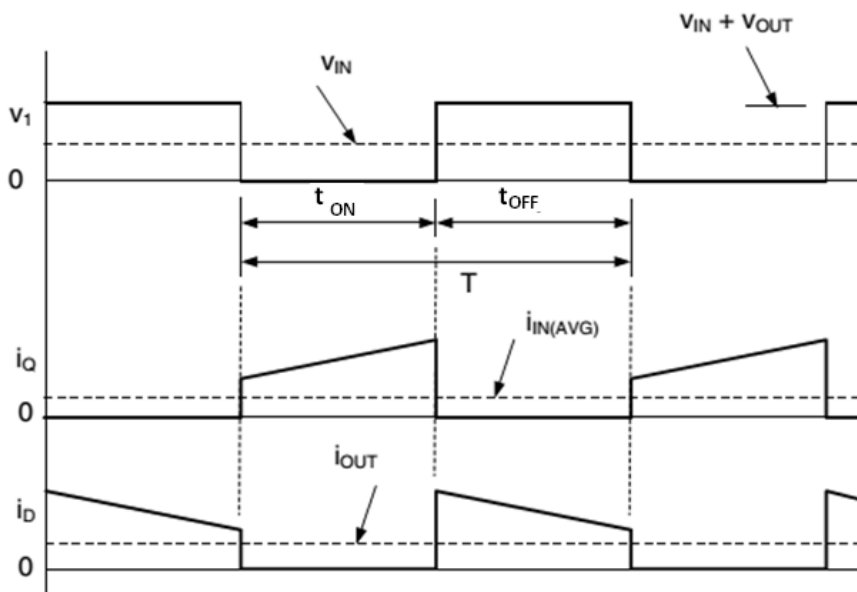
Figure 2.13 Buck-Boost converter: a) circuit; b) waveforms[17,19].

In the first step, the transistor is conducting and the current flows through the primary winding increasing linearly. The energy is stored in the transformer core. At this time, the diode on secondary side is reversed and the energy is transferred to the load from the capacitor C_{OUT}. In the next step, the transistor is off preventing current flow in the primary winding. Because reversed coupling of windings, the energy is stored in the core is transformed and transmitted by the secondary winging and to the positively biased diode to the capacitor C_{OUT} and output. The transfer function of flyback in CCM mode is stated as

$$V_{OUT} = V_{IN} \frac{Ns}{Np} \frac{t_{ON}}{t_{OFF}}$$

(2.9)

23

a)
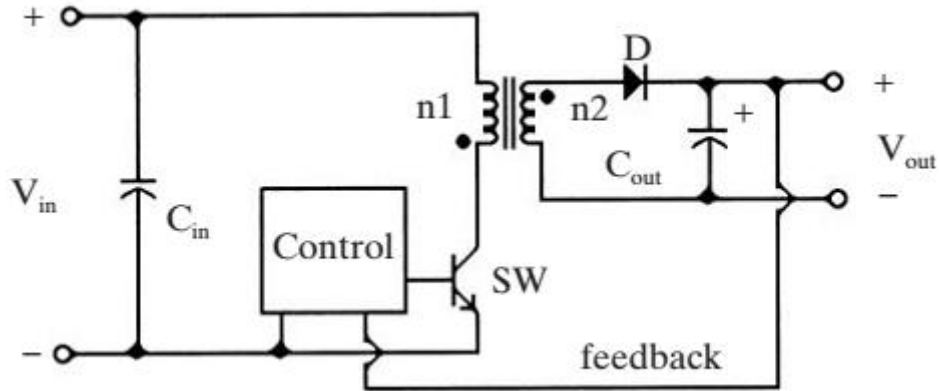
b)
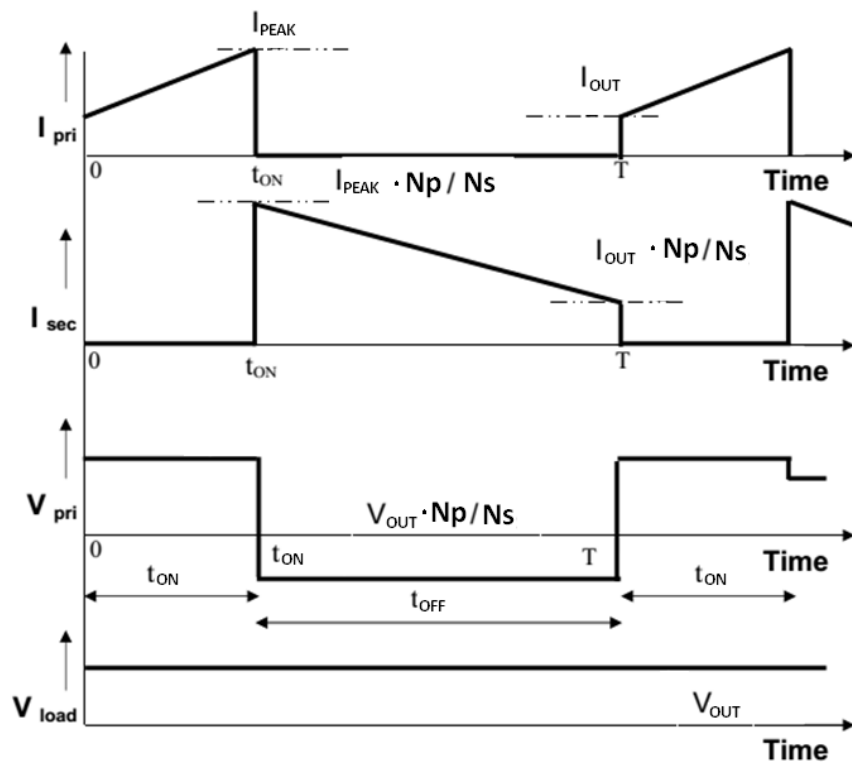
Figure 2.14 Flyback converter: a) circuit, b) waveforms[17,19].

2.4.6 Half-bridge converter

This topology is used for applications with higher power in the range of 150-500W. It is more complex than the ones previously discussed. The topology diagram is shown in Figure 2.15. The transformer has one primary winding with Np turns and one winding with tap with Ns turns on each section. Two capacitors are in series between the supply voltage and the ground. They divide input voltage in a half. The primary winding is connected at this mid-point. The second end of the winding is connected between the two push-pull transistors: the high side is connected to the power supply line and a bottom is connected to ground. During operation, the transistors are switched alternately causing an alternating current in the primary winding. On the secondary side is a full-wave rectifier using a center tap winding and two diodes. Choke and output capacitor creates a filter and store energy. Duty-cycle

control signal is divided in half for each transistor. The output voltage is defined by the formula

$$V_{OUT} = \frac{1}{2} \cdot V_{IN} \cdot D \cdot \frac{Ns}{Np} \qquad (2.10)$$
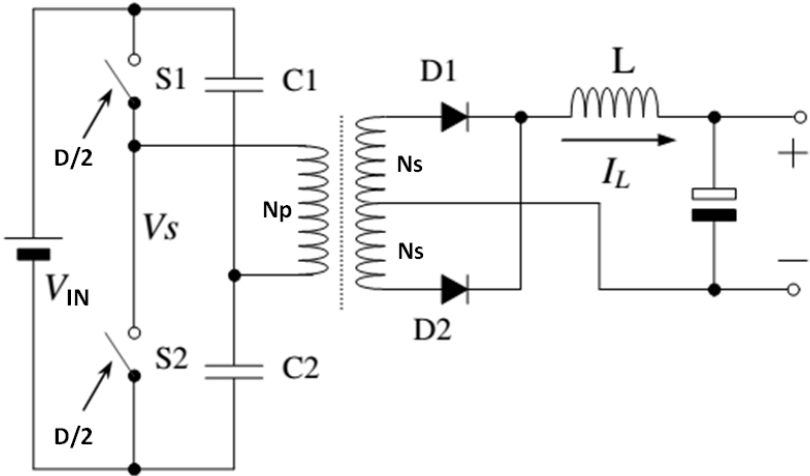
Figure 2.15 Half-bridge converter circuit [17].

The waveforms of voltages and currents are shown in Figure 2.16
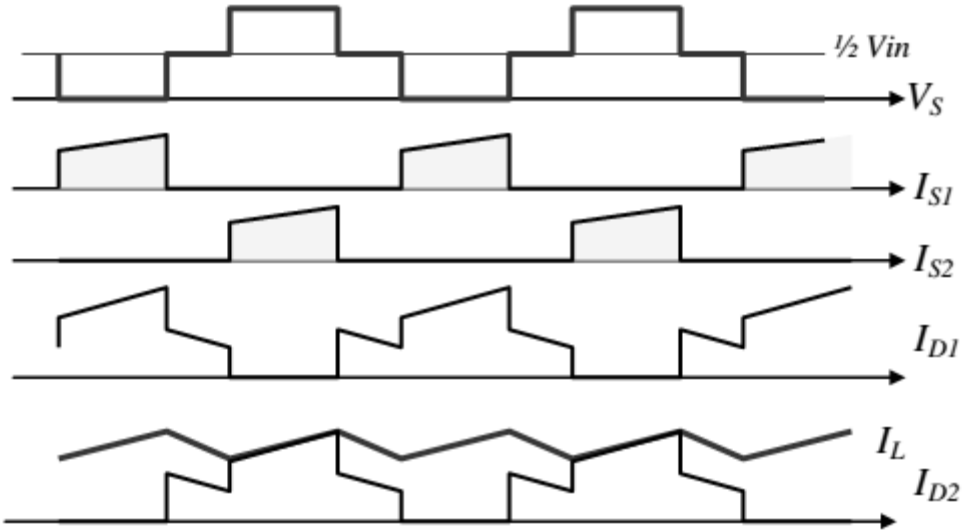
Figure 2.16 Half-bridge converter waveforms [17].

2.5 Power factor correction

Electrical devices drawing energy from the power line present complex impedance consisting of resistance and reactance. All devices, different from pure resistance, draw from the power line more energy than they use. This is very important for energy production and transmission, because it forces to supply more energy than the energy actually required. The Power Factor (PF) is a measure of how energy is efficiently used. It represents the real part of the complex power [22].

In a simple alternating current (AC) circuit consisting of a source and a linear load, both the current and voltage are sinusoidal. The power factor is defined as the cosine of the phase angle between the voltage and the current, or as the ratio of active power to apparent power (formula 2.11). The ideal value is 1 thus the current and voltage are in phase, which is the most efficient use of energy.

$$PF = cos\varphi = \frac{P}{S} \tag{2.11}$$

The apparent power S is drawn from the grid. The real power P is part of the apparent power, and is consumed by the device to carry the work. The reactive power Q is the energy that the device draws from the power line and circulates in the circuit but it is not used to perform useful work. The apparent power is the vector sum of real and reactive power or root mean square of the two of them. This can be represented by the power triangle (Figure 2.17). The angle φ defines a phase shift between voltage and current [23].
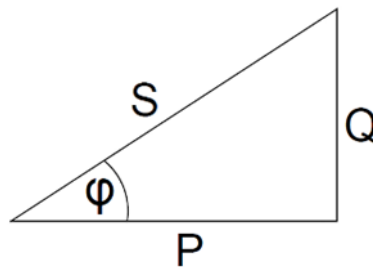
Figure 2.17 Power triangle.

The previously-stated definition of power factor related to phase angle is valid when considering ideal sinusoidal waveforms for both current and voltage. However, most power supplies draw a non-sinusoidal current. When the current is not sinusoidal and the voltage is sinusoidal, the power factor consists of two factors: 1) the displacement factor ($K\varphi$) related to phase angle and 2) the distortion factor (Kd) related to wave shape. Equation 1 represents the power factor as the relationship of the displacement and distortion factor[23].

$$PF = \frac{Irms(1)}{Irms} \cdot cos\varphi = Kd \cdot K\varphi \tag{2.12}$$

Where Irms(1) is the Root Mean Square (RMS) value current's fundamental component and Irms is the current's RMS value. When the power factor is not equal to 1, the current waveform does not follow the voltage waveform. This results not only in power losses, but may also cause harmonics that can disrupt other devices connected to the line. The closer the power factor is to 1, the less the current harmonics will be and more power will be contained in the fundamental frequency. Therefore, the purpose of the power factor correction (PFC) circuit is to minimize the input current distortion and make the current in phase with the voltage.

In a typical switched-mode power supply without power factor correction the first stage, without the input EMI filter, is a full wave rectifier with capacitor C_{IN} as shown in Figure 2.18a [24]. The purpose of the capacitor is to smooth voltage ripple on the output. Current and voltage waveforms are shown in Figure 2.18b.

a)

b)
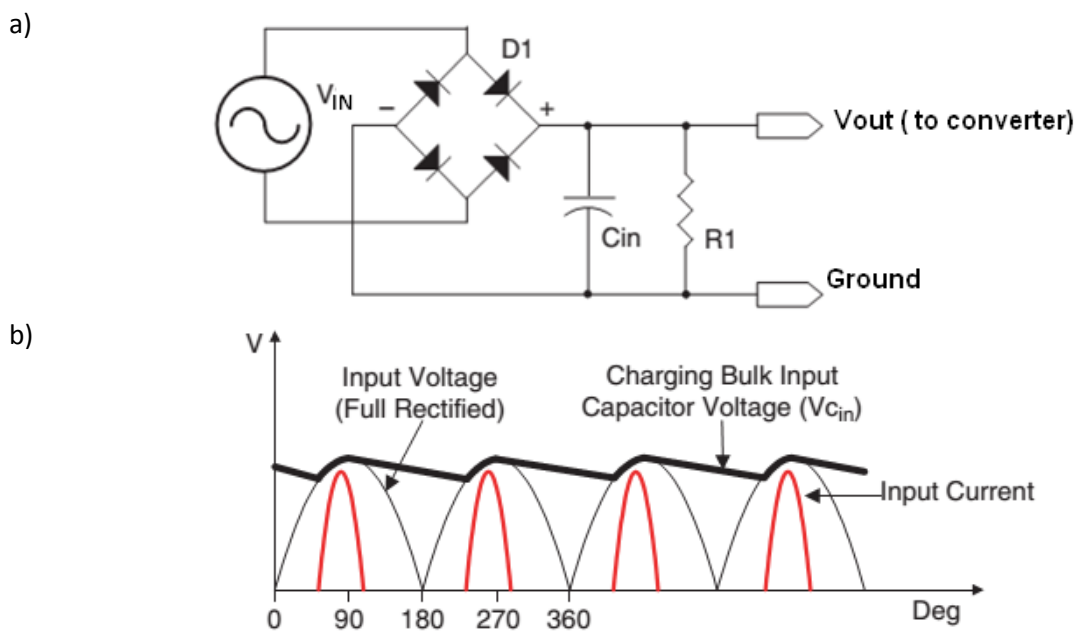
Figure 2.18 a) Full wave rectifier circuit and b) voltage and current waveforms[23].

Most of time, the energy is transferred from the capacitor to the load and the capacitor voltage decreases. This capacitor is charged when its voltage is less than the input voltage. It is so only for a short time, when the input voltage is close to the peak voltage Vpeak. In this small period, the capacitor is charged to the peak voltage. This leads to very high current surges from the power supply line. All the circuitry in the supply chain must be capable of carrying this huge peak current. Since the current is not sinusoidal, it causes harmonic distortion and low power factor. To improve this situation, it should be provided continuous current flow during the AC mains waveform. Power factor connecting circuits can be divided into passive and active topologies.

27

2.5.1 Passive power factor correction

Passive methods for PFC use additional passive components in conjunction with the diode bridge rectifier and form filters. Passive filters can broadly be classified into series filters, shunt filters, and a hybrid combination of the two. Series filters introduce an impedance in series with the utility to reduce harmonic currents. Shunt filters provide a low-impedance path for the harmonic currents generated by the rectifiers so that they are not reflected in the current drawn from the utility [25]. One of the simplest methods of passive PFC is to add an inductor at the AC-side of the diode bridge, in series with the line voltage as shown in Fig. 2.19a. The line current has Kd = 0.888, $\cos\varphi$ = 0.855. The maximum power factor that can be obtained by this configuration is 0.76 [24].

a)

b)
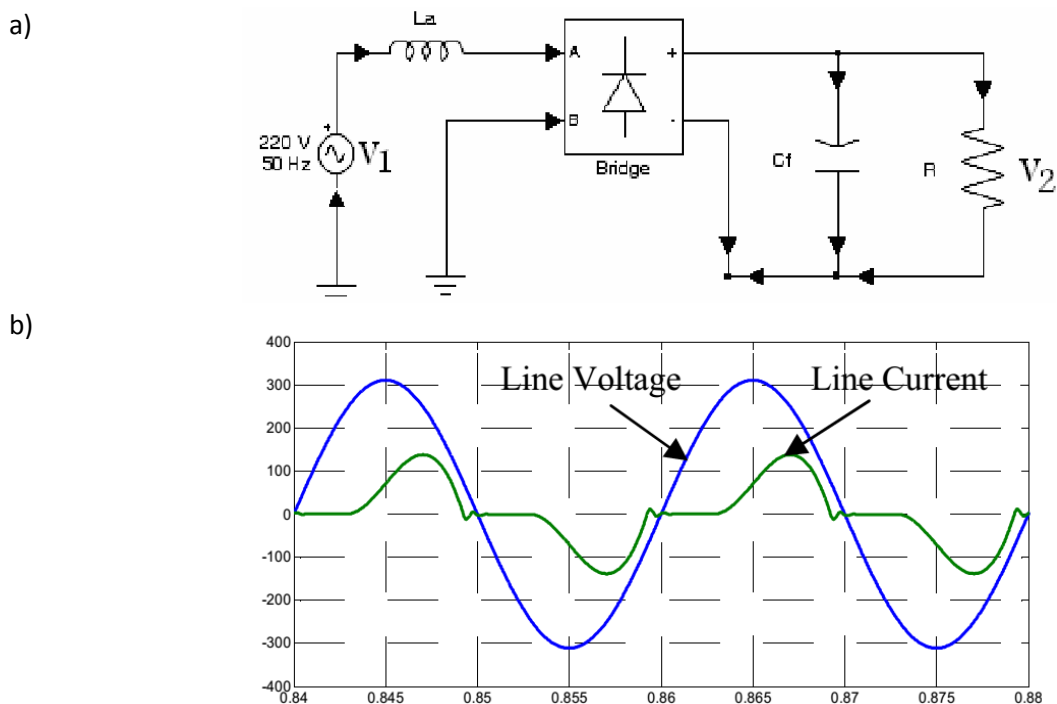
Figure 2.19 Passive PFC with AC-side inductor: a) circuit; b) Line voltage and line current with resistive load R=500Ω, Cf=470µF and La=130mH [24].

Another example of a passive PFC circuit is to connect in series a capacitor and one inductor at the AC-side of the diode bridge, in series with the line voltage as shown in Figure 2.20a. The inductor and capacitor creates a resonant circuit at the frequency of the power line. From the waveforms depicted in Figure 2.20b can be seen that the shape of the current is close to sinusoidal. The line current has a Kd = 0.993, $\cos\varphi$ = 0.976 and PF = 0.969, and output voltage is V2 = 250V.

a)

b)
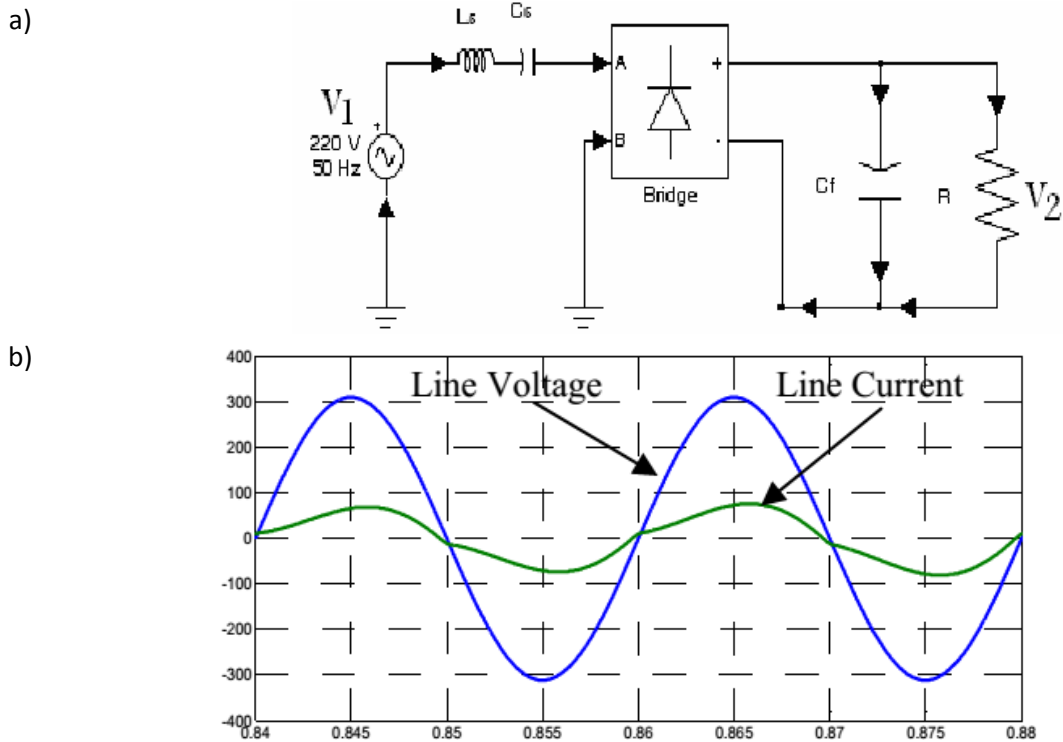
Figure 2.20 Rectifier with series-resonant band-pass filter: a) circuit; b) line voltage and line current with V1=220Vrms, resistive load R=500Ω, Cf= 470μF, Ls= 1,5H and Cs=6,75μF [24].

Passive methods for power factor correction have certain advantages, such as simplicity, reliability and ruggedness, insensitivity to noise and surges, no generation of high frequency electro-magnetic interface (EMI). However, they have several significant drawbacks. Solutions based on filters are heavy and bulky, because line-frequency reactive components are used. They are designed for specific load hence performance can vary for different loads. They also have a poor dynamic response and lack voltage regulation.

2.5.1 Active power factor correction

The active PFC is based on the switched-mode devices. There are placed between the input rectifier and the storage capacitor. The PFC controller monitors the main voltage, switch current and output voltage accordingly. It drives the power transistor so, that the average value of the pulsating current should follow the input voltage in both shape and phase. The most popular topology in PFC applications is the boost topology, showed in Figure 2.21 [27]. It is not the only type, however.
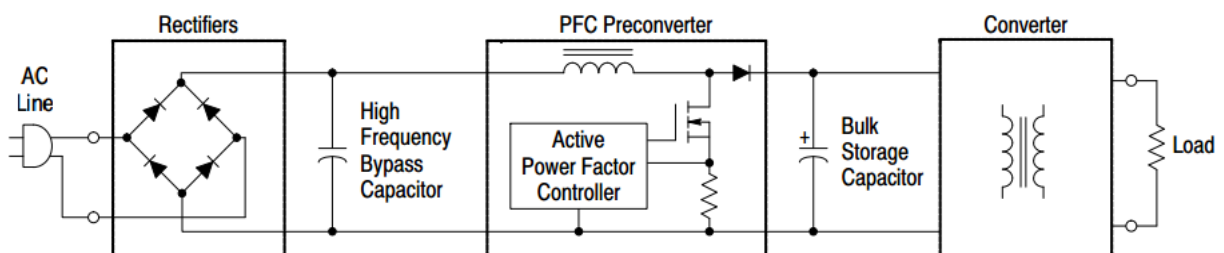
Figure 2.21 The PFC application based on boost topology [22].

Regarding the power factor correction stage, the boost converter is widely used because of its advantages. It allows low-distorted input currents and almost unity power factor. Moreover, it offers high efficiency, around 95%, and the ground-connected switch simplifies the driver circuit. There are also some drawbacks to this solution. The output voltage is always higher than the peak input voltage. There is high current during start-up, due to the charge of the large output capacitor. Furthermore there is a lack of current limitation during overload and short circuit conditions, due to the direct connection between line and load [27] [28].

One can distinguish two main control strategies of boost PFC circuit: CCM and DCM. In fact, the real DCM is rarely used. Instead of DCM most control circuits operate in a mode known as the boundary current-mode (BCM) or critical conduction-mode (CrCM), which is a special case of DCM where the inductor current never stays at the zero current.
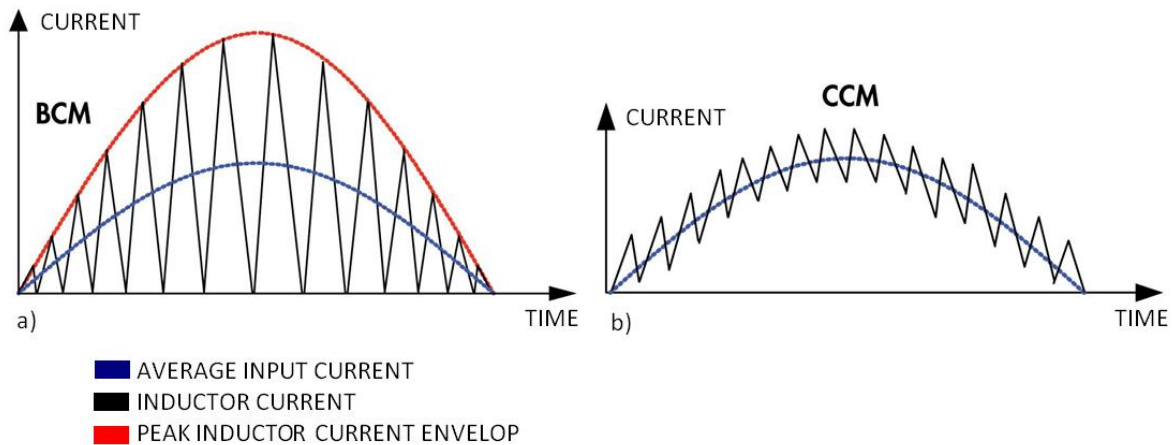
Figure 2.22 Current waveforms in boost PFC circuit: a) boundary conduction mode; b) continuous conduction mode [30].

The main advantage of BCM is that the control method and the implementation is simple [29]. It consists of a controller that turns on the power switch until inductor current reaches the upper limit. Then, the switch is turned off until the inductor current just reaches zero. Then the cycle starts over again, repeating at a relatively high frequency. It is showed in Figure 2.22a. The upper limit is given by a varying reference voltage that fallows the rectified line voltage in shape. Its magnitude is increased or decreased depending on output bus voltage. The characteristic features for BCM are: 1) power transistor has zero-current turn-on therefore reduced switching loss; 2) switching frequency is variable and depends on instantaneous main voltage and 3) there is high input ripple current and high RMS current. The latter ones limit BCM PFC applications for relatively low range of power. In addition, an input filter has to be added to meet EMI requirements.

For higher-power applications, the CCM approach is used. This configuration operates mostly with fixed switching frequency. During the period, the inductor current increases and decreases linearly, but its average value follows the rectified line voltage in

30

shape. The inductor current reaches zero only when the line voltage crosses through zero. Current waveforms are shown in Figure 2.22b. Traditional CCM controllers are based on an analog multiplier, which scales the reference signal [29]. The reference signal is obtained from several control loops, each with their own compensation network. This makes the design more difficult and complex. The transistor in CCM is hard-switched. It means that current flows by the transistor during switching. It incurs switching losses. However, RMS current is lower in contrast to equivalent BCM design what means less conduction losses. In CCM configuration, current has small ripple what cause better power factor and electro-magnetic compatibility.

3. Design Considerations

Before starting project development, the initial requirements of the project were indentified. The next step consists of the search and analysis of existing solutions. The review of applications and technologies available on the market brings many answers and narrows down the scope of search. Available catalogs and component samples from manufacturers were a precious help in this stage. After selecting the topology and settle a development, the time came for a detailed analysis of the circuit. Each topology has its own features and points at which particular attention should be paid. It was necessary to explore thoroughly the mechanisms of operation and identify the weaknesses. The next step was to find methods to improve the operation of the devices. Datasheets and numerous publications and reports are a great source of knowledge to learn practical solutions commonly used in the electronic industry.

3.1 Architecture selection

The aim is to design a power supply controller for LED lighting module. A digital system should be employed to control operation based on signals from sensors. The controller should be suitable to supply the set of two LED modules STARK-LLE24-1250-840-CLA, which are available in the laboratory. Each module consists of two separate lines made of 11 LED diodes of 0,5W. Due to supply from power line, it is necessary to use galvanic isolation to separate the device. The power range is less than 40W. Flyback converter is seems to be an appropriate choice. However, adequate stabilization of the current for the LEDs and lighting control would be difficult to achieve using only the flyback converter. Therefore, it was decided to use an additional switched-mode LED driver in Buck topology. In addition, to improve the performance and adapt the device to the needs of main power it was decided to use active power factor correction. The flyback converter provides a reduction of supply voltage and galvanic isolation, while Buck controller stabilizes the LED current. The microcontroller collects and analyzes signals from the environment and controls the operation of Buck driver.

LEDs are characterized by theirs high efficiency, unfortunately, they require a driver that stabilizes the current. Each functional block leads to losses that affect the efficiency of the overall system. Therefore, the main requirement posed in the project is to provide the highest possible performance of each block of the developed system. To improve the device, it is required to analyze the main source of losses in the circuit and methods to prevent their occurrence. One of the main sources of losses in SMPS are switching losses on semiconductor devices. They result from the fact that during the transistor switching there is a voltage drop. The idea is to reduce the switching losses of the transistor by switching it when there is no current flow: zero current switch (ZCS); or the voltage drop is zero: zero voltage switch (ZVS). To achieve this, resonant circuits are used. The secondary-side rectifier is another place where energy is dissipated. There is always a voltage drop on the rectifier

diodes. Current, which flows through diodes, causes power dissipation. Using Schottky diodes with a smaller voltage drop reduces losses. Another way is to use a MOSFET transistor. When transistor is fully opened, its channel is characterized by a certain, small resistance R_{DSon}. Therefore, the voltage drop R_{DSon} depends only on the drain current I_D and the resistance of the channel R_{DSon}. Switching transistors must be synchronized with the operation of the converter. This type of circuit is called a synchronous rectifier and in some cases can be more effective. In the flyback converters, a transformer is a specific element. During operation, energy is stored in its core. Unfortunately, due to the parasitic leakage inductance of windings, not all the energy is transferred to the secondary side. Some part of this energy is wasted. A better solution is to recycle it back to the power source.

Unfortunately, devices with very high efficiency are also very complex and technically advanced. Since this project was achieved under academic conditions, several possible difficulties had to be considered. In paper [26], the author compares the high performance resonant half-bridge converter with quasi-resonant flyback converter with two switches. It follows that the flyback converter in this configuration can achieved efficiencies above 90% over a wide load range. This was a particularly important feature for the targeted objectives. Careful design consideration assured that the solution meets the design requirements, with many advantages, and feasible construction. The components were available at the stock, and the cost was not a barrier. The entire system is based on the IC FAN6920. An interesting feature is that this Integrated Circuit (IC) contains in its structure combined PFC and quasi-resonant flyback controller. In addition, the manufacturer provided the documentation with detailed operating description. Therefore, it was decided to use this IC.
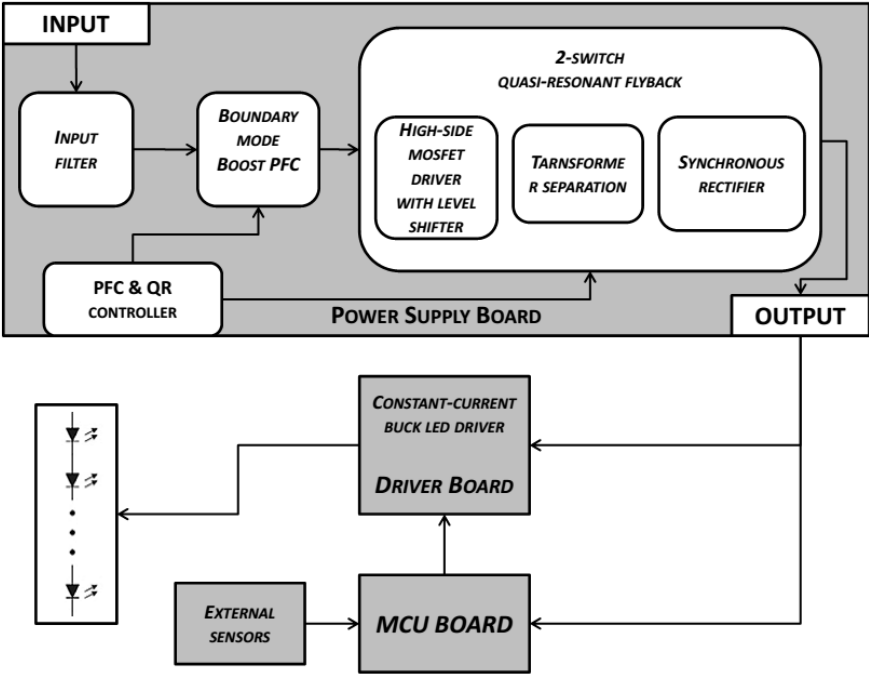
Figure 3.1 Block diagram of developed project.

After choosing the configuration an IC, a module diagram was set (Figure 3.1). The project was divided into three boards: power supply board, Buck LED driver board and microcontroller board. Mains voltage is connected to the power supply board. The first block is the input EMI filter. The next block is the PFC circuit, which supplies voltage for the flyback quasi-resonant converter. The structure of the converter can be divided into sub-circuits: high-side MOSFET driver, separation transformer and synchronous rectifier. The PFC block and flyback converter are managed by one controller. The flyback converter provides power to the LED Buck driver and microcontroller board. The LED driver supplies the LED module with the necessary current. The microcontroller (MCU) collects signals from external sensors, and based on it, establishes the dimming signal strategy of the LED driver. This provides sufficient light intensity. Detailed information on the construction, operation and project development will be discussed in the following sections.

3.2 Flyback converter operation detailed

Conventional flyback converter uses a single MOSFET switch, which is referred to the ground. Owing to this, the MOSFET drive circuit is simple and effective. However, this approach involves a voltage stress during operation. As mentioned in the previous section, the energy transfer takes place in two steps, and the transformer acts as storage element. The transformer windings are coupled causing that the voltage of each side is reflected to the another. (Figure 3.2).

a)

b)

$$V_{SW} = V_{IN} + V_{OUT} \cdot \frac{Np}{Ns} + V_{SPIKE}$$
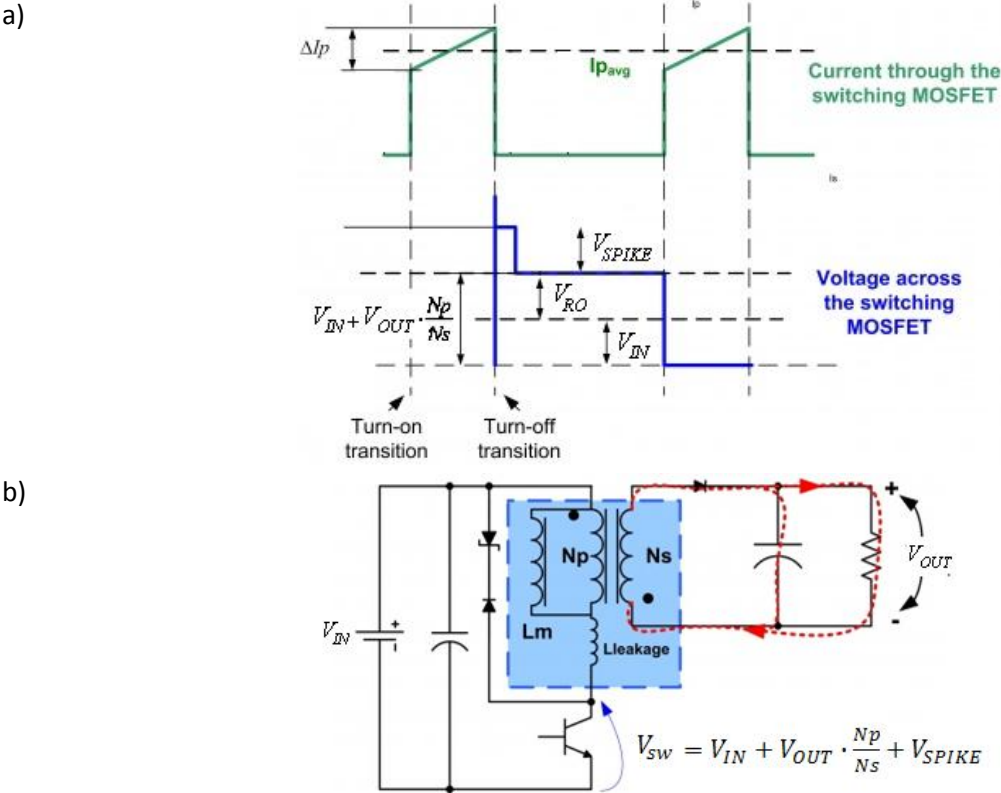
Figure 3.2 Voltage reflection and leakage inductance in flyback converter: a) waveforms b) circuit [32].

35

When the switch is turned on, in the primary winding, voltage drop is approximately equal to the input voltage V_{IN}. At this time, the secondary-side diode is reverse biased with voltage

$$V_D = V_{OUT} + V_{IN} \cdot \frac{Ns}{Np}$$

(3.1)

where V_{OUT} is the output voltage, and Np and Ns is the turns of respectively the primary and secondary windings. In the second step the situation reverses. When the switch is turned off and current flows in the secondary winding, the voltage on the switch is equal to the sum of the input voltage and the voltage reflected from the secondary side V_{RO}

$$V_{sw} = V_{IN} + V_{RO} = V_{IN} + V_{OUT} \cdot \frac{Np}{Ns}$$

(3.2)

This means that the voltage on the switch can reach high values, depending on the transformer turn ratio and output voltage. In a real application, the windings of flyback transformer are not coupled ideally. The leakage inductance is formed as a part of the primary inductance that is not mutually coupled with the secondary inductance [32]. Unfortunately, the energy stored by the leakage inductance in the transformer will not be transferred to the secondary and to the load. This energy need to be dissipated somehow. Moreover, during switch commutation, the leakage inductance is source of voltage spikes and resonance with parasitic capacitance of switch and transformer. There are two methods to dissipate leakage energy. One of them is to use a snubber circuit consisting of a capacitor, a resistor and a diode, which suppress voltage spikes and damps resonance. However, energy is transformed into heat. The second method is to clamp voltage spikes, which allows to recycle energy.

3.3   Two-switch quasi-resonant flyback converter approach

Due to the increasing demand for energy and environmental issues, the electronic devices are required to be more and more efficient. This presents a high challenge for designers of power supply circuits. In order to meet them, the resonant circuit and soft-switching techniques are used. However, they are complex and can cause problems in designing. Two-switched quasi-resonant (QR) flyback converter is a solution, which, as a flyback converter, has a simple structure, and uses several additional components to improve performance and efficiency. Adding a high-side MOSFET switch to the conventional flyback power converter, design brings benefits, especially in higher input-voltage applications. In two-switch approach, the leakage energy is recycled back to the input what improves efficiency and cancels need for a snubber circuit. It also reduces voltage stresses on the MOSFET switch due to clamping of the switch voltage to the input voltage.

The two-switch flyback converter is depicted in Figure 3.3. The secondary side is similar to conventional flyback converter. On the secondary winding of transformer T_r, there are a rectifier diode D_{OUT} and output filter capacitor C_{OUT}. The primary side consists of two

MOSFET switches, two clamping diodes and the primary winding of T_r. In the primary circuit, the original MOSFET switch Q_1 (called low-side transistor) remains in series between the low side of the transformer and input return. An added transistor Q_2 (high side) is in series between V_{IN} and the high side of the transformer primary. Clamp diodes D_1 and D_2 are placed between the low side of the primary winding and input return, and between V_{IN} and the high side of the primary winding, respectively.
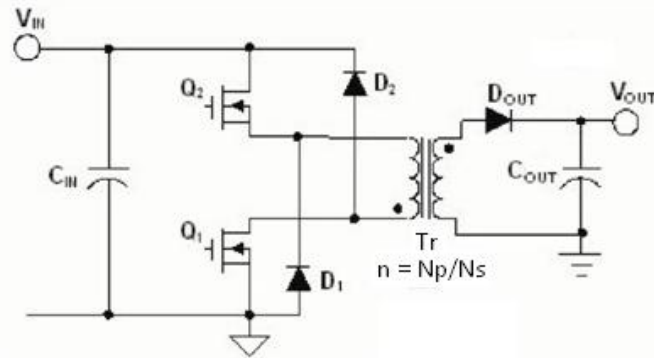
Figure 3.3 Two-switch flyback converter circuit [33].

The two-switch flyback can be operated in either discontinuous or continuous conduction mode just like the single-switch flyback converter. However, quasi-resonant operation is based on discontinuous conduction mode or on boundary conduction mode.

Operation of two-switch quasi-resonant flyback converter can be described in 4 phases (Figure 3.4). Both MOSFET switches are operating simultaneously. In phase 1, when Q_1 and Q_2 are turned on, current flows from V_{IN} to primary ground through switches and primary winding. Energy is supplied to the transformer core. In this time, the sum of input voltage reflected to the secondary side and the output voltage is applied across the secondary-side rectifier. During the commutation of switches (phase 2), voltage spike, caused by leakage inductance is added to V_{DS}^{nom} and clamped to input voltage by D_1 and D_2. As a result, the leakage energy is recycled back to the input to improve efficiency. The dissipative snubber circuit that often required in the single-switch approach is no longer needed. When the primary MOSFETs are turned off (phase 3), the energy is released to the secondary side. The input voltage together with the output voltage reflected to the primary V_{RO}, are imposed on the MOSFET. Thus, the maximum nominal voltage across the MOSFET V_{DS}^{nom} and diode V_D^{nom} are given as [34]:

$$V_{DS}^{nom} = \frac{V_{IN} + n \cdot (V_{OUT} + V_F)}{2} = \frac{V_{IN} + V_{RO}}{2} \tag{3.3}$$

$$V_D^{nom} = V_{OUT} + \frac{V_{IN}}{n} \tag{3.4}$$

where $n = \frac{Np}{Ns}$. When all energy is transferred to secondary side and the inductor current reaches zero, the drain-to-source voltage (V_{DS}) begins to oscillate by the resonance between the primary-side inductor and the MOSFET output parasitic capacitance with an amplitude of V_{RO} and on the offset of $V_{IN}/2$ (phase 4). Quasi-resonant switching is achieved by turning on the MOSFET when V_{DS} reaches its minimum value in valleys. This reduces the MOSFET turn on switching loss caused by the capacitance loading between the drain and source of the MOSFET [35].
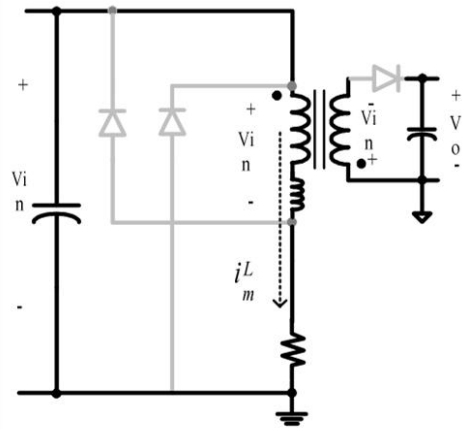
Phase 1: Q1&Q2 On

Phase 2: Q1&Q2 Off, D1, D2 on
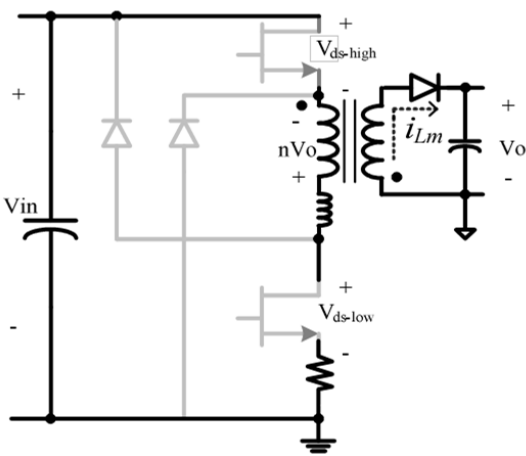
Phase 3&4: Q1&Q2 off, D1&D2 off
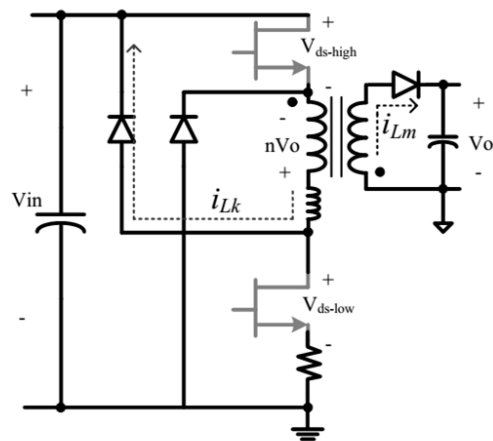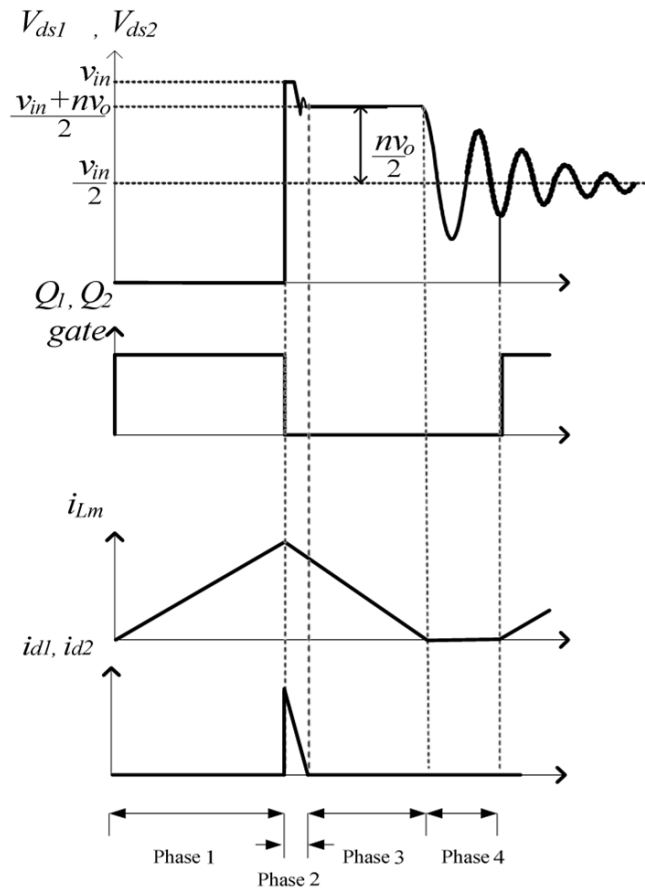
Figure 3.4 Two-switch quasi-resonant flyback converter operations [36].

38

The controller detects valleys and based on it, drives the switches. On full load, first valley is latched, and switches are turned on one moment after the inductor current reaches zero. In this situation, the converter operates in boundary condition mode. When the load is decreasing, the converter enters into green-mode. It detects the next valleys and latches on one of them, according to load conditions. As a result, the converter goes into discontinuous condition mode and the efficiency is upgraded.

In configurations with high-side switch, the control of its gate can bring a problem. When the upper-side transistor is turned on, the voltage at the source is approximately V_{IN}. The voltage at the gate must be greater than the source voltage to allow transistor conduction. It follows that the gate drive voltage must be greater than voltage V_{IN}. One of the most widely used methods to supply power to the high-side gate is to use high-voltage gate drive integrated circuit with bootstrap. Figure 3.5 describes its operation.
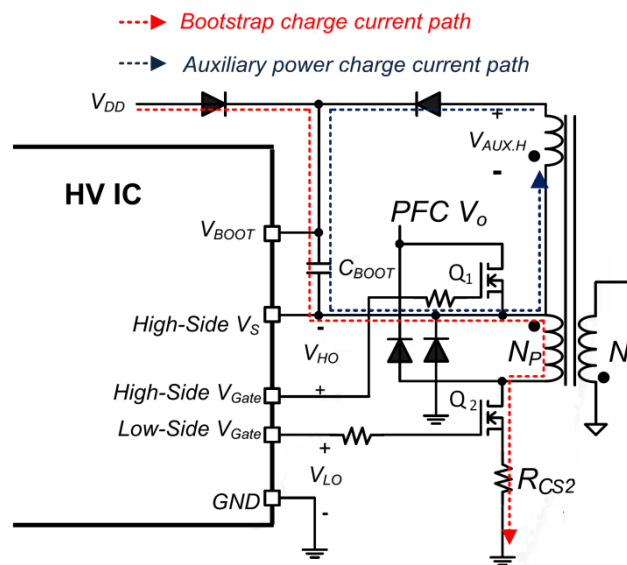
Figure 3.5 MOSFET gate driving approach for high-side switch with bootstrap technique [35].

Traditionally this method is used to drive push-pull transistors, which are driven alternately. In this case, source of high side (Q_2) switch is on floating potential. When low-side switch (Q_1) is turned on, source of Q_2 is grounded. Low voltage power supply V_{DD} charges the capacitor C_{BOOT}. When both transistors are switched, the source of Q_2 goes to input voltage potential what changes C_{BOOT} potential. As a result, C_{BOOT} boost voltage V_{BOOT} to value equal approximately V_{IN} + V_{DD}. Moreover, between Vs and V_{BOOT} is still voltage V_{DD} that supplies Q_2 gate. However, in two-switch flyback both MOSFET transistor switches simultaneously. Therefore, once the Q_2 turns on, its source V_S equals V_{IN}, the V_{DD} is not able charge the C_{BOOT}. Therefore, additional high side auxiliary winding is needed to charge C_{BOOT} capacitor and draw power for Q_2 gate.

3.4   Detailed specification and requirements

As mentioned earlier, the project had to be suitable to supply power for two LED modules: STARK-LLE24-1250-840-CLA (Figure 3.6).

Figure 3.6 LED module STARK-LLE24-1250-840-CLA [37].

According to datasheet [37], it can be shortly described in points.

- Luminous flux range 1,100 up to 1,440 lm
- Efficiency of the module up to 125 lm/W
- High color rendering index: CRI > 80
- Color temperature: 4,000 K
- life-time: 50,000 hours
- In table 3.1 the is more specific data

More detailed specification is contained in the table 3.1.

Table 3.1 Specific technical data of LED module STARK-LLE24-1250-840-CLA [37].

Typ. luminous flux	Typ. luminous flux	Typ. forward current	Min. forward voltage	Max. forward voltage	Typ. power consumption	Efficacy of the module
1240 lm	1190 lm	300mA	30,0V	36,5	9.8W	123lm/W
1410 lm	1360 lm	350 mA	30,1V	36,7V	11,6W	119 lm/W

Based on the specifications of the module STARK-LLE24-1250-840-CLA and referring to previous considerations, the detailed requirements of the flyback power supply was stated:
- device is supplied from power line and isolation is required,
- input voltage range: 220-240Vac (50 Hz) with tolerance $\pm$10%,
- main output: V_{OUT} = 42,5V, I_{OUT} = 0,7A,
- second output V_{OUT2}= 12V, I_{OUT2}= 0,1A,
- output power: 35W,
- efficiency: 81% (PFC stage: 90%, flyback stage 90%),
- PFC output voltage: V_{O_PFC} = 400 V,
- minimum PFC switching frequency: > 30 kHz,
- minimum flyback switching frequency: > 66 kHz.

As mentioned above the controller FAN6920MR was used in this project. It controls the PFC and the flyback section and manages entire power supply. The chip is built in 16 pins case. The function of each pin is described in table 3.2. The controller is highly integrated and its structure is complex. The block diagram is shown in Figure 3.7. The exact details about operation of each block are contained in datasheet of the controller [40]. To control the main transistors in the flyback converter, the integrated circuit AUIRS21811S was used [38]. This is a high-side and low-side MOSFET driver, which can operate up to 600V. It supports high driving current of 2A and fast switching time typically 135ns. On the secondary side, it was decided to use a synchronous rectifier controlled by the integrated circuit FAN6204 [39]. FAN6204 is a secondary-side synchronous rectification (SR) controller to drive SR MOSFET for improving efficiency. FAN6204 can be applied in continuous or discontinuous conduction mode (CCM and DCM) and quasi-resonant (QR) flyback converters based on the proprietary innovative linear-predict timing-control technique.

Table 3.2 Pin definition of controller FAN6920MR [40].

Pin	Name	Desction
1	RANGE	The RANGE pin's impedance changes according toVIN pin voltage level. When the input voltage detected by the VIN pin is higherthan a threshold voltage, it sets to low impedance; whereas it sets to high impedance if input voltage is at a high level.
2	COMP	Output pin of the error amplifier. It is a transconductance-type error amplifier for PFC output voltage feedback. Proprietary multi-vector current is built-in to this amplifier; therefore, the compensation for PFC voltage feedback loop allows a simple compensation circuit between this pin and GND.
3	INV	Inverting input of the error amplifier. This pin is used to receive PFC voltage level by a voltage divider and provides PFC output over- and under-voltage protections. This pin also controls the PWM startup. Once the FAN6920MR is turned on and VINV exceeds in 2.3V, PWM starts.
4	CSPFC	Input to the PFC over-current protection comparator that provides cycle-by-cycle current limiting protection. When the sensed voltage across the PFC current-sensing resistor reaches the internal threshold (0.82V typical), the PFC switch is turned off to activate cycle-by-cyclecurrent limiting.
5	CSPWM	Input to the comparator of the PWM over-current protection and performs PWM current-mode control with FB pin voltage. A resistor is used to sense the switching current of the PWM switch and the sensing voltage is applied to the CSPWM pin for the cycle-by-cycle current limit, currentmode control, and high / low line over-power compensation according to DET pin source current during PWM tON time.
6	OPFC	Totem-pole driver output to drive the externalpower MOSFET. The clamped gate output voltage is 15.5V.
7	VDD	Power supply. The threshold voltages for startup and turn-off are 12V and 7V, respectively. The startup current is less than 30µA and the operating current is lower than 10mA.
8	OPWM	Totem-pole output generates the PWM signal to drive the external power

|		MOSFET. The clamped gate output voltage is 17.5V.
9	GND	The power ground and signal ground.
10	DET	This pin is connected to an auxiliary winding ofthe PWM transformer through a resistor divider for the following purposes: • Producing an offset voltage to compensate the threshold voltage of PWM current limit for overpower compensation. The offset is generated inaccordance with the input voltage when the PWM switch is on. • Detecting the valley voltage signal of drain voltage of the PWM switch to achieve the valley voltage switching and minimize the switching loss on the PWM switch. • Providing output over-voltage protection. A voltage comparator is built in to the DET pin. The DET pin detects the flat voltage through a voltage divider paralleled with auxiliary winding. This flat voltage is reflected to the secondary winding during PWM inductor discharge time. If output over voltage and this flat voltage are higher than 2.5V, the controller stops all PFC and PWM switching operation. The protection mode is auto-recovery.
11	FB	Feedback voltage pin used to receive the output voltage level signal to determine PWM gate duty for regulating output voltage. The FB pin voltage can also activate open-loop, overload protection and output-short circuit protection if the FB pin voltage is higher than a threshold of around 4.2V for more than 50ms.The input impedance of this pin is a 5kΩ equivalent resistance. A 1/3 attenuator is connected between the FB pin and the input of the CSPWM/FB comparator.
12	RT	Adjustable over-temperature protection and external protection triggering. A constant current flows out from the RT pin. When RT pin voltage is lower than 0.8V (typical), protection is activated and stops PFC and PWM switching operation. This protection is auto-recovery.
13	VIN	Line-voltage detection for brownin / out protections. This pin can receive the AC input voltage level through a voltage divider. The voltage level of the VIN pin is not only used to control RANGE pin's status, but it can also perform brownin / out protection for AC input voltage UVP.
14	ZCD	Zero-current detection for the PFC stage. This pin is connected to an auxiliary winding coupled to PFC inductor winding to detect the ZCD voltage signal once the PFC inductor current discharges to zero. When the ZCD voltage signal is detected, the controller starts a new PFC switching cycle. When the ZCD pin voltage is pulled to under 0.2V (typical), it disables the PFC stage and the controller stops PFC switching. This can be realized with an external circuit if disabling the PFC stage is desired.
15	NC	No connection
16	HV	High-voltage startup pin is connected to the AC line voltage through a resistor for providing a high charging current to VDDcapacitor.

*Figure 3.7 Internal Block diagram of FAN6920MR [40].*
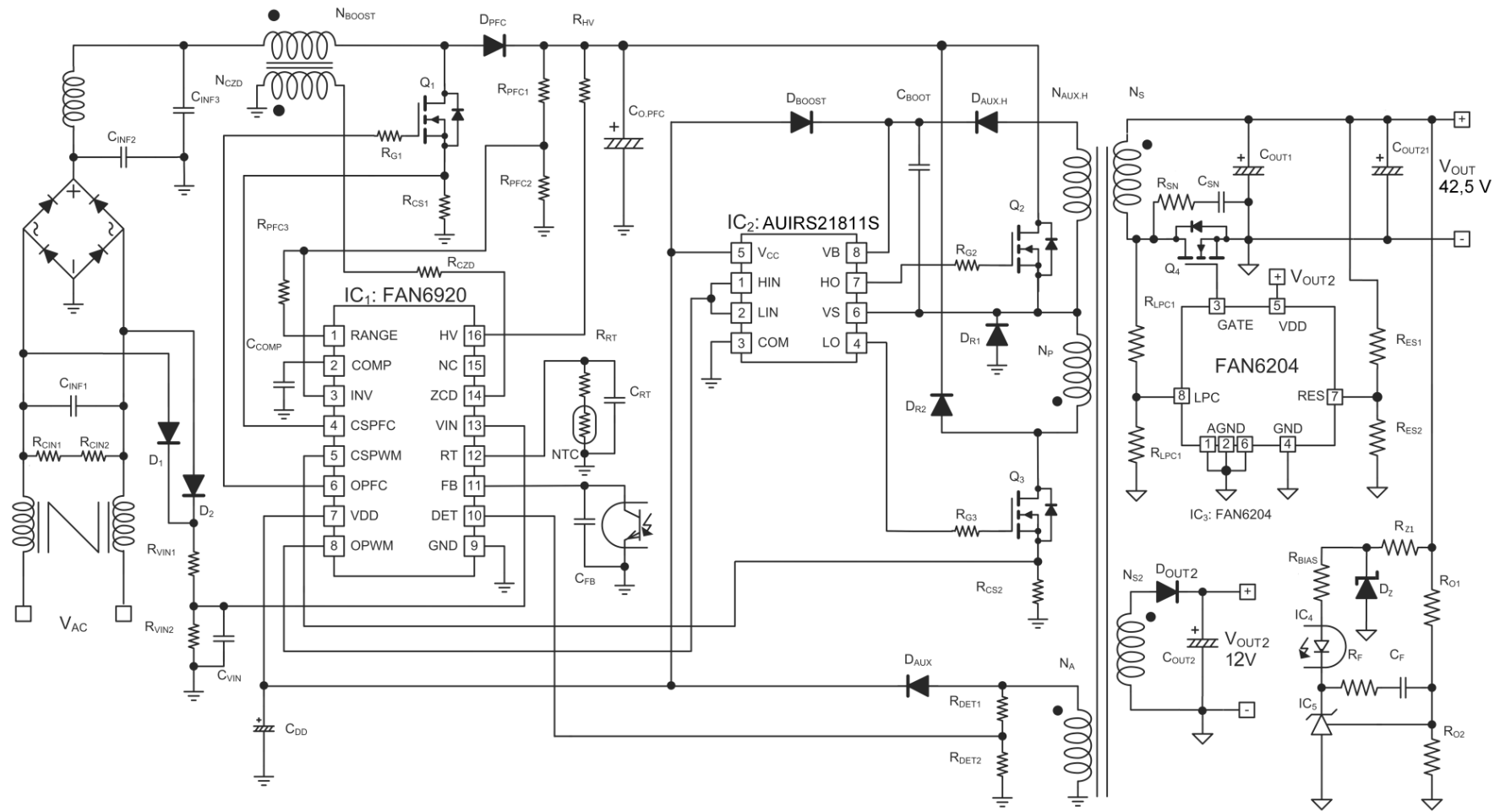
Figure 3.8 Power supply board schematic (adopted from [35]).

3.5 Component Dimensioning

Figure 3.8 shows a schematic of designed power supply. The design procedure with all necessary dimensioning operations is described below.

3.5.1 PFC section

The relation between voltage and current in inductor is given as:

$$V \cong L \frac{\Delta i}{\Delta t} \qquad (3.5)$$

In a boost converter, the voltage-second balance equation for the inductor is:

$$V_{IN}(t)t_{ON} = (V_{OUT} - V_{IN}(t))t_{OFF} \qquad (3.6)$$

From that, we obtain switching frequency for boost PFC circuit:

$$f_{SW} = \frac{1}{t_{ON} + t_{OFF}} = \frac{1}{t_{ON}} \frac{V_{O\_PFC} - \sqrt{2}V_{LINE}}{V_{O\_PFC}} \qquad (3.7)$$

where: V_{LINE} is RMS line voltage (220-240 VAC $\pm$ 10%, 50 Hz); t_{ON} is the MOSFET conduction time; $V_{O.PFC}$ is the PFC output voltage (400V). The MOSFET conduction time with a given line voltage at a nominal output power is given as [22]:

$$t_{ON} = \frac{2P_{OUT}L}{\eta V_{LINE}^{2}} \qquad (3.8)$$

Where η is efficiency (81%); L is the boost inductance; P_{OUT} is the nominal output power (35W).From equation 3.7 and 3.8, the switching frequency is:

$$f_{SW} = \frac{\eta V_{LINE}^{2}}{2P_{OUT}L} \frac{V_{O\_PFC} - \sqrt{2}V_{LINE}}{V_{O\_PFC}} \qquad (3.9)$$

The boost inductor value is determined by the output power and the minimum switching frequency. The minimum switching frequency is obtained for highest line voltage (264V). Using previous date, the inductor value is given:

$$L = \frac{\eta V_{LINE\_MAX}^{2}}{2P_{OUT}f_{SW\_MIN}} \frac{V_{O\_PFC} - \sqrt{2}V_{LINE\_MAX}}{V_{O\_PFC}} = 1.77\text{mH} \qquad (3.10)$$

Once the inductance value is decided, the maximum peak inductor current at the nominal output power is obtained under low-line condition as[22]:

$$I_{L.PK} = \frac{2\sqrt{2}P_{OUT}}{\eta V_{LINE\_MIN}} = 0,625 \ A \qquad (3.11)$$

The number of turns of the boost inductor should be determined considering the core saturation. The minimum number is given as [22]:

$$N_{BOOST} \geq \frac{I_{L\_PK}L}{A_e \Delta B}$$

(3.12)

where A_e is the cross-sectional area of core and ΔB is the maximum flux swing of the core in Tesla. ΔB should be set below the saturation flux density. Based on catalog of Ferroxcube international soft ferrites core producer [41], the core E 20/10/6 was chosen for the PFC inductor. The cross-sectional area of core equals 32 mm^2 and ΔB of 0,3T is suitable [42]. The number of turns of the boost inductor is:

$$N_{BOOST} = 116$$

(3.13)

Since the PFC stage operates in BCM, information about current in PFC inductor has to be given. Auxiliary winding N_{ZCD} on PFC inductor provides information to FAN6920MR controller. Internal current detect threshold V_{ZCD} equals 2.1V. The number of auxiliary turns is given by:

$$N_{ZCD} > \frac{V_{ZCD}\,N_{BOOST}}{V_{O\_PFC} - \sqrt{2}V_{LINE\_MAX}} = 9{,}14$$

(3.14)

With a margin, N_{ZCD} is determined as 20 turns. FAN6920 has pulse-by-pulse current limit function. It senses current using resistor R_{CS1} and compares with internal current limit threshold V_{CS_PFC} equals 0,82V. R_{CS1} was calculated for maximum inductor current with margin 20~30% using:

$$R_{CS1} = \frac{V_{CS\_PFC}}{I_{L\_PK}(1 + magrin)} = 1\Omega$$

(3.15)

3.5.2 DC-DC stage

The transformer is one of the most important elements is flyback converter. Its turn ratio has influence on transfer function (equation 2.9) and determinates many values in the overall project. By increasing turn ratio, the capacitive switching loss and conduction loss of the MOSFET are reduced. This also reduces the voltage stress of the secondary-side rectifier (equation 3.1). However, it is limited by input voltage due to V_{RO} (equation 3.3). After analysis of circuit, the turn radio between primary and secondary side of main transformer was stated as:

$$n = \frac{Np}{Ns} = 8{,}5$$

(3.16)

According to equation 3.3 and 3.4 nominal voltage of switches and rectifier is:

$$V_{DS}^{nom} = \frac{V_{O\_PFC} + n(V_{OUT} + V_{F})}{2} = \frac{V_{IN} + V_{RO}}{2} = 382{,}75V \tag{3.17}$$

$$V_D^{nom} = V_{OUT} + \frac{V_{IN}}{n} = 90V \tag{3.18}$$

The converter operates with minimum switching frequency $f_{S.QR.MIN}$ when is full-loaded. Maximum duty-cycle is calculated as

$$D_{max} = \frac{V_{RO}}{V_{RO} + V_{O\_PFC}}\left(1 - f_{S\_QR\_MIN}t_f\right) = 0{,}455 \tag{3.19}$$

where t_f is drain voltage fall time. It depends of MOSFET output capacitance and primary-side inductance. The value is assumed as 1 μs. Then, the primary-side inductance is obtained as:

$$L_m = \frac{\eta_{QR}(V_{O\_PFC}D_{MAX})^2}{2f_{S\_QR\_MIN}P_{OUT}} = 5{,}974mH \tag{3.20}$$

Once L_m is determined, the maximum peak current and RMS current of the MOSFET in normal operation are obtained as:

$$I_{DS\_PK} = \frac{V_{O\_PFC}D_{MAX}}{L_m\, f_{S\_QR\_MIN}} = 0{,}444A \tag{3.21}$$

$$I_{DS\_RMS} = I_{DS\_PK}\sqrt{\frac{D_{MAX}}{3}} = 0{,}173A \tag{3.22}$$

For the flyback transformer the core RM-8 was chosen [42]. The cross-sectional area A_e for RM-8 core is $64\,mm^2$. The maximum flux density swing in normal operation is stated as $\Delta B = 0{,}25\,T$. The minimum number of turns is given:

$$Np = \frac{L_m I_{DS\_PK}}{A_e \Delta B} \approx 166 \tag{3.23}$$

Then the number of secondary winding turns is given:

$$Ns = \frac{Np}{n} \approx 20 \tag{3.24}$$

Knowing the number of secondary winding turns, another winding can be calculated. The auxiliary winding N_{AUX} is necessary to supply voltage for controller and MOSFET driver (V_{DD}=14V). The high auxiliary winding $N_{AUX.H}$ provides sufficient voltage for high-side MOSFET gate driving $V_{AUX.H} = 12V$ The second secondary winding Ns_2 create low voltage output for general purpose also $V_{OUT2} = 12V$.

$$N_{AUX} = \frac{V_{DD} + V_F}{V_{OUT} + V_F} Ns \approx 7 \qquad (3.25)$$

$$N_{AUX.H} = \frac{V_{AUX.H} + V_F}{V_{OUT} + V_F} Ns \approx 6 \qquad (3.26)$$

$$Ns_2 = \frac{V_{OUT2} + V_F}{V_{OUT} + V_F} Ns \approx 6 \qquad (3.27)$$

3.5.3 Synchronous rectifier

The FAN6204 utilizes a proprietary linear-predict timing control to determine the turn-on and turn-off timing of SR MOSFET. This control technique detects the voltage of the transformer winding and output voltage instead of MOSFET current. The application circuit is shown in Figure 3.9.
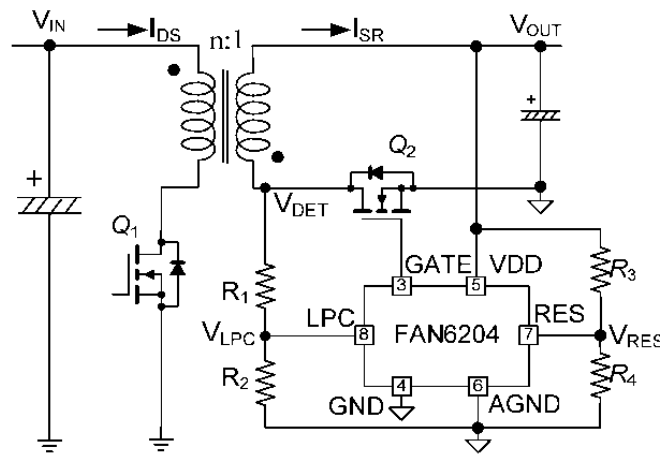

Figure 3.9 Typical application circuit for flyback converter [39].

Its operation is based on prediction of MOSFET current. It sense the secondary winding voltage and output voltage by pins respectively LPC and RES. Sensed signals are drawn to two independent voltage-controlled current sources, which charge an internal capacitor. As a result, the obtained capacitor voltage is a replica of the MOSFET current. Based on it, the MOSFET switch is driven appropriately. The main consideration on the design of this circuit is to select correct voltage dividers for LPC and RES lines. The dividers have to meet following conditions according to Figure 3.9

for $R_1 + R_2$:

$$0{,}83\, V_{LPC\_EN} \frac{R_2}{R_1 + R_2} \left(\frac{V_{IN}}{n} + V_{OUT} \right) > V_{LPC\_TH\_HIGH} + V_{DD\_HYST} \qquad (3.28)$$

$$\frac{R_2}{R_1 + R_2} \left(\frac{V_{IN}}{n} + V_{OUT} \right) < V_{LPC\_DIS} \qquad (3.29)$$

48

where LPC enable voltage $V_{LPC\_EN} = 1V$, LPC high threshold $V_{LPC\_TH\_HIGH} = 0,05V_{DD}$, voltage hysteresis $V_{DD\_HYST} = 0,3V$ and LPC enable voltage $V_{LPC\_DIS} = 4V$;

for $R_3 + R_4$:

$$V_{LPC\_EN} < \frac{R_4}{R_3 + R_4} V_{OUT} < V_{LPC\_DIS} \qquad (3.30)$$

Because of the certain proportion of internal current sources, the voltage dividers have to be selected to proportion K which is in range from 5 to 5,5 fallowing the formula:

$$K \frac{R_2}{R_1 + R_2} = \frac{R_4}{R_3 + R_4} \qquad (3.31)$$

Using formulas above, fallowing values for elements were chosen: $K = 5.18$, $R_1 = 560k\Omega$, $R_2 = R_4 = 10k\Omega$, $R_3 = 100k\Omega$.

3.5.4 Buck converter for the LED driver

The LEDs modules are power supplied from driver board, which is based on integrated circuit LM3414HV. The LM3414HV is constant current buck LED driver. It accepts input voltages from 4.5VDC to 65VDC and deliver up to 1A average LED current with ±3% accuracy. Its efficiency is up to 96%. The integrated low-side N-channel power MOSFET and current sensing element realize simple and low component count circuitry, as no bootstrapping capacitor and external current sensing resistors are required. An external small-signal resistor to ground provides very fine LED current adjustment and thermal fold-back functions. The circuit is based on the standard application, for which the schematic is depicted in Figure 3.10.
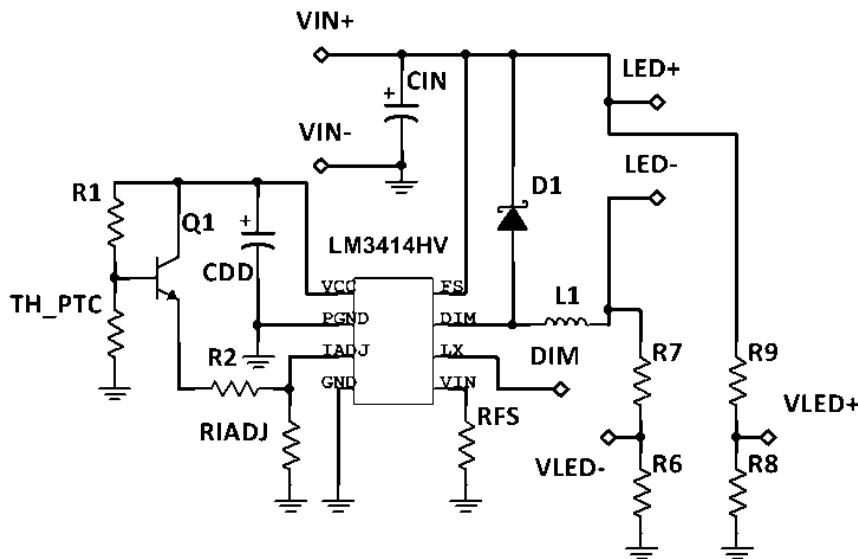

Figure 3.10 Schematic of the Buck LED driver board.

The LM3413 operation frequency ranges from 250 kHz to 1000 kHz. The frequency was set at 400 kHz to keep switching losses low but obtain small inductor also. The operation frequency of IC is inversely proportional to resistor R$_{FS}$ witch proportional factor $20 \cdot 10^6$ according to the formula:

$$f_S = \frac{20 \cdot 10^6}{R_{FS}}$$

(3.32)

The integrated circuit LM3414 stabilizes the LED average current, based on resistor R_{IADJ} following the formula:

$$I_{LED} = \frac{3125 \cdot 10^3}{R_{IADJ}}$$

(3.33)

For $R_{IADJ} = 4{,}42 k\Omega$, LED current should be equal to 707mA. Knowing switchin frequency and LED current, the buck inductor is calculated as:

$$L \geq \frac{(V_{IN} - V_{LEDmin})V_{LEDmin}}{I_{LED}V_{IN}f_S K} \approx 100 \mu H$$

(3.34)

Where V_{IN} is input voltage of the flyback power supply, V_{LEDmin} is minimum forward voltage for the diodes, and $K = \frac{I_{RIP\_PK}}{I_{LED}} = 0{,}4$ is ratio between peak to peak inductor current ripple and average current of LEDs.

3.6   Microcontroller system

The previous section described the design of the power supply and LED driver. To ensure sufficient lighting in the operation area and make the system cost effective, the active control dimming should be provided. A simple and convenient solution is to use a microcontroller that reads the signals from the sensors in real time and sends a control signal to the LED driver to accommodate lighting intensity. In addition, connection of a radio module to the microcontroller provides wireless communication with the user.

For microcontroller system implementation, the open-source platform Arduino was used [46]. Arduino platform provides a wide range of boards and expansion modules that allows to build complex systems. Arduino also provides a software development environment. Arduino language is based on the C language. A set of libraries and functions provided with software makes the easy setup and simplifies programming and operation of the periphery. Arduino boards are based on 8-bit microcontrollers Atmel AVR. Most of the Arduino boards have a built-in USB - serial port that emulates a serial port via a USB interface. This enables a convenient programming without additional programmer. Serial port emulation also enables simple communication between the microcontroller and the computer via serial port monitor software.

In the project two Arduino boards were used: Arduino Nano and Arduino UNO. Both are based on the processor Atmel Atmega 328P. ATmega328 is an 8-bit microcontroller is characterized by [47]:

- Operation at a frequency of 16 MHz (on the Arduino platform),
- 32KBytes Programmable Flash program memory,
- Two 8-bit Timers / Counters,
- One 16-bit Timer / Counter,
- 6-channel 10-bit ADC,
- Programmable Serial USART,
- SPI Serial Interface.

One of the Arduino board is operating on the LED driver's side and is responsible for the LEDs control (LED MCU module). The second board acts as a bridge of communication between the LED MCU module and the computer (communication bridge module). The system block diagram is shown in Figure 3.11.
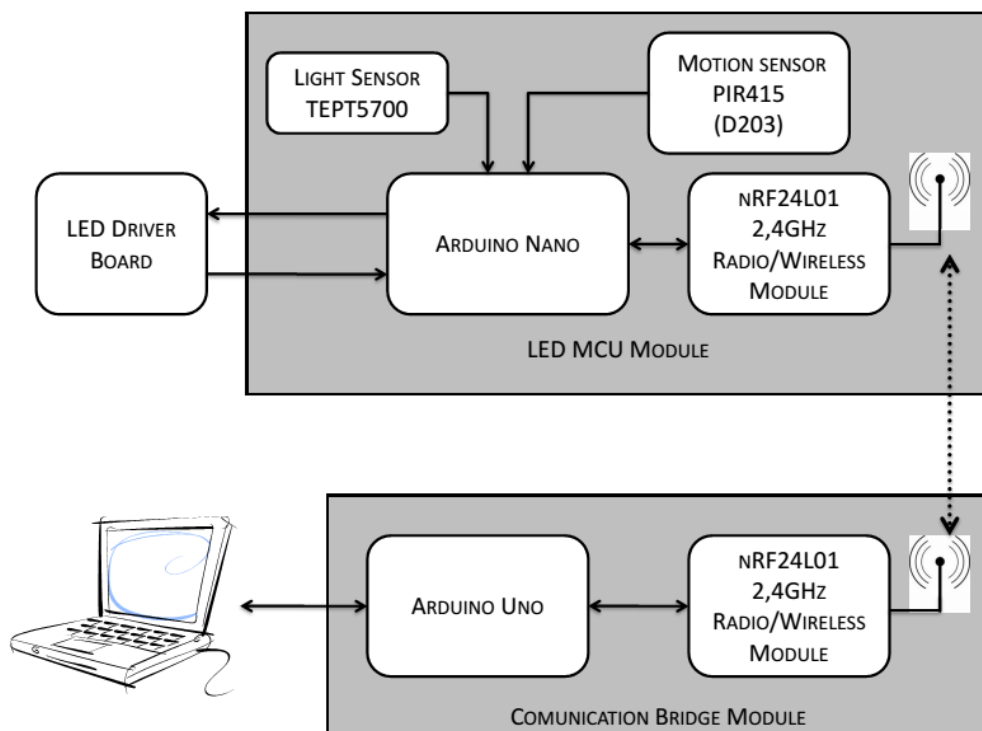

Figure 3.11 Microcontroller system diagram.

3.6.1 LED Microcontroller Module

The LED MCU Module, the Arduino Nano board is the central unit. The input signals are derived from the ambient light sensor, motion sensor and LED driver. The light sensor is based on phototransistor TEPT5700 [48]. It is sensitive to visible light much like the human eye and has peak sensitivity at 570 nm. Its conductivity is dependent on the current light intensity. An additional resistor is connected between the collector of phototransistor and the supply voltage. In this way, voltage on the collector is inversely proportional to the light intensity. This voltage is read by the microcontroller.

The motion sensor used consists of commercial device, PIR415 Velleman [49]. In its construction, the component D203 is the actual sensory device. The PIR415 device has no outputs and it is not used in common way. Motion signal is drawn from the internal point of its PCB. This signal goes high when motion is detected within the sensor. The microcontroller receives and signals from the sensors. Based on this signals, it supplies a PWM signal with a frequency of 1 kHz and variable duty-cycle, which is proportional to the desired luminous flux of LEDs. The inductor voltage and the voltage across the resistor RIADJ are collected from LED driver board. Based on its values, the actual power and consumed energy are determined. The microcontroller communicates with the wireless module nRF24L01 to send data and configure operating parameters.

Figure 3.12 shows a lighting profile and a block diagram of the program. After initialization, the program enters the main loop. In the main loop, the program checks motion mode status and then senses signal from the motion sensor. If both conditions are not met, the program gets a signal from the light sensor and creates a signal for the LED. If the motion is detected, the program enters the motion mode and increases duty-cycle of PWM control signal to specified level. The timer is started and counts motion mode time. When motion mode is active and motion sensor is triggered, the program resets the timer and its start counting again. If the timer reaches a designated amount and in the meantime, no further movement is detected, the program exits the motion mode and reduces the light intensity to the level specified by the light sensor. At the end, program checks if any data were received from the radio module. If so, the program reads it, analyzes it and configures or transmits the requested information. During operation, one time per 100ms program receives the data from the LED driver, and on its basis calculates the actual power and estimated the energy consumed.

a)

b)
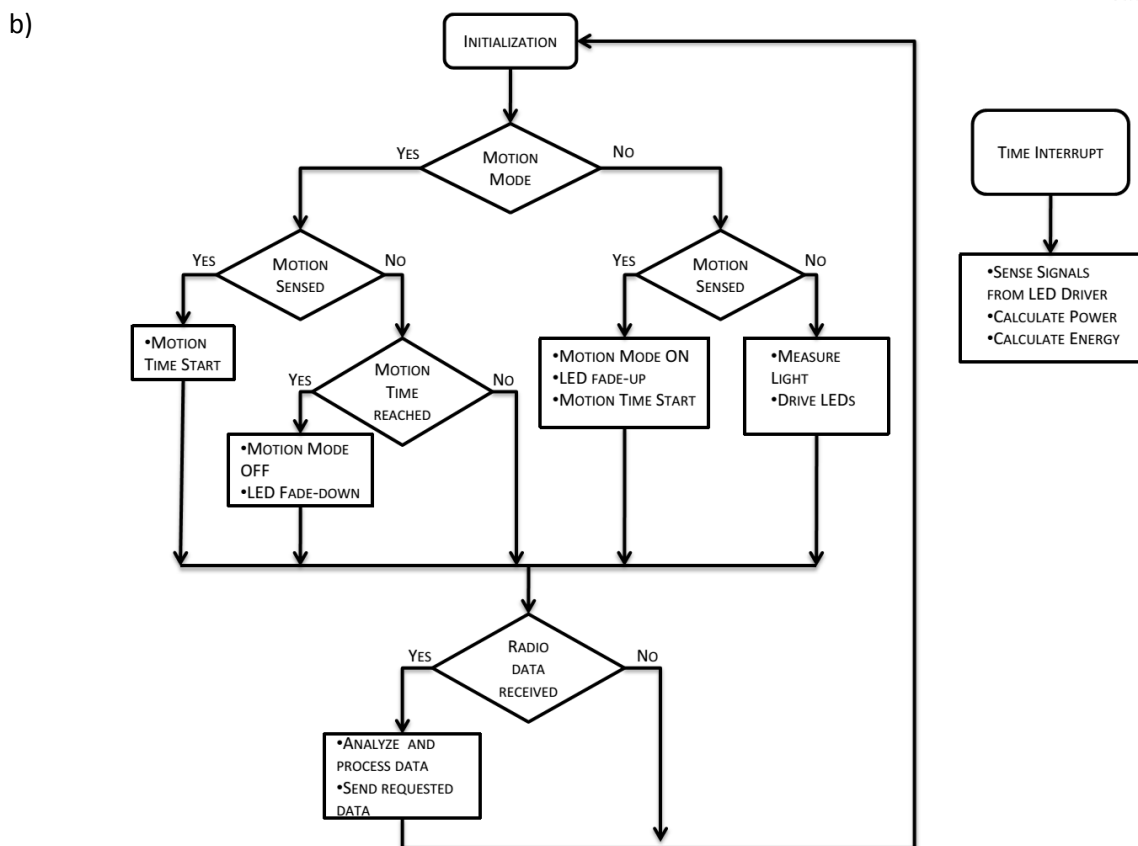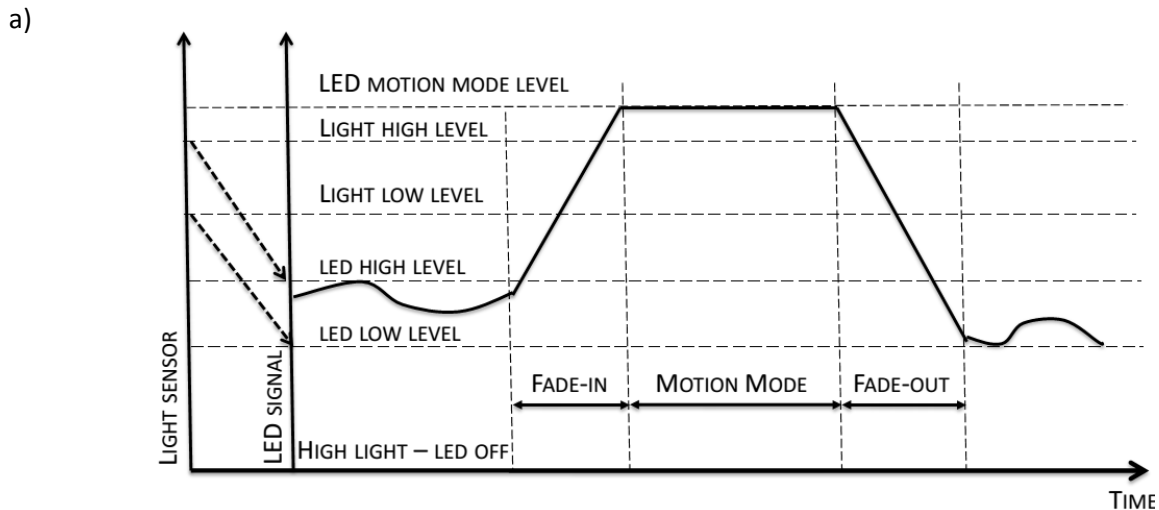
Figure 3.12 Lighting profile a) and block diagram of implemented algorithm in LED MCU module b).

3.6.1 Communication bridge module

The communication module is responsible for the exchange of information between your computer and the LED MCU using wireless transmission. After initialization, the program goes into standby. If any data is received from the serial port, the program enters the communication menu. In the menu, some parameters can be changed such as levels of illumination in standby and motion mode, time of motion mode and light sensor sensitivity. Also request for the current light level signal LED, power and energy consumed can be send.

53

4.Assembly and Measurements

In the previous chapter was described the operation and design of the modules that composed the developed LED supply device. The next step was the construction of the designed system and test for determining its properties. This chapter will include the design of transformers power supply and PCB design. Then in will be described preparation process for measurement, studies and analysis of the system. At the end, the results of measurements will be presented.

4.1   Transformer Design

Design of the transformer is a critical process, which affects the operation of the system and its performance. It must be analyzed in many aspects. When designing, the attention must be paid to the core material and core size. This has influence for the thickness of the winding wires and the number of layers. To increase the energy storage and to prevent core saturation, also it is needed to have a gap in the core column.

The first thing is the choice of the core material, which is appropriate for the application and for the operating conditions. As mentioned in the previous section, the construction of transformers flyback and PFC stages, the cores E 20/10/6 and RM - 8 were selected. Both cores are derived from the manufacturer EPCOS and are made of manganese zinc (MnZn) ferrite material codenamed N87. This material is intended for operation in power applications up to 500 kHz [50].

Another issue is the order of the windings placed on the inductor [31].It is typical to place the primary winding or its part as first on the bottom of the winding stack. This minimizes the length of wire and reduces the conduction loss in the wire. The EMI noise radiation can be reduced, since the other windings can act as Faraday shields. The winding order in a transformer has a large effect on the leakage inductance. The secondary winding, which supplies the highest power, should be placed closest to the primary for the best coupling and lowest leakage inductance. To achieve it, the most common method is a sandwich winding where the primary winding is divided on two parts and high power secondary winding is placed between them. In addition, windings should be spaced evenly across the width of the inductor window instead of being bunched together. Choosing the order of winding, attention should be taken for isolation between windings especially for primary and secondary side. However, each isolation layer decreases the available space of winding window. Taking in consideration information above, the order of flyback transformer was designed as depicted on Figure 4.1. In the PFC stage, the transformer has only two winding thus the main winding was placed on bottom of the inductor stuck, and auxiliary winding is placed on top of it.
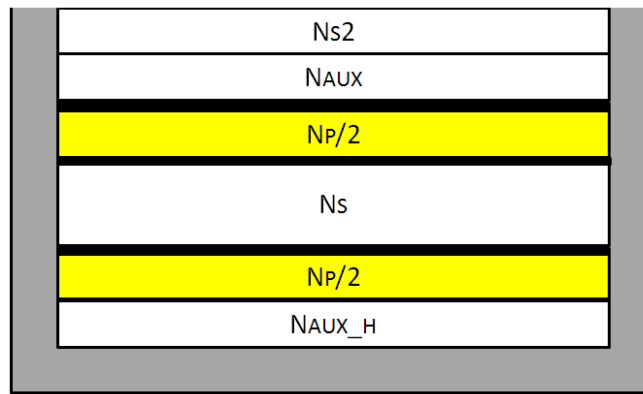
Figure 4.1 Order of winding in the designed flyback transformer.

When order of winding has been set, the diameter of winding wire has to be selected. The cross section of the wire, and thus diameter, has an impact on its resistance and hence loss in the transformer. To ensure the lowest losses, the cross section of wire should be as large as possible. However, the limitation is winding window area. The wire diameter is determined based on the RMS current flowed through the wire. The current density is typically $5 A/mm^2$ when the wire is longer than 1 meter [31]. When the wire is short with a small number of turns, a current density of $6 - 10\ A/mm^2$ is also acceptable. For designed purposes it was assumed a current density of $6\ A/mm^2$. The skin effect has to be taken in consideration. Skin effect is based on a non-uniform distribution of current in the conductor. Its value is higher at the surface of the conductor and smaller in its interior. This phenomenon only occurs when the flow of alternating current. A rate of skin effect is the current's penetration depth of the conductor. The skin effect causes the effective resistance of the conductor to increase at higher frequencies where the skin depth is smaller, thus reducing the effective cross-section of the conductor. For the present purpose the skin effect depth was assumed 0,21mm.

The last step is to make a gap in the transformer column. The gap increases the amount of energy that can be stored in the core and prevents saturation of the core. The gap was necessary for both transformers. The gap should be performed only in the middle column to maintain the lowest possible leakage inductance. The gap is made by grinding the middle column of the two halves core using sandpaper. During grinding, the special care should be taken, because the ferrite material is very hard, fragile and easy to damage. The gap width was chosen appropriately, having in consideration the number of turns of each winding and the primary winding inductance. Each core has inductance factor A_L assumed in the manufacturer datasheets. The relationship between the inductance, number of turns and the factor A_L is derived by:

$$L = A_L \cdot n^2$$

(4.1)

Creating a gap in the middle column of the core, the A_L factor decreases. A suitable gap width was selected by checking the inductance of the primary winding during grinding.

When the desired value was reached, other windings inductances were checked. Table 4.1 presents detailed data of designed transformers.

Table 4.1 Transformers specification.

	Turns	Calculated inductance	Measured inductance	Pins of inductor		Diameter
				Dot end		
Flyback transformer						
Primary winding high Np/2	83	1,488 mH	1,542 mH	4	8	0,22mm
Primary winding low Np/2	83	1,488 mH	1,471 mH	7	4	0,22mm
Secondary winding Ns	20	86,4 µH	88,2 µH	3	11	4x 0,28mm
Secondary winding Ns2	6	7,77 µH	9,9 µH	2	1, 10, 12	0,22mm
Auxiliary winding	7	10,59 µH	13,3 µH	5	6	0,22mm
High auxiliary winding	6	7,77 µH	9,9 uH	9	8	0,22mm
PFC transformer						
Main winding N_{boost}	116	1,77 mH	1,769 mH	3	5	0,28mm
Auxiliary winding N_{zcd}	20	52,62 µH	52,58 µH	1	2	0,28mm

4.2. Design of the PCBs

Within the project, two PCBs have been designed: the power supply board and the LED driver board. The PCB designs were created in the DipTrace 2.4. This software has a powerful but intuitive interface, which allows you to create advanced projects. It also offers a rich library of components. Diptrace software is divided into four modules, each of which is designed for different tasks in the subsequent stages of the project:

- Schematic - is used to draw schematics,
- PCB Layout - the main module to design PCB, it allows to create boards from the schematic and has autorouting function,
- Component Editor - used to create elements for the module Schematic,
- Pattern Editor - used to create case models for the PCB Layout program.

The designs were created in the PCB Layout module without using the Schematic and autorouting function. Both boards are a single layer. When designing, attention was paid to the routing paths. The big challenge was to rout ground paths on the power supply board. This was due to the fact, that the controller FAN6920 senses signals from different parts of the board, which must have a common reference point. Therefore, it was decided to rout ground in shape of star, in which the reference points for the individual signals are combined in one place at the capacitor C_{DD} .

After designing the PCB boards, the project was sent to the workshop at the university, where the PCBs were made using a CNC milling machine. Then the boards were cleaned and coated with rosin to protect against oxidation and make soldering easier. The

next step was to solder all components. This started with SMD components on the bottom side of the board. Then small parts on the upper side were soldered. At the very end transformers, transistors and connectors were assembled. Figure 4.2 and 4.3 depicted the assembled PCBs.

*Figure 4.2 Photograph of Power supply board.*

Figure 4.3 Photograph of LED driver board.

4.3   Measurements set-up

Before measurements, the necessary equipment and the testing set-up had to be prepared. In the project, the power supply was supplied from main power. Therefore, to maintain security and allow the measurements of the input signal parameters an isolation transformer was built. It consists of two identical conventional power transformers connected in series such that the secondary windings of both transformers are connected to each other. Therefore, when the mains voltage is connected to the primary winding of the first transformer, the primary winding of the second transformer get a voltage equal to the

input voltage. In the laboratory, the supply voltage was 220V AC. The diagram of the isolation transformer is shown in Figure 4.4.
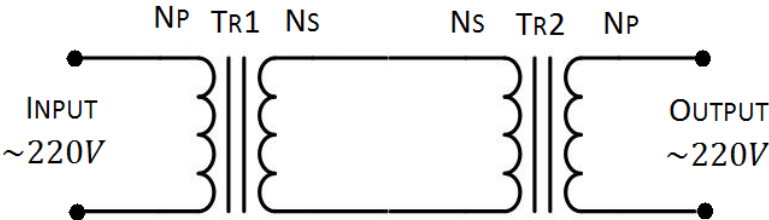

Figure 4.4 Schematic of the isolation transformer.

To perform the measurements, tested devices had to be loaded. To obtain the characteristics of the devices, a regulated load should used. For this purpose, two additional devices were built. To load the flyback power supply, a regulated current source has been assembled. It is similar to that in Figure 2.7 but with the possibility of adjusting the reference voltage by using a potentiometer. In this manner, a regulated resistive dummy load was obtained. Energy dissipated by the transistor was radiated through heat sink with fan. To test the LED driver, the load had to be constructed which acts as the LEDs. A good LED substitute is a Zener diode in the reverse bias [10]. There is a voltage drop across them as in the LEDs, which are polarized in the conduction direction. In this way, the Zener diode was made using one high-power bipolar transistor. In order to ensure regulation of the voltage drop, which would emulate different number of LEDs, the regulated Zener diode TL431 was used. Schematic of regulated high power Zener diode is shown in Figure 4.5.
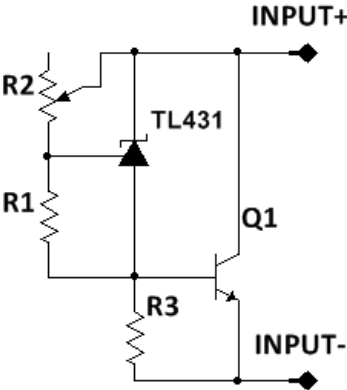

Figure 4.5 Schematic of high power regulated Zener diode.

The voltage of the Zener diode at the INPUT terminals is determined by the resistance R1 and R2 according to the formula:

$$V_{DZ} = V_{BE} + (\frac{R_2}{R_1} + 1)V_{ref}$$

(4.1)

where V_{BE} is base-emiter voltage of Q_1 and V_{ref} is internal reference of TL431 equal 2,5V.

All measurements were carried out using two digital oscilloscopes Tektronix TDS2012B and TDS3032C. To study the input currents 1Ω resistors were used where measured voltage is proportional to the current. Figure 4.6 shows the connection of probes, which was used to test voltage and current input and output.
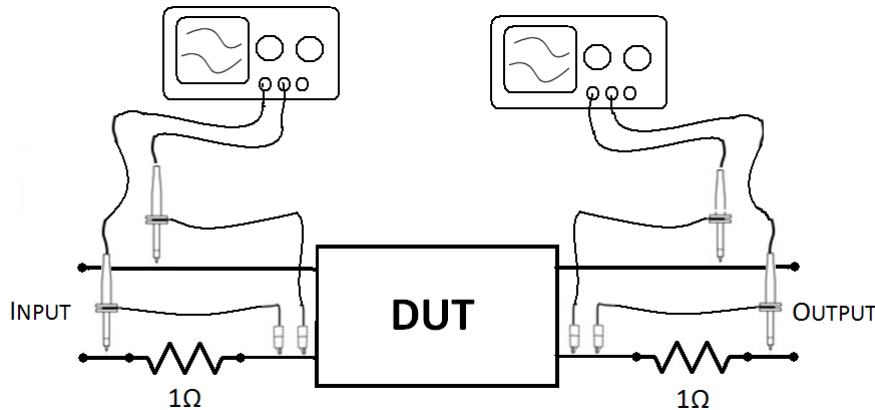

Figure 4.6 Circuit diagram for measuring input and output voltage and current.

4.4 Device analysis

At the beginning, the power supply board was tested. The voltage of the output of the rectifier bridge and the drain current of the transistor PFC stage was measured. The waveforms are depicted in Figure 4.7. The peak drain current envelope follows the rectified line voltage in shape. However, there is the gap in the middle of each half of power line period where voltage reaches highest value. This is due to the peaks of the sine wave voltage. Probably the main cause is resistance of winding in separation transformer or poor quality of main power voltage. Maximum current value is about 500mA, what is below the calculated value. The next step was to compute power factor, using formula 2.12. The RMS value of the input voltage and current was measured for different load conditions. The oscilloscope provides some advanced option. One of them is to perform Fast Fourier Transform (FFT) from input signal. To obtain the amplitude of the first harmonic of the input current, this function was used. This allowed to calculate the distortion factor (Kd). However, it was not possible a carry out reliable measurement of the phase shift for a light load.

60
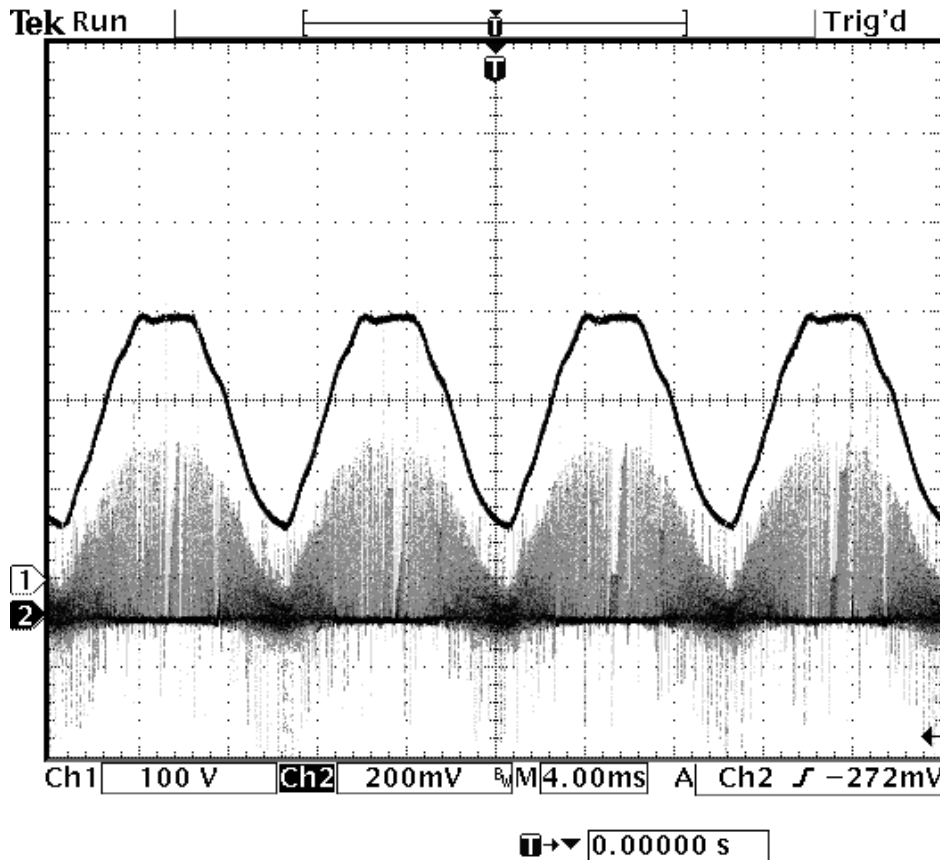
Figure 4.7 Rectified voltage (channel 1), drain current of the transistor PFC stage (channel 2).

For low load, the power supply operates in burst mode. It consists of a periodical turning on and off the stage PFC to save energy. Burst mode stops when the input current reached about 110mA. At a time when the PFC stage is disabled, the input current leads the voltage by about 82.5°. This determines the capacitive impedance, which may be due to the capacity of the filter input. Figure 4.8 shows the averaged waveforms (using the oscilloscope acquisition function) at the input of the power supply for full load. When the PFC stage operates above burst mode, the current leads before voltage only about 20 °. The power factor was calculated for no-burst mode operation. The results are presented in Figure 4.9. The maximum value of PF is more than 0.92.
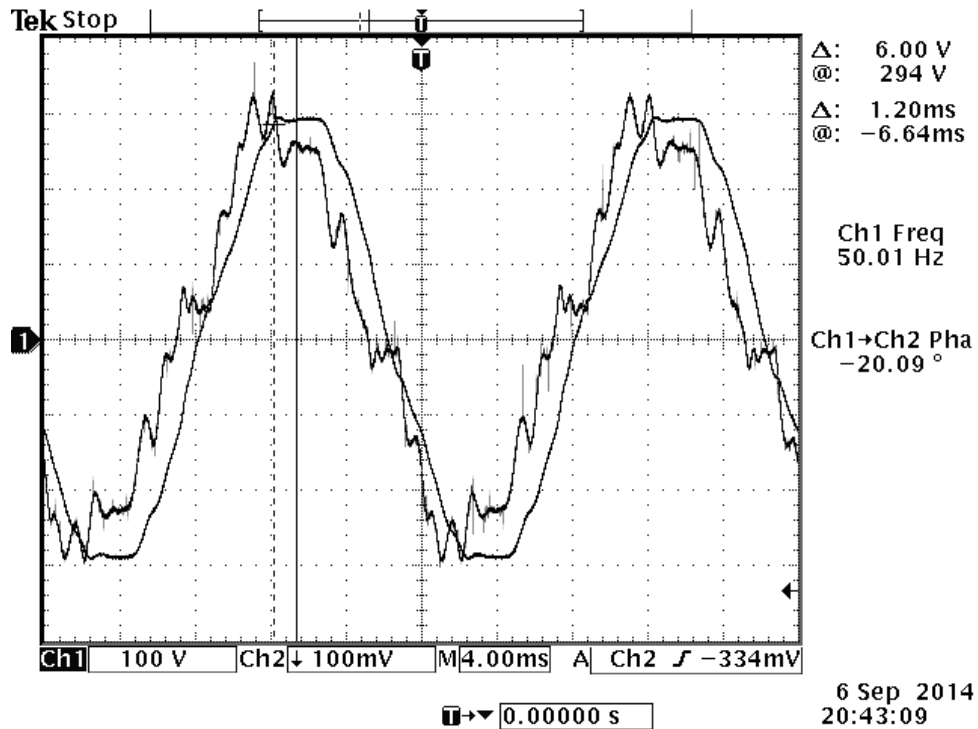
*Figure 4.8 Input Voltage (channel 1) and input current (channel 2).*
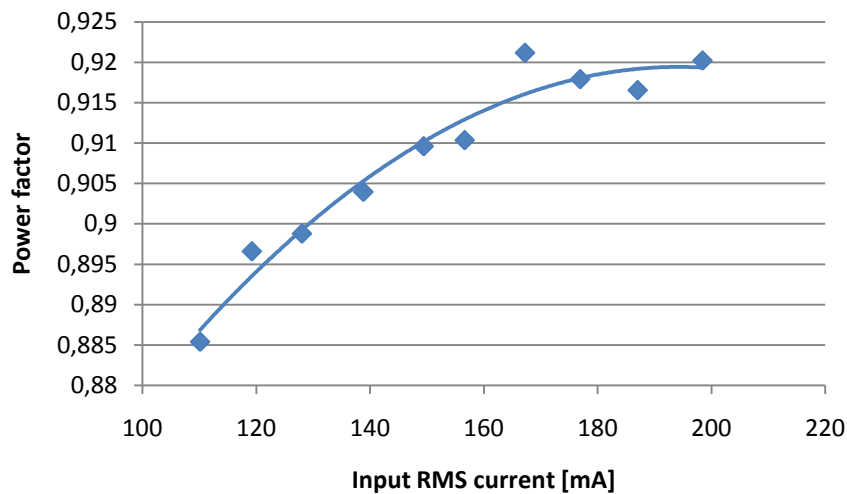
Figure 4.9 Power factor as function of input current.

Figure 4.10 presents the detecting valleys of the resonance voltage at the low transistor drain of the resonant flyback converter. When load is about 120 mA, the controller turns on the transistors when it detects 5th valley. For full load, transistors are switched on when 1st valley is detected. In this instance, the voltage on the lower transistor is approximately 44 V. Depending on the load, it can be noticed a different overshoot and ringing when switching off the transistor. This situation is better shown in Figure 4.11. For light load, voltage at the lower transistor drain is clamped for about 100 ns. At this time, the leakage inductance energy is transferred to the load. When the power supply is loaded, the

62

leakage inductance accumulates more energy, and its discharge is approximately 600ns. Smaller ringing is noted for heavy load.
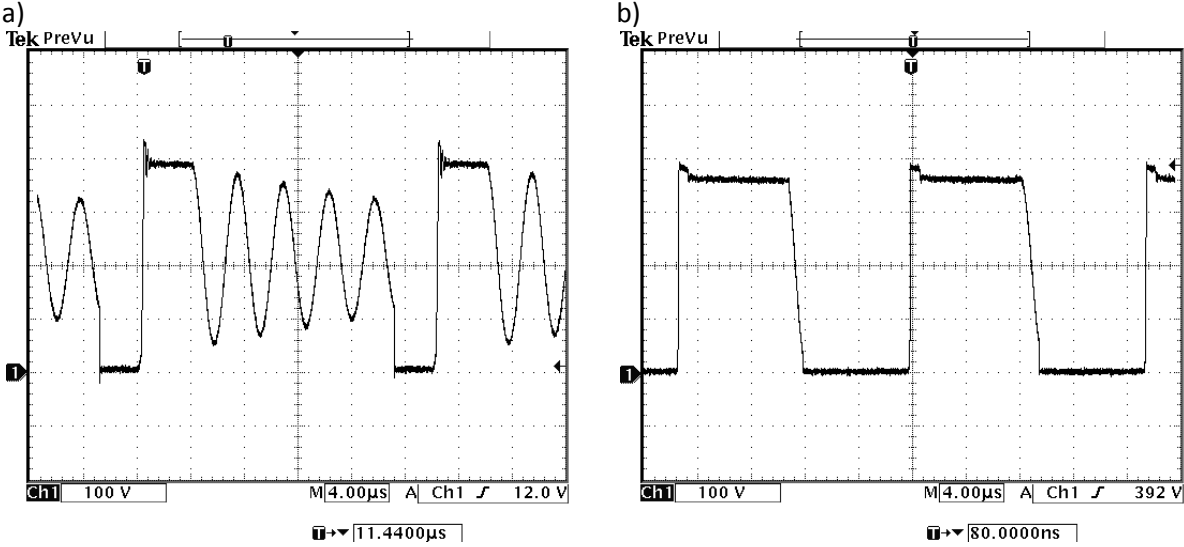

Figure 4.10 The Valleys detection: a) for light load ; b) for full load.
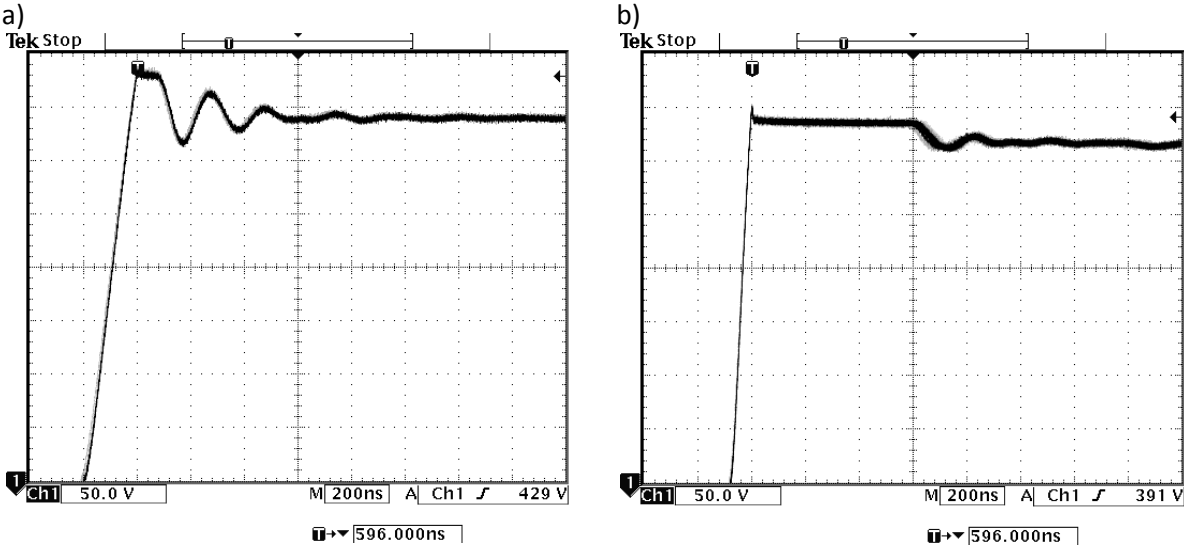
Figure 4.11 Drain voltage of low side transistor during turning off and leakage energy releasing: a) low load; b) full load.

In Figure 4.12 the waveform of the LED current on the output of LED driver is depicted. The peak to peak inductor current ripple is equal about 280mA. The ratio between current ripple and output current is equal to 0,4 consistent with assumed K factor during calculation. During switching, the current spikes are observed. A reason of these spikes lies in slow reaction of artificial Zener diode as the load.

63
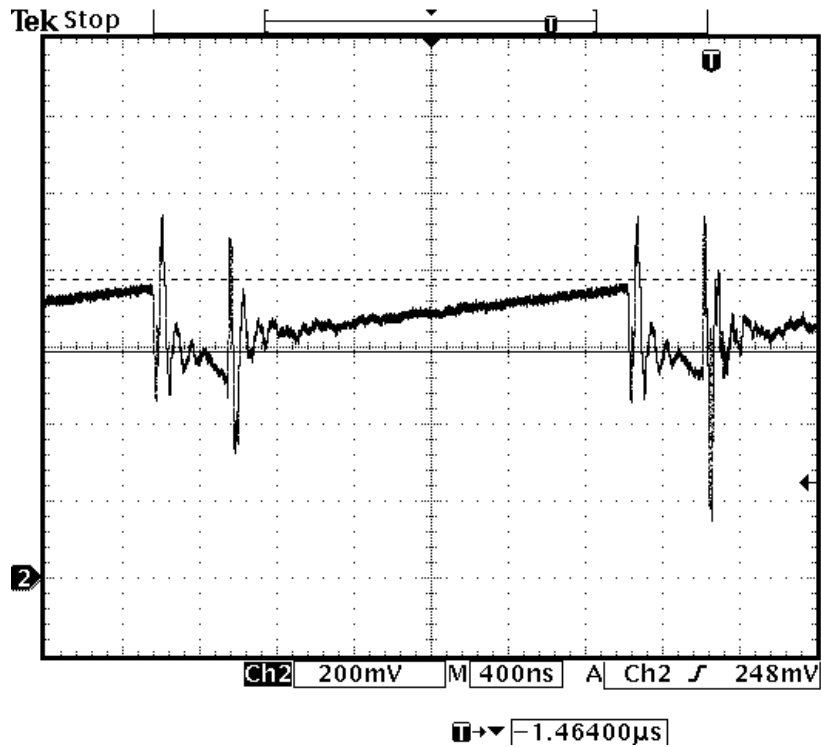
Figure 4.12 LED current on output of LED driver for LED voltage equal 35V.

4.5   Measurement results

In the following section, the results of measurements are presented. They contain the characteristics of the tested devices. The measurements were done using the connection diagram from Figure 4.6. The two oscilloscopes were sensing input and output voltage and current. To obtain the power supplied to device and drawn from device, the function of multiplication the waveforms was done on oscilloscopes. This brings waveform of the power. The real power was also calculated by oscilloscopes by averaging the power waveform. Based on this the efficiency was determined. The characteristics as function of the load were calculated with respect to nominal maximum load: 35W - 100%.

Figure 4.13 presents overall efficiency and losses of power supply module. The 80% efficiency, which was established in requirements on beginning of design, is obtained above the 25% load. The maximum efficiency 92% is achieved for full load. There are very satisfactory results. It means that the average efficiency of each PFC and flyback converters has above 95%. It is worth to note, that during standby mode, without any load, device drawn below 0,5W. In Figure 4.14 it is shown the output voltage as function of load. The voltage load is falling slightly on full load about 0,3V. It is considered that it is good result and demonstrates a satisfactory operation of control loop.
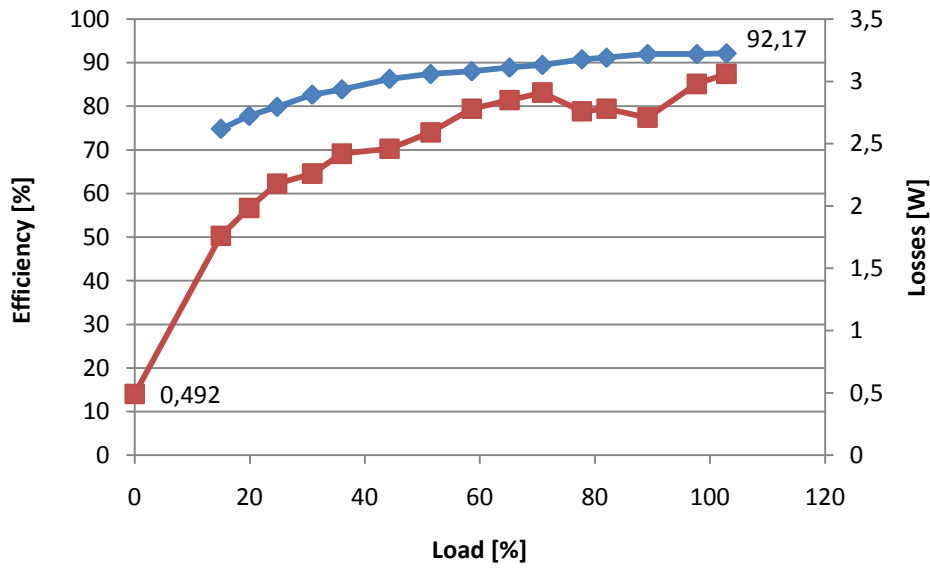
Figure 4.13 Efficiency of power supply – blue color, and losses in power supply – red color as function of load.
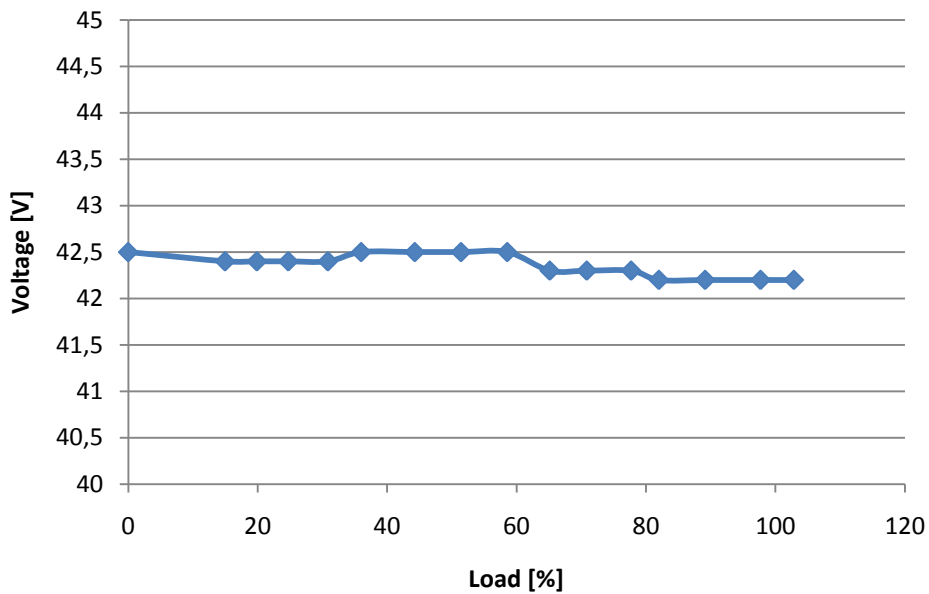
Figure 4.14 Output voltage as function of load.

In the following part, the characteristics of the LED driver are examined. Figure 4.15 shows the efficiency and current stability depending on the voltage drop across the load. In wide range of operation, the output voltage efficiency is above 90%. The peak value is achieved for voltage 35V and it is almost 97%. The output current decreases with the increase of the output voltage. The characteristic is below the set value and the maximum difference is about 34 mA. This means that the stabilization of the LED current has a tolerance of 4.8%, which is above the 3% limit assured by the manufacturer. Figure 4.16 presents the relation between efficiency and duty-cycle of PWM dimming signal for three different values of output voltages. It shows that for output voltages 25V and 35V, the

efficiency decreases by about 12% with lowering duty-cycle. For a voltage 15V, the drop of the efficiency is about 18%. Figure 4.17 shows the dependence of delivered active power as function of duty-cycle for 3 different output voltages. It can be seen that the relationship between the power delivered and the duty-cycle of the control signal is nearly linear and is not dependent on the output voltage.
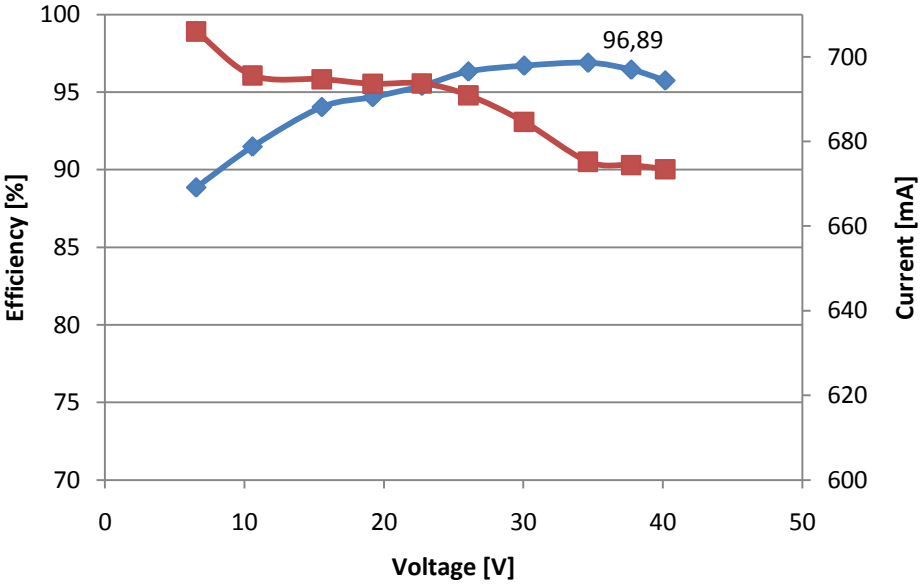

Figure 4.15 Efficiency – blue color, and output current – red color as function of voltage of LED driver.
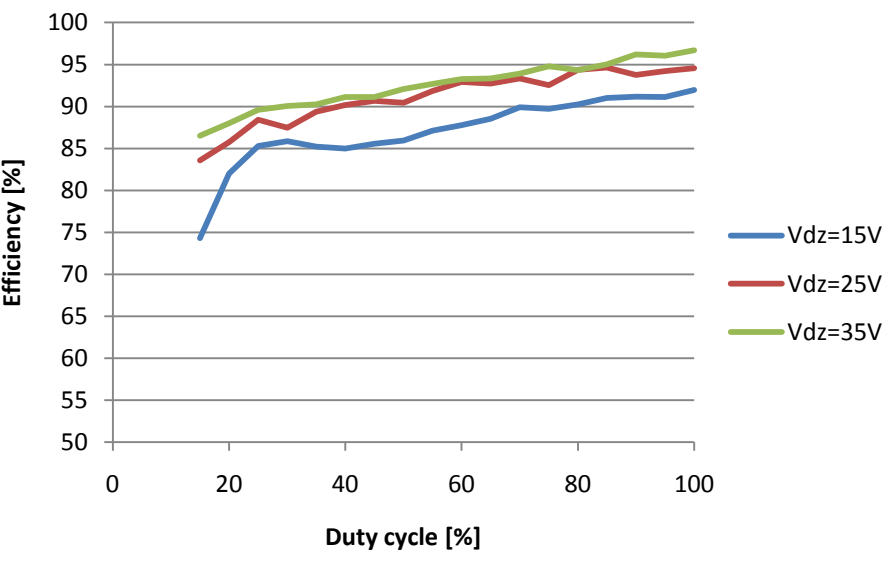

Figure 4.16 Efficiency of LED driver as function of control signal's duty-cycle, for 3 values of voltage.
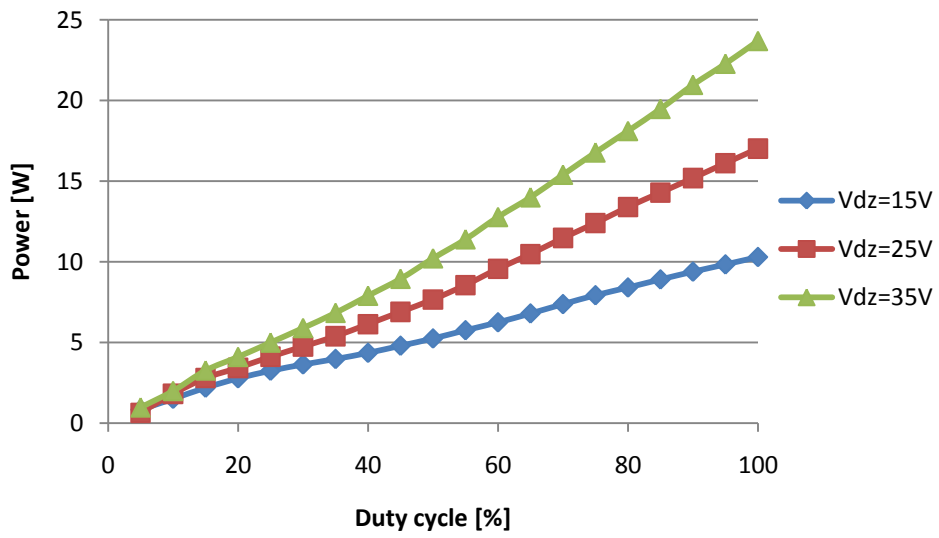
Figure 4.17 Output power as function of control LED signal's duty-cycle for 3 values of voltage.

5. Conclusions

LEDs technology is an evolving trend in the lighting industry in recent years, due to their capabilities and wide variety of possible applications. The main object of this thesis was to develop an intelligent LED driver for modern lighting systems. The targeted goal for this device was to obtain high overall efficiency. A digital management system also had to be developed to allow appropriate control of light intensity and wireless monitoring.

As part of the project, a main power supply and a LED driver were designed. The power supply provides power for the entire system. It consists of an active Power Factor Correction stage and a two-transistor quasi-resonant flyback converter. The LED driver provides the necessary current to the LED and easily allows light intensity control using a PWM dimming approach. In addition, the microcontroller system was implemented. It consists of two modules, which communicate wirelessly. The first module is responsible for the measurement of ambient conditions and adjusting the appropriate light intensity of the LEDs. The second module acts as a communication bridge between the first module and a computer.

The overall system was implemented with commercially available devices and custom designed PCBs. The developed prototype operated properly. All the components cooperated with each other, and provided adequate control of the LED light intensity according to ambient conditions, coping with both twilight sensing and motion detection. The measured results of the power supply and the LED driver showed that the requirements were fulfilled. The power supply supplied a stable voltage for wide load range. In addition, stabilization of LED driver current did not raise reservations. The results of efficiency measurement were particularly important. Both devices achieved efficiency values higher than expected, with efficiency reaching 92% under full lighting and maximal load conditions. It was also ascertained that efficiency decrease due to low dimming stayed around 75%, which represents a good performance metric, for comparison with other solutions. This proved the validity of the selected configurations and the correct development of the design.

The developed project is a complete device. It was tested in the laboratory conditions and ready for examination in the existing LED lighting application. With high efficiency and intelligent active control, it allows low power consumption and high illumination capabilities when required. In addition, wireless communication provides monitoring and allows system adjustment for the customer's needs.

5.1 Future work

The currently developed design makes up a complete device but it is still a prototype. Before it can be consider as the final product, it has to be tested and tuned up in the existing lighting system. This would bring information about the device behavior and find possible drawbacks, and in consequence provide more reliable product. In particular, it would be important to have electromagnetic compatibility tests to ascertain if the electromagnetic interference generated by the device copes with the standard values for this class of equipment.

Apart from that, there are also possible exploitation venues that could take this device as a starting point. In particular it would be interesting to duplicate the device and build an illumination system, where LED drivers would be connected in a network as nodes. Each of the nodes would share sensor signals between each other to provide even better lighting control and save power. The main field of study is to design this network, develop the schedule of the communication and the lighting profiles according to installed application. The example of the system would be a road lamp network. One, or more, lamps would send the information about passing car or pedestrian to the next lamps. In this case, other lamps would have the information in advance and suitable conditions to adapt their light intensity.

Another possibility concerns the modules individually. Designed power supply can be treat as high-efficient general purpose power supply and it can be used in plenty of application for instance in cooperation with efficient power class D amplifiers.

During working on this thesis, in the same time, there was another developing project in laboratory concerning visible light communications provided by lighting system. The objective of this project was to develop LED driver, which would besides controlling the light, also supply the data signal to the LED to transmit information in the light flux. In this respect, the designed prototype can be a good base to study possible approaches. Concerning light intensity modulation, the LED peak-to-peak current ramp is dependent on the operating frequency, thus also on R_{FS}. It seems feasible to transmit data by acting on the frequency adjustment input.

References

[1]   David A. Jones, *Electrical engineering: the backbone of society",* Proceedings of the IEE: Science, Measurement and Technology, 1991

[2]   The International Energy Agency, *Key World Energy Statistic*, 2013, http://www.iea.org/publications/freepublications/publication/KeyWorld2013.pdf

[3]   U.S. Energy Information Administration, *The International Energy Outlook*, 2013, https://www.eia.gov/forecasts/ieo/pdf/0484(2013).pdf

[4]   United Nations Framework Convention on Climate Change, *Kyoto Protocol*, 1998

[5]   European Commission, *Citizens' summary EU climate and energy package*, 2012, http://ec.europa.eu/clima/citizens/summary/docs/climate_package_en.pdf

[6]   Aalto University School of Science and Technology Department of Electronics Lighting Unit, *Guidebook on Energy Efficient Electric Lighting for Buildings*, Espoo, 2010, www.ecbcs.org/docs/ECBCS_Annex_45_Guidebook.pdf

[7]   McKinsey & Company, *Lighting the way: Perspectives on the global lighting market*, 2nd ed, 2012, http://www.mckinsey.com/~/media/mckinsey/dotcom/client_service/automotive and assembly/lighting_the_way_perspectives_on_global_lighting_market_2012.ashx

[8]   Peter R. Boyce, *Human Factors in Lighting*, CRC Press, Boca Raton, 2014

[9]   The International Energy Agency, *Light's Labour's Lost: Policies for Energy-efficient Lighting*, 2006, http://www.iea.org/publications/freepublications/publication/light2006.pdf

[10]   Steve Winder, *Power Supplies for LED Driving*, Elsevier, Burlington , 2008

[11]   Vinod Kumar Khanna, *Fundamentals of Solid-State Lighting*, CRC Press, Boca Raton, 2014

[12]   Illuminating Engineering Society of North America, *Lighting Handbook: Reference and Applications*, New York, 2000

[13]   E. Fred Schubert, *Light-emitting Diodes*, Cambridge University Press, New York, 2006

[14]   U.S. Department of Energy, *Color Quality of White LEDs*, 2008, http://www.cool.conservation-us.org/byorg/us-doe/color_quality_of_white_leds.pdf

[15]   Philips online catalog, 2014, http://www.ecat.lighting.philips.com/l/

[16] Cree.com, *Cree First to Break 300 Lumens-Per-Watt Barrier*, Durham, NC, March, 2014, http://www.cree.com/News-and-Events/Cree-News/Press-Releases/2014/March/300LPW-LED-barrier

[17] Marty Brown, *Power Supply Cookbook*, Newnes, 2001

[18] National Semiconductor, *LED Drivers for High-Brightness Lighting Solutions Guide*, 2011, http://www.ti.com/lit/sl/snvy001/snvy001.pdf

[19] Johnny C. Bennett , Practical Computer Analysis of Switch Mode Power Supplies, CRC Press, Boca Raton, 2005

[20] Marty Brown , *Practical Practical Switching Power Supply Design*, Academic Press, California , 1990

[21] Jean Picard*, Under the Hood of Flyback SMPS Designs*, SLUP261, Texas Instruments, 2011, www.ti.com/lit/ml/slup261/slup261.pdf

[22] ON Semiconductor*, Power Factor Correction (PFC) Handbook*, HBD853/D, 2014, *www.onsemi.com/pub/Collateral/HBD853-D.PDF*

[23] Fairchild Semiconductor Corporation, *Power Factor Correction (PFC) Basics*, Application Note 42047, 2004, www.fairchildsemi.com/an/AN/AN-42047.pdf

[24] H.Z.Azazi , E.EL-Kholy, S.A.Mahmoud , S.S.Shokralla, *Review of Passive and Active Circuits for Power Factor Correction in Single Phase, Low Power ACDC Converters*, Cairo University, Egypt, 2010, www.sdaengineering.com/mepcon10/papers/154.pdf

[25] Timothy L. Skvarenina*, The power electronics handbook*, CRC Press, Boca Raton, 2002

[26] Hangseok Choi, *Dual-Switch Quasi-Resonant Flyback Converter: Cost Effective Alternative to LLC Resonant Converters*, Fairchild Semiconductor, 2011, http://www.fairchildsemi.com/collateral/whitepapers/Dual-Switch-Quasi-Resonant-Flyback-Converter.pdf

[27] L. Rossetto, G. Spiazzi, P. Tenti, *Control Techniques for Power Factor Correction Converters*, University of Padova, Padova – ITALY, http://www.dei.unipd.it/~pel/Articoli/1994/Pemc/Pemc94.pdf

[28] Oscar García, José A. Cobos, Roberto Prieto, Pedro Alou, Javier Uceda, *Single Phase Power Factor Correction: A Survey*, IEEE TRANSACTIONS ON POWER ELECTRONICS, 2003

[29] ERIC PERSSON, *Understanding PFC*, International Rectifier, El Segundo, CA, 2006, http://www.electronicproducts.com/Analog_Mixed_Signal_ICs/Understanding_PFC.aspx

[30] Christopher Bridge, *Why we don't need silicon carbide diodes for PFC*, Fairchild Semiconductor, 2009, http://www.embedded.com/design/power-management-design/4019569/Why-we-don-t-need-silicon-carbide-diodes-for-PFC

[31] Hang-Seok Choi, *Transformer Design Consideration for Off-line Flyback Converters Using Fairchild Power Switch*, AN- 4140, Fairchild Semiconductor Corporation, 2003, www.fairchildsemi.com/an/AN/AN-4140.pdf

[32] L. Rossetto, G. Spiazzi, P. Tenti, *Control Techniques for Power Factor Correction Converters*, University of Padova, Padova – ITALY, http://www.dei.unipd.it/~pel/Articoli/1994/Pemc/Pemc94.pdf

[33] Youhao Xi and Bob Bell, *Two-switch topology boosts forward, flyback designs*, National Semiconductor, 2008, http://www.eetimes.com/document.asp?doc_id=1273232

[34] Aries Huang, *SMPS design: Switch mode power supply based on Dual Switch Flyback Topology* , Fairchild Semiconductor, 2006, http://www.eeherald.com/section/design-guide/dual-switch-flyback-converter.html

[35] AN-6920MR, *Integrated Critical-Mode PFC / Quasi-Resonant Current-Mode PWM Controller FAN6920*, Rev. 1.0.1, Fairchild Semiconductor Corporation, 2010, www.fairchildsemi.com/an/AN/AN-6920MR.pdf

[36] Fairchild Semiconductor Corporation, *Dual Switch Flyback Converter Solution: The Ideal Solution for 75~200W Power Supplies*, http://www.icbank.com/icbank_data/online_seminar_image/Flyback_Converter_Solution.pdf

[37] TALEX module STARK LLE 24-280-1250 Datasheet, Tridonic, 2014, http://www.tridonic.com/com/en/download/data_sheets/TALEXXmodule_STARK_LLE24_CLASSIC_en.pdf

[38] AUIRS21811S Datasheet, International Rectifier, 2010, http://www.irf.com/product-info/datasheets/data/auirs21811s.pdf

[39] FAN6204 Datasheet, Rev. 1.0.3, Fairchild Semiconductor Corporation, 2013, www.fairchildsemi.com/ds/FA/FAN6204.pdf

[40] FAN6920MR Datasheet, Rev. 1.0.8, Fairchild Semiconductor Corporation, 2013, www.fairchildsemi.com/ds/FA/FAN6920MR.pdf

[41] Ferroxcube Catalog: Soft Ferrites and Accessories Data Handbook 2013, Ferroxcube International Holding, 2013, http://www.ferroxcube.com/FerroxcubeCorporateReception/datasheet/FXC_HB2013.pdf

[42]   E 20/10/6 Ferrite Core Datasheet, EPCOS, 2013,
        www.epcos.com/inf/80/db/fer_07/e_20_10_6.pdf

[43]   RM 8 Ferrite Core Datasheet, EPCOS, 2013,
        http://www.epcos.com/inf/80/db/fer_13/rm_8.pdf

[44]   LM3414HV Datasheet, SNVS678E, Texas Instruments Incorporated, 2013,
        http://www.ti.com/lit/ds/symlink/lm3414hv.pdf

[45]   LM3414HV 1A 65V LED Driver Evaluation Board, Application Note 2076, National
        Semiconductor, 2010, http://www.ti.com/lit/ug/snva451b/snva451b.pdf

[46]   Home page of Arduino board, http://arduino.cc/

[47]   ATMEGA 328P Datasheet, Atmel Corporation, 2014,
        http://www.atmel.com/images/Atmel-8271-8-bit-AVR-Microcontroller-ATmega48A-
        48PA-88A-88PA-168A-168PA-328-328P_datasheet_Complete.pdf

[48]   TEPT5700 Datasheet, Rev. 1.7, Vishay Semiconductors, 2014,
        http://www.vishay.com/docs/81321/tept5700.pdf

[49]   PIR415 User Manual, Velleman nc, 2013,
        http://www.velleman.eu/downloads/3/pir415a705.pdf

[50]   SIFERRIT material N87 Datasheet, EPCOS AG, 2006,

[51]   http://www.eeweb.com/blog/anthony_catalano

[52]   http://en.wikipedia.org/wiki/Lighting

Appendix A: Bill of Materials

Part	Value		Note	Case
Two-switches quasi-resonant Flybac k converter				
Resistors				
RPFC1	9,9	MΩ	1% 0,125W / 3xR	1206
RPFC2	62	kΩ	1% / 0,25W	1206
RPFC3	250	kΩ	5% / 0,25W	1206
RVIN1	9,4	MΩ	1% / 0,6W / 2xR	THT
RVIN2	60,4	kΩ	1% / 0,25W	1206
RZCD	47	kΩ	5% / 0,25W	1206
RHV	156	kΩ	1% / 0,33W / 4xR	1206
RRT	7,5	kΩ	1% / 0,25W	1206
RCS1	1	Ω	5% / 1W	THT
RCS2	1,2	Ω	1% / 0,6W	THT
RG1	10	Ω	1% / 0,25W	THT
RG2	10	Ω	1% / 0,25W	THT
RG3	10	Ω	1% / 0,25W	THT
RDET1	105	kΩ	1% / 0,25W	1206
RDET2	20	kΩ	1% / 0,25W	1206
RCIN	3	MΩ	10% / 0,25W /3xR	1206
RCSF1	1	kΩ	5% / 0,25W	1206
RCSF2	1	kΩ	5% / 0,25W	1206
RLPC1	560	kΩ	1% / 0,25W	1206
RLPC2	10	kΩ	1% / 0,25W	1206
RRES1	100	kΩ	1% / 0,25W	1206
RRES2	10	kΩ	1% / 0,25W	1206
RSN	360	Ω	1W	
RO1	240	kΩ	1% / 0,25W	1206
RO2	15	kΩ	1% / 0,25W	1206
RBIAS	330	Ω		1206
RF	1,2	kΩ		1206
Capacitors				
CINF1	330	nF	X2CAP / 275V	
CINF2	470	nF	450V	
CINF3	470	nF	450V	
CVIN	2,2	μF		
CCOMP	470	nF		
CAUX	100	μF	63V	
CRT	100	nF		
CIC1	100	nF		
CIC2	100	nF		
CIC3	2x100	nF		
CFB	47	nF		

CO.PFC	47	μF	450V	
CSN	2,2	nF		
CF	10	nF		
COUT1	330	μF	63V	
COUT2	330	μF	63V	
CBOOT	0,1	μF		
Diodes				
D1	S1JL		600V / 1A	SMF
D2	S1JL		600V / 1A	SMF
DPFC	STTH1R06	Ultra-Fast	600V / 1A	SMA
DBOOST	STTH1R06	Ultra-Fast	600V / 1A	SMA
DAUX	RGF1D	Fast	200V / 1A	SMA
DAUX.H	RGF1D	Fast	200V / 1A	SMA
DR1	STTH1R06	Ultra-Fast	600V / 1A	SMA
DR2	STTH1R06	Ultra-Fast	600V / 1A	SMA
DBR	DF08S-E3/77	Bridge	800V	DFS
DZ		Zener		DO-41
MOSFETs				
Q1	STP13NM60N			TO220
Q2	STP13NM60N			TO221
Q3	STP13NM60N			TO222
Q4	FDS86242			SOP8
IC				
IC1	FAN6921MR		PFC + 2QR	SOP16
IC2	AUIRS21811S		Gate Driv 600V	SOP8
IC3	FAN6204		SR	SOP8
IC4	K817P9		CMR 200-400%	DIP4
IC5	AP431AG		2,5V shunt 0,5%	SOP8
Other				
NTC	TTC104 10K		5%	
LDM	20	mH	200nH CM	
LCM	125	nH		
LED DRIVER BOARD				
RFSF	49,9	kΩ	1% / 0,25W	1206
RIADJ	4,42	kΩ	1% / 0,25W	1206
RT1	8,25	kΩ	1% / 0,25W	1206
RT2	422	Ω	1% / 0,25W	1206
PTC	3,9	kΩ	1%	THT
RVI1	560	kΩ	1% / 0,25W	1206
RVI2	100	kΩ	1% / 0,25W	1206
RVI3	39	kΩ	1% / 0,25W	1206
RVI4	39	kΩ	1% / 0,25W	1206
RDS1	560	kΩ	1% / 0,25W	1206
RDS2	100	kΩ	1% / 0,25W	1206

| RDS3	39	kΩ	1% / 0,25W	1206
RDS4	39	kΩ	1% / 0,25W	1206
Q1	BC847B	NPN		SOT23
IC1	LM3414HV			
CIN	100	uF		
CVCC	1	uf		
CIC1	2x100	nF		
DZ1	5,1	V		DO-41
DZ2	5,1	V		DO-41

Appendix B: PCB Design
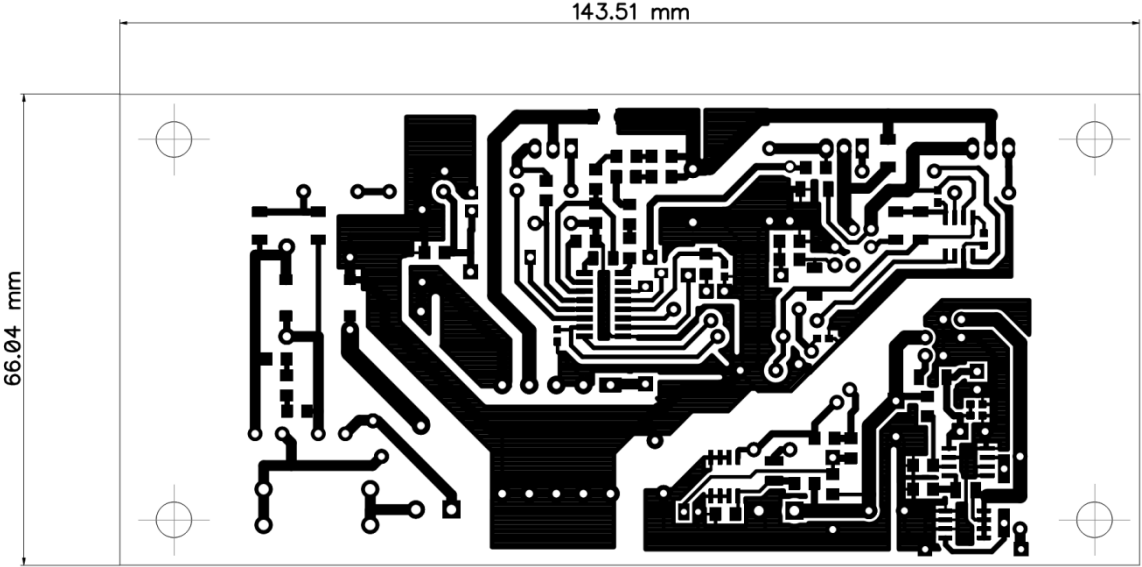


Figure 7.1 Power supply board's bottom layer.
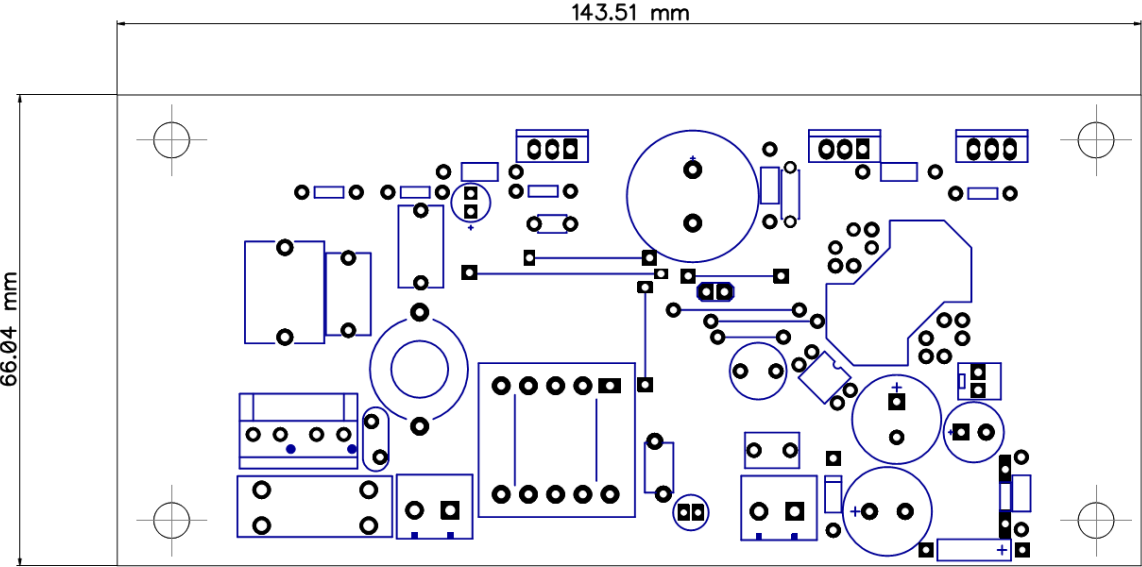
Figure 7.2 Power supply board's top layer component placement.
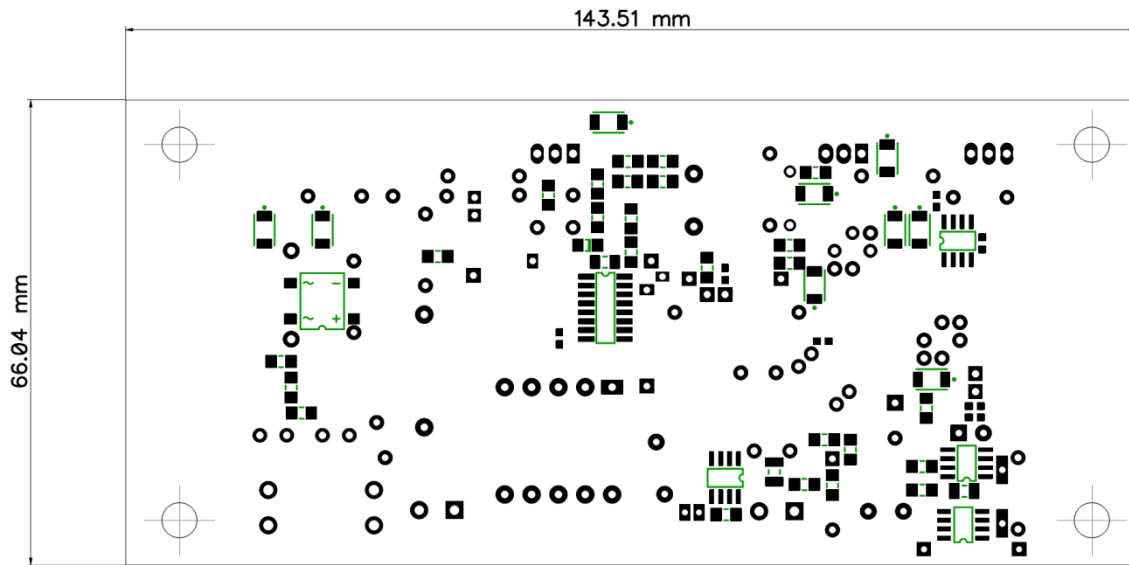
*Figure 7.3 Power supply board's top layer component placement.*
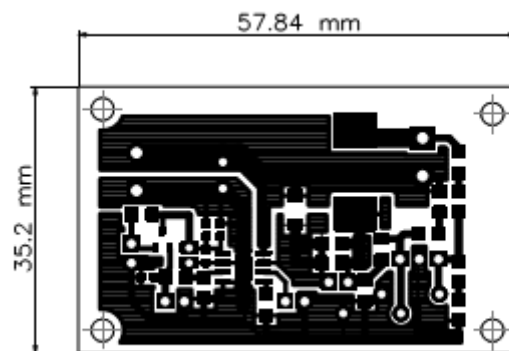
*Figure 7.4 Power supply board's bottom layer.*
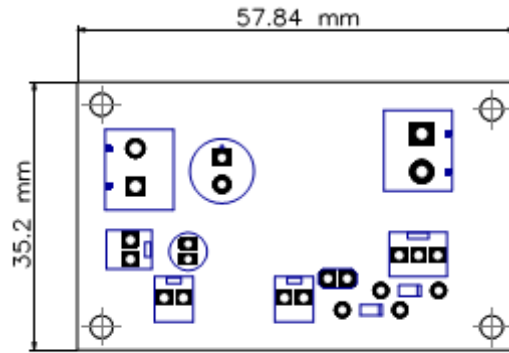
Figure 7.5 LED driver board's top layer component placement.
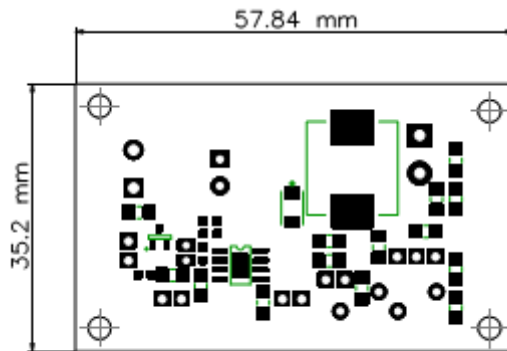


Figure 7.6 LED driver board's bottom layer component placement.

Appendix C: Arduino code

LED MCU module

```
#include <MsTimer2.h>
#include <TimerOne.h>
#include <SPI.h>
#include <Mirf.h>
#include <nRF24L01.h>
#include <MirfHardwareSpiDriver.h>
/** Radio Pins:
 * Hardware SPI:
 * MISO -> 12
 * MOSI -> 11
 * SCK -> 13
 * Configurable:
 * CE -> 8
 * CSN -> 7
//  INPUTS
const unsigned int LightSensePin = A0;  // Analog input pin to sense light sensor.
const unsigned int MotionSensePin = A1;  // Analog input pin to sense motion sensor.
const unsigned int CurrentSenseResistorPin = A2;  // Analog input pin from current sense resistor on driver
board.
const unsigned int HighInductorSenseVoltagePin = A3;   // Analog input pin sensing high side voltage of
inductor on driver board.
const unsigned int LowInductorSenseVoltagePin = A4;    // Analog input pin sensing low side voltage of
inductor on driver board.
//  OUTPUTS
const int OutLEDsignalPin = 9; // PWM output pin for LED.
//const int OutLEDsignalPin2 = 3; // PWM output pin for LED.
//  INTERNAL VALUES
unsigned int LightSense = 0;
unsigned int LightValue = 0;
unsigned int MotionValue = 0;
volatile unsigned int LedLevel = 0;
volatile unsigned int LedLevelBuffer = 0;
unsigned int LowLightTH = 800;  //78,125
unsigned int HighLightTH = 928; //90,625
unsigned int LowLedLevel = 50;
unsigned int HighLedLevel = 150;
unsigned int MotionLedLevel = 928;  //90,625
unsigned long TimeMotionStart = 0;
unsigned long TimeMotionLimit = 3000;      // millisecond
unsigned char FadeUpDelay = 2; //millisecond per step
unsigned char FadeDownDelay = 20; //millisecond per step
const unsigned char sendingDelay = 0;
const unsigned int currentLED=0,7;
volatile unsigned int HighInductorVoltage;
volatile unsigned int LowInductorVoltage;
volatile unsigned int CurrentSense;
unsigned long Etot=0;
unsigned int Pold=0;
unsigned int Pnew=0;
unsigned int Energy_consumed = 0;
const int PowerSenseInterval = 1000; // milliseconds
boolean MotionSense = 0;
boolean MotionModeStatus = 0;
boolean PowerCalcStatus = 0;
int sensorValue = 0;          // value read from the pot
int outputValue = 0;          // value output to the PWM (analog out)
volatile unsigned int pwmValue = 50;
volatile unsigned int out = 0;
//byte data[Mirf.payload];
//////////////////////////////////////////////////////////////////////
unsigned int  PowerCalc()
{
if (!PowerCalcStatus)
        {
        unsigned int DD = LelLevel'
        PO=0.0007*DD*DD+0.1637*x+0.3507;
        return PI=PO/(EffCalc1(PO)*EffCalc2(PO));
}
//////////////////////////////////////////////////////////////////////
void Energy_Consumed()
{
        Pnew=PowerCalc();
        Etot=PowerSenseInterval*(Pold+Pnew)/2;
        Pold=Pnew;
};


unsigned int EffCalc2(x)
{
```

```
return Eff2=-000.6*x*x+0.1704*x+84,928;
}
unsigned int EffCalc1(x)
{
return Eff2=-0,0024*x*x+0,464+69,67;
}
/////////////////////////////////////////////////////////////////
void LedSignal()
{
  if (LightValue > HighLightTH)LightValue = HighLightTH;
  if (LightValue < (LowLightTH)) {
    LedLevel = 0;
    delay (1000);
  }
  else
  {
    LedLevelBuffer = map(LightValue, LowLightTH, HighLightTH, LowLedLevel, HighLedLevel);
  }
  if (LedLevelBuffer > (LedLevel)) {
    LedLevel++;
  }
  else if (LedLevelBuffer < (LedLevel)) {
    LedLevel--;
  }
}
/////////////////////////////////////////////////////////////////
void SensorMeasurements()
{
  LightValue = analogRead(LightSensePin);
  delay(2);
  MotionValue = analogRead(MotionSensePin);
  delay(2);
  //LightValue = map(LightSense, 0, 1023, 0, 100);
}
/////////////////////////////////////////////////////////////////
void LedDecreasing()
{
  PowerSense();
  LedLevel = map(LightValue, LowLightTH, HighLightTH, LowLedLevel, HighLedLevel);
  LedLevelBuffer = MotionLedLevel;
  while ((LedLevel <= LedLevelBuffer) && !MotionSense)
  {
    LedLevelBuffer--;
    Timer1.setPwmDuty(OutLEDsignalPin, LedLevelBuffer);
    delay(FadeDownDelay);
    MotionSense = digitalRead(MotionSensePin);
  }
  PowerSense();
  //else return 1;
  if (!MotionSense)   {LedLevelBuffer = LedLevel;}
  else {MotionModeStatus = HIGH;}
}
/////////////////////////////////////////////////////////////////
void LedIncreasing()
{
  while (LedLevel < MotionLedLevel)
  {
    LedLevel++;
    Timer1.setPwmDuty(OutLEDsignalPin, LedLevel);
    delay(FadeUpDelay);
  }
  LedLevelBuffer = MotionLedLevel;
}
/////////////////////////////////////////////////////////////////
void comunicationMode()
{
  volatile unsigned int stat = 0;
  Serial.println("I received some!!!");
  Mirf.getData((byte *) &stat);
  Serial.print("value\t:");
  Serial.println(stat);
  switch (stat)
  {
    case 1:
      Serial.println("Wybrales 1");
      LowLightTH = receiveObject(stat);
      break;
    case 2:
      Serial.println("Wybrales 2");
      HighLightTH = receiveObject(stat);
      break;
    case 3:
      Serial.println("Wybrales 3");
      LowLedLevel = receiveObject(stat);
      break;
    case 4:
      Serial.println("Wybrales 4");
      HighLedLevel = receiveObject(stat);
```

84

```
        break;
      case 5:
        Serial.println("Wybrales 5");
        MotionLedLevel = receiveObject(stat);
        break;
      case 6:
        Serial.println("Wybrales 6");
        TimeMotionLimit = receiveObject(stat);
        break;
      case 8:
        Serial.println("Wybrales 8");
        if (!Mirf.isSending())
        {
          Mirf.setTADDR((byte *)"serv1");
          noInterrupts();
          Mirf.send((byte *) &LightValue);
          while (Mirf.isSending()) {}
          interrupts();
        }
        break;
      case 9:
        Serial.println("Wybrales 9");
        if (!Mirf.isSending())
        {
          Mirf.isSending();
          Mirf.send((byte *) &LedLevel);
          while (Mirf.isSending()) {
          }
        }
        break;
      default:
        Serial.println("Transmition error");
        break;
  }
}
/////////////////////////////////////////////////////////////////////
unsigned int receiveObject(unsigned int sendReply)
{
  unsigned int waitTime = millis();
  volatile unsigned int object = 0;
  Mirf.setTADDR((byte *)"serv1");
  noInterrupts();
  Mirf.send((byte *)&sendReply);
  while (Mirf.isSending()) {    }
  interrupts();
  Mirf.isSending();
  delay(sendingDelay);
  while (!Mirf.dataReady())
  {
    if ( ( millis() - waitTime ) > 1000 )
    {
      Serial.println("Timeout on response from server!");
      return 0;
    }
  }
    Serial.print("Received:\t");
  Mirf.getData((byte *) &object);
  Mirf.setTADDR((byte *)"serv1");
  noInterrupts();
  Mirf.send((byte *)&object);
  while (Mirf.isSending()) {  }
  interrupts();
  Serial.println(object);
  return object;
}
/////////////////////////////////////////////////////////////////////
void setup() {

  pinMode(OutLEDsignalPin, OUTPUT);
  // initialize serial communications at 9600 bps:
  Serial.begin(9600);

  Timer1.initialize(1000);  // 1000 us = 1 kHz
  Timer1.pwm(OutLEDsignalPin, 0);
  //MsTimer2::set(PowerSenseInterval, Power_Sense); // 100ms period
  //MsTimer2::start();



  // Setup pins / SPI.
  // To change CE / CSN Pins:
  // Mirf.csnPin = 9;
  // Mirf.cePin = 7;
  Mirf.csnPin = 7;
  Mirf.cePin = 8;
  Mirf.spi = &MirfHardwareSpi;
  Mirf.init();
  Mirf.setRADDR((byte *)"clie1"); // * Configure receiving address.
```

85

```
    Mirf.payload = sizeof(unsigned int);//Set the payload length to sizeof(unsigned long) the return type of
millis().payload on client and server must be the same.
    Mirf.channel = 0;       // channel
    Mirf.config();
    Mirf.setTADDR((byte *)"serv1"); //Set the send address.
    Serial.println("Beginning ... ");
    delay(3000);
}
///////////////////////////////////////////////////////////////////
void loop() {
    if (Mirf.dataReady())
    {     comunicationMode();   }
    MotionSense = digitalRead(MotionSensePin);
    delay(2);
    if (MotionModeStatus)
    {
        if (MotionSense)    {       TimeMotionStart = millis();     }
        else     {
            if ((millis() - TimeMotionStart) > TimeMotionLimit)
            {
                MotionModeStatus = LOW;
                LedDecreasing();
            }
        }
    }
    else
    {
        if (MotionSense && (LightValue > LowLightTH))
        {
            MotionModeStatus = HIGH;
            LedIncreasing();
            TimeMotionStart = millis();
        }
        else
        {
            SensorMeasurements();
            LedSignal();
            Timer1.setPwmDuty(OutLEDsignalPin, LedLevel);
        }
    }
}
///////////////////////////////////////////////////////////////////
void serialEvent()
{
    while (Serial.available())Serial.read();

    Serial.println("Values in range (1 - 1023");
    Serial.print("1. Low threshold of light sensor:\t");
    Serial.println(LowLightTH);
    Serial.print("2. High threshold of light sensor:\t");
    Serial.println(HighLightTH);
    Serial.print("3. Minimum level of standby luminance:\t");
    Serial.println(LowLedLevel);
    Serial.print("4. Maximum level of standby luminance:\t");
    Serial.println(HighLedLevel);
    Serial.print("5. Maximum level of luminance when motion detected:\t");
    Serial.println(MotionLedLevel);
    Serial.print("6. Time of motion detect mode (in miliseconds):\t");
    Serial.println(TimeMotionLimit);
}
```

Comunication bridge module

```
#include <SPI.h>
#include <Mirf.h>
#include <nRF24L01.h>
#include <MirfHardwareSpiDriver.h>
#include <stream.h>

unsigned int pwmValue=50;

unsigned int LowLightTHCopy = 800;   //78,125
unsigned int HighLightTHCopy =928;   //90,625
unsigned int LowLedLevelCopy = 50;   //18,75
unsigned int HighLedLevelCopy = 150; //50
unsigned int MotionLedLevelCopy = 928;   //90,625
unsigned long TimeMotionLimitCopy = 3000;     // millisecond
const unsigned char sendingDelay = 1;

void setup(){
  Serial.begin(9600);
  Mirf.csnPin = 7;
  Mirf.cePin = 8;
  Mirf.spi = &MirfHardwareSpi;       //      Set the SPI Driver.
  Mirf.init();                                       //      Setup pins / SPI.
  Mirf.setRADDR((byte *)"serv1");   //Configure receiving address.
  Mirf.payload = sizeof(unsigned int);       //Set  the  payload  length  to  sizeof(unsigned  int)  the  return  type
payload on client and server must be the same.
  Mirf.channel = 0;        // channel
  Mirf.config();
  Mirf.setTADDR((byte *)"clie1");    //Set the send address.
  Serial.println("Beginning ... ");
}
void loop()
{
}
void serialEvent(){Comunication();}

void Comunication()
{
  while(Serial.available())Serial.read();
  Serial.println("Welcome  in  Led  Driver  Communication.\nWhich  value  do  you  want  to  change:\n1.  Low  threshold  of
light  sensor.\n2.  High  threshold  of  light  sensor.\n3.  Minimum  level  of  standby  luminance.\n4.  Maximum  level  of
standby  luminance.\n5.  Maximum  level  of  luminance  when  motion  detected.\n6.  Time  of  motion  detect  mode");
  Serial.println("You  can  also\n  7.  Print  all  values.\n  8.  Check  light  sensor  level.\n  9.  Check  LED  driving
signal.");
  while(!Serial.available()){
  }
  switch (Serial.read())
  {
  case '1':
    Serial.println("Are you sure to change this value? [y: 1/n: 0]");

    while(!Serial.available()){
    }
    if(!(Serial.read()-'0')) {
      Serial.println("Operation cancelled by user.");
      break;
    }
    changeLowLightTH();
```

87

```
    break;
case '2':
  Serial.println("Are you sure to change this value? [y: 1/n: 0]");

  while(!Serial.available()){
  }
  if(!(Serial.read()-'0')) {
    Serial.println("Operation cancelled by user.");
    break;
  }
  changeHighLightTH();
  break;
case '3':
  Serial.println("Are you sure to change this value? [y: 1/n: 0]");

  while(!Serial.available()){
  }
  if(!(Serial.read()-'0')) {
    Serial.println("Operation cancelled by user.");
    break;
  }
  changeLowLedLevel();
  break;
case '4':
  Serial.println("Are you sure to change this value? [y: 1/n: 0]");

  while(!Serial.available()){
  }
  if(!(Serial.read()-'0')) {
    Serial.println("Operation cancelled by user.");
    break;
  }
  changeHighLedLevel();
  break;
case '5':
  Serial.println("Are you sure to change this value? [y: 1/n: 0]");

  while(!Serial.available()){
  }
  if(!(Serial.read()-'0')) {
    Serial.println("Operation cancelled by user.");
    break;
  }
  changeMotionLedLevel();
  break;
case '6':
  Serial.println("Are you sure to change this value? [y: 1/n: 0]");

  while(!Serial.available()){
  }
  if(!(Serial.read()-'0')) {
    Serial.println("Operation cancelled by user.");
    break;
  }
  changeTimeMotionLimit();
  break;
case '7':
  Serial.println("Values in range (1 - 1023");
  Serial.print("1. Low threshold of light sensor:\t");
  Serial.println(LowLightTHCopy);
  Serial.print("2. High threshold of light sensor:\t");
```

```
      Serial.println(HighLightTHCopy);
      Serial.print("3. Minimum level of standby luminance:\t");
      Serial.println(LowLedLevelCopy);
      Serial.print("4. Maximum level of standby luminance:\t");
      Serial.println(HighLedLevelCopy);
      Serial.print("5. Maximum level of luminance when motion detected:\t");
      Serial.println(MotionLedLevelCopy);
      Serial.print("6. Time of motion detect mode (in miliseconds):\t");
      Serial.println(TimeMotionLimitCopy);
      break;
    case '8':
      Serial.print("Light sensor level =\t");
      receiver(8);
      break;
    case '9':
      Serial.print("LED signal =\t");
      receiver(9);
      break;
    default:
      Serial.println("Error!");
      break;

  }
}
/////////////////////////////////////////////////////////////////
void changeLowLightTH()
{
  unsigned int tempValue=0;
  volatile unsigned int comp=0;

  Serial.println("Put value in range 1-1024:");
  while(!Serial.available()){
  }
  tempValue=Serial.parseInt();
  if(1<=tempValue&&tempValue<=1024&&tempValue<HighLightTHCopy)
  {
    LowLightTHCopy = sender(1,tempValue);
  }
  else
  {
    Serial.println("Wrong value! Out of range or greater than HighLightTH" );
  }
  Serial.println("\n-------------\n");
}
/////////////////////////////////////////////////////////////////
void changeHighLightTH()
{
  unsigned int tempValue=0;
  volatile unsigned int comp=0;      //block name:      "variable name"
  unsigned int waitTime= 0;
  Serial.println("Put value in range 1-1024:" );
  while(!Serial.available()){
  }
  tempValue=Serial.parseInt();
  if(1<=tempValue&&tempValue<=1024&&tempValue>LowLightTHCopy)
  {
    HighLightTHCopy = sender(2,tempValue);

  }
  else
  {
```

```
    Serial.println("Wrong value! Out of range or lower than LowLightTH" );
  }
  Serial.println("\n-------------\n");
}
////////////////////////////////////////////////////////////////
void changeLowLedLevel()
{
  unsigned int tempValue=0;
  volatile unsigned int comp=0;
  unsigned int waitTime= 0;
  Serial.println("Put value in range 1-1024:" );
  while(!Serial.available()){
  }
  tempValue=Serial.parseInt();
  if(1<=tempValue&&tempValue<=1024&&tempValue<HighLedLevelCopy)
  {
    LowLedLevelCopy = sender(3,tempValue);

  }
  else
  {
    Serial.println("Wrong value! Out of range or greater than HighLedLevel" );
  }
  Serial.println("\n-------------\n");
}
////////////////////////////////////////////////////////////////
void changeHighLedLevel()
{
  unsigned int tempValue=0;
  volatile unsigned int comp=0;
  unsigned int waitTime= 0;
  Serial.println("Put value in range 1-1024:" );
  while(!Serial.available()){
  }
  tempValue=Serial.parseInt();
  if(1<=tempValue&&tempValue<=1024&&tempValue>LowLedLevelCopy)
  {
    HighLedLevelCopy = sender(4,tempValue);

  }
  else
  {
    Serial.println("Wrong value! Out of range or lower than LowLedLevel" );
  }
  Serial.println("\n-------------\n");
}
////////////////////////////////////////////////////////////////
void changeMotionLedLevel()
{
  unsigned int tempValue=0;
  volatile unsigned int comp=0;
  unsigned int waitTime= 0;
  Serial.println("Put value in range 1-1024:" );
  while(!Serial.available()){
  }
  tempValue=Serial.parseInt();
  if(1<=tempValue&&tempValue<=1024&&tempValue>HighLedLevelCopy)
  {
    MotionLedLevelCopy = sender(5,tempValue);

  }
```

```
  else
  {
    Serial.println("Wrong value! Out of range or lower than HighLedLevel" );
  }
  Serial.println("\n-------------\n");
}
/////////////////////////////////////////////////////////////////
void changeTimeMotionLimit()
{
  unsigned int tempValue=0;
  volatile unsigned int comp=0;
  unsigned int waitTime= 0;
  Serial.println("Put value in range 1-1024:" );
  while(!Serial.available()){
  }
  tempValue=Serial.parseInt();
  if(1<=tempValue&&tempValue<=4294967294)
  {
    TimeMotionLimitCopy = sender(6,tempValue);

  }
  else
  {
    Serial.println("Wrong value! Out of range or lower than HighLedLevel" );
  }
  Serial.println("\n-------------\n");
}
/////////////////////////////////////////////////////////////////
unsigned int sender(unsigned int  caseNum, unsigned int sendValue)
{
   unsigned int data=0;
   //volatile
  unsigned int waitTime= millis();

  data=caseNum;   //block
  Serial.println("TU1");
  Mirf.setTADDR((byte *)"clie1");
  noInterrupts();
  Mirf.send((byte*) &data);
  while(Mirf.isSending()){    }
  interrupts();
  //waiting to finish transmission
  //Mirf.isSending();       // turn on RX mode
  Serial.println("TU2");
  delay(sendingDelay);      // turn on RX mode
  data=0;
  //waitTime= millis();
  Serial.println("1");
  Mirf.isSending();
  while(!Mirf.dataReady()){//waiting for receive data
    if ( ( millis() - waitTime ) > 100 ) {
      Serial.println("Timeout on response from server!");
      return data;
    }
  }
  Mirf.getData((byte *) &data);      //get data
  if(data!=caseNum)        {
    Serial.println("Status Error!");
    return data=0;
  }        //check block
  Mirf.setTADDR((byte *)"clie1");
```

91

```
  noInterrupts();
  Mirf.send((byte*)&sendValue);
  while(Mirf.isSending()){ }
  interrupts();
  data=0;
  Mirf.isSending();
  while(!Mirf.dataReady()){//waiting for receive data
    if ( ( millis() - waitTime ) > 100 ) {
      Serial.println("Timeout on response from server!");
      return data;
    }
  }
    Serial.println("Finished sending");
  Serial.print("value =\t" );
  Mirf.getData((byte *) &data);      //get data

  Serial.println(data);
  return data;
}


void receiver(unsigned int  caseNum)
{
  volatile unsigned int data=0;
  unsigned int waitTime= 0;
  data=caseNum;   //block
  Mirf.setTADDR((byte *)"clie1");
  noInterrupts();
  Mirf.send((byte*) &data);
  while(Mirf.isSending()){    }      //waiting to finish transmission
  interrupts();
  Mirf.isSending();         // turn on RX mode
  delay(sendingDelay);     // turn on RX mode
  data=0;
  waitTime= millis();
  while(!Mirf.dataReady()){//waiting for receive data
    if ( ( millis() - waitTime ) > 100 ) {
      Serial.println("Timeout on response from server!");
      return;
    }
  }
  Mirf.getData((byte *) &data);      //get data
  Serial.println(data);
}
```